PART TWO

DATA INTERPRETATION

Chapter 1
Introduction to the Data

1.1 INTRODUCTION

Resistivity/phase (RP) and complex resistivity (CR) are geophysical techniques in which electrical current is transmitted into a grounded dipole at specific frequencies, and the returned voltage is measured by a second dipole some distance away. The responses are measured at several frequencies, processed, and analyzed for characteristics indicative of hydrocarbon alteration, minerals, or other pertinent geologic information.

The terms "resistivity/phase" and "complex resistivity" refer to specific methods which are an extension of the more general induced polarization (IP) method. IP has been as widely used in the mining industry over the past 30 years as the seismic reflection method has been in the petroleum industry. RP and CR measure the same phenomena and the presentation of data from the two methods is identical. Throughout this volume, the use of "resistivity/phase" implies the following:

1. Measurements are made of both amplitude and phase angle.
2. Measurements are made in the frequency domain at three or more discrete frequencies.
3. The data are specially processed in order to recover electromagnetic coupling information by separating it from the induced polarization response.

The use of "complex resistivity" implies the following:

1. Measurements are made of both amplitude and phase angle.
2. Measurements are made in the frequency domain at 6 to 24 odd Fourier harmonic frequencies.
3. The data are specially processed in order to recover electromagnetic coupling information by separating it from the induced polarization response.

These distinctions will become clear upon reading the information to follow.

A third technique, controlled source audiofrequency magnetotellurics (CSAMT), is also used in petroleum applications and is discussed in section 1.7.

1.2 DEFINITIONS AND PLOTTING CONVENTIONS

Voltage and Phase Angle

In order to impress an electromagnetic field into the ground, an electric current is transmitted directly into a grounded dipole. A source current is used in which the sense of current flow alternates periodically at some specified frequency. The flow of this periodic, time-varying current in the earth produces an electromagnetic field. This field is affected by the presence of electrical inhomogeneities, such as ore deposits, alteration zones, structure, variations in pore fluids, etc. The electromagnetic field produces a voltage gradient in the ground. It is the purpose of an electrical survey to measure the amplitude and the time-dependency of this voltage gradient using a grounded "receiving" dipole.

The voltage measurement between any two points is influenced by the shape of the original source current waveform and any perturbations caused by inhomogeneities in the earth. The perturbations are the things which are interpreted for their geologic significance.

A periodic, time-varying signal may be completely measured using the following two parameters:

1. Magnitude of the response (voltage)
2. Shift in time of the received signal with respect to the transmitted signal (phase angle)

A series of measurements of magnitude and phase angle as a function of time/frequency establishes the shape of the received signal with respect to the transmitted signal.

If the grounding geometry of the dipoles and the magnitude of the original current are known, the *apparent resistivity* of the ground can be calculated using the voltage gradient measurements. This is one of the three primary interpretation parameters used in petroleum exploration with the resistivity/phase and complex resistivity techniques. Phase angle refers to how well the ground stores up electrical charge with time, a process which is commonly called induced polarization. The phase angle measurement is also influenced by electromagnetic coupling, which is an artifact of the grounding geometry of the measuring system and of the geology. When the data are processed, the induced polarization and electromagnetic effects are separated from one another by means of a proprietary Zonge Engineering decoupling algorithm, resulting in the additional two interpretational parameters of *apparent polarization* and *residual electromagnetic (REM)* data.

The unit used for apparent resistivity measurements is the ohm-meter. High apparent resistivities indicate media which resist current flow; low numbers indicate media through which current flows easily. The unit used for induced polarization data is the milliradian. High numbers indicate media with a high electrical energy storage capacity; low numbers indicate media with low energy storage capacity. REM data are normalized and hence are unitless.

Figure 1.1 illustrates how the phase angle measurement is made. At time t=0, a sinusoidal electric current is applied to the ground. The induced electromagnetic field results in an instantaneous voltage, V_0. Capacitive properties of the ground cause it to charge up, and the voltage continues to rise to a peak of V at some time t. The time it takes for this voltage rise to occur, expressed as a function of the sinusoidal frequency, is the phase angle. In other words, phase angle is the amount

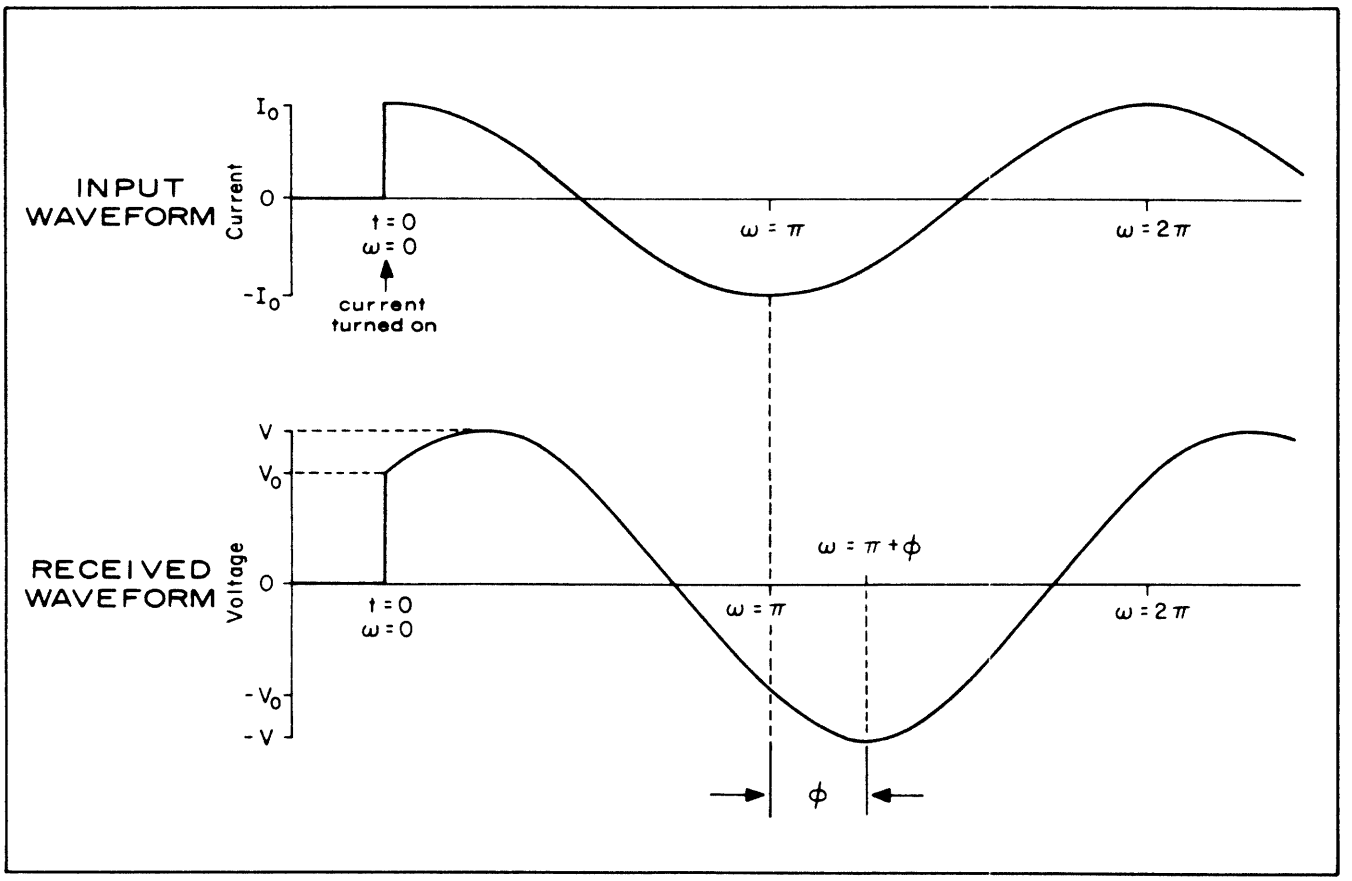

Figure 1.1. Definition of phase angle (ϕ). For the sinusoidal signals shown, phase angle is the delay in angular frequency (ω) between the peak of the input current and the peak of the received voltage.

by which the voltage lags the current. Units are in radians; a phase lag of 180 degrees (π radians) corresponds to signals which are completely out of phase (i.e., while one is at its minimum value, the other is at its maximum value). According to common convention, a negative phase angle is assigned to a measurement in which the voltage lags the current, while a positive phase angle refers to a case in which the current lags the voltage. In most ground environments, nearly all phase angles are negative. As a matter of convenience, then, the convention in electrical geophysics application is to reverse the sign of all phase angle data. Hence, all data which have positive signs correspond to voltage lagging the current; conversely, data which have negative signs correspond to voltage leading the current, a situation which occasionally results from peculiar geometric effects.

Complex Plane Plots

The two defining parameters of magnitude and phase angle permit one to plot a data point at a given frequency in polar coordinates, as illustrated in Figure 1.2(a). An equivalent plot can be constructed in terms of rectangular coordinates, as shown in Figure 1.2(b). The latter is called a "complex plane" plot, since it involves the use of complex numbers to describe the locations of the plot points. Following the standard convention used in electrical engineering, the horizontal axis is called the "real" or "in-phase" axis, since points located on it are in phase with their source, i.e., there is no phase shift between the two. The vertical axis is called the "imaginary," "quadrature," or "out-of-phase" axis, since data points which have a

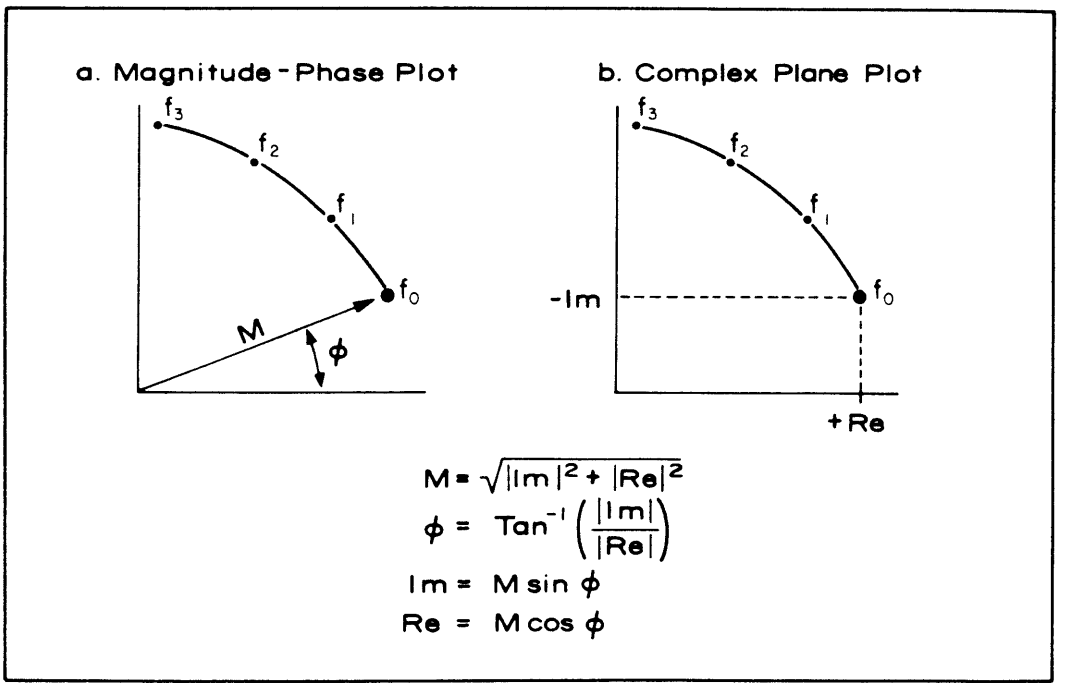

Figure 1.2. Example of a magnitude-phase plot and a complex plane plot of data at frequencies f_0, f_1, f_2, and f_3. The plots show the conversion from magnitude (M) and phase angle (ϕ) to real (Re) and imaginary (Im) coordinates.

non-zero vertical axis component are out of phase by 90 degrees ($\pi/2$ radians) with respect to their source and are described mathematically by imaginary numbers. Please note that in Figure 1.2, the negative imaginary component is up, not down, since convention dictates that negative phase angles are to be measured counter-clockwise from the positive real axis.

Pseudosection Plots

All oilfield data in this volume and nearly all resistivity/phase and complex resistivity data obtained by Zonge Engineering are acquired with the dipole-dipole array. This array employs a transmitting dipole of length "a" and a collinear receiving dipole of the same length. The separation between the two, called the "n" spacing (expressed in terms of "a"), is varied in order to control the depth of penetration.

Figure 1.3(a) shows how dipole-dipole data are normally plotted. By convention, the plot point is located midway between the transmitting and receiving dipoles at the intersection of two 45 degree lines projected from their midpoints. By plotting data at various separations and for various dipole positions on the ground, one can come up with a pseudosection plot similar to that of Figure 1.3(b). The pseudosection is not a true cross-section of the ground, for several important reasons. First, the depth of penetration is not strictly controlled by the "n" and "a" spacings, but is also dependent upon other factors, such as ground resistivity, geologic contacts, layering, etc. Secondly, the number value assigned to any given plot point does not represent the actual value of the rocks at that point, but rather the weighted averaged value of all the material affecting the measurement, with the near-surface material exerting a disproportionately high influence on all the data. The plot points, then, are strictly a matter of convention and convenience; effects observed in a pseudosection must be interpreted in order to arrive at an inferred geoelectric section. This is why the data plots are called "pseudosections."

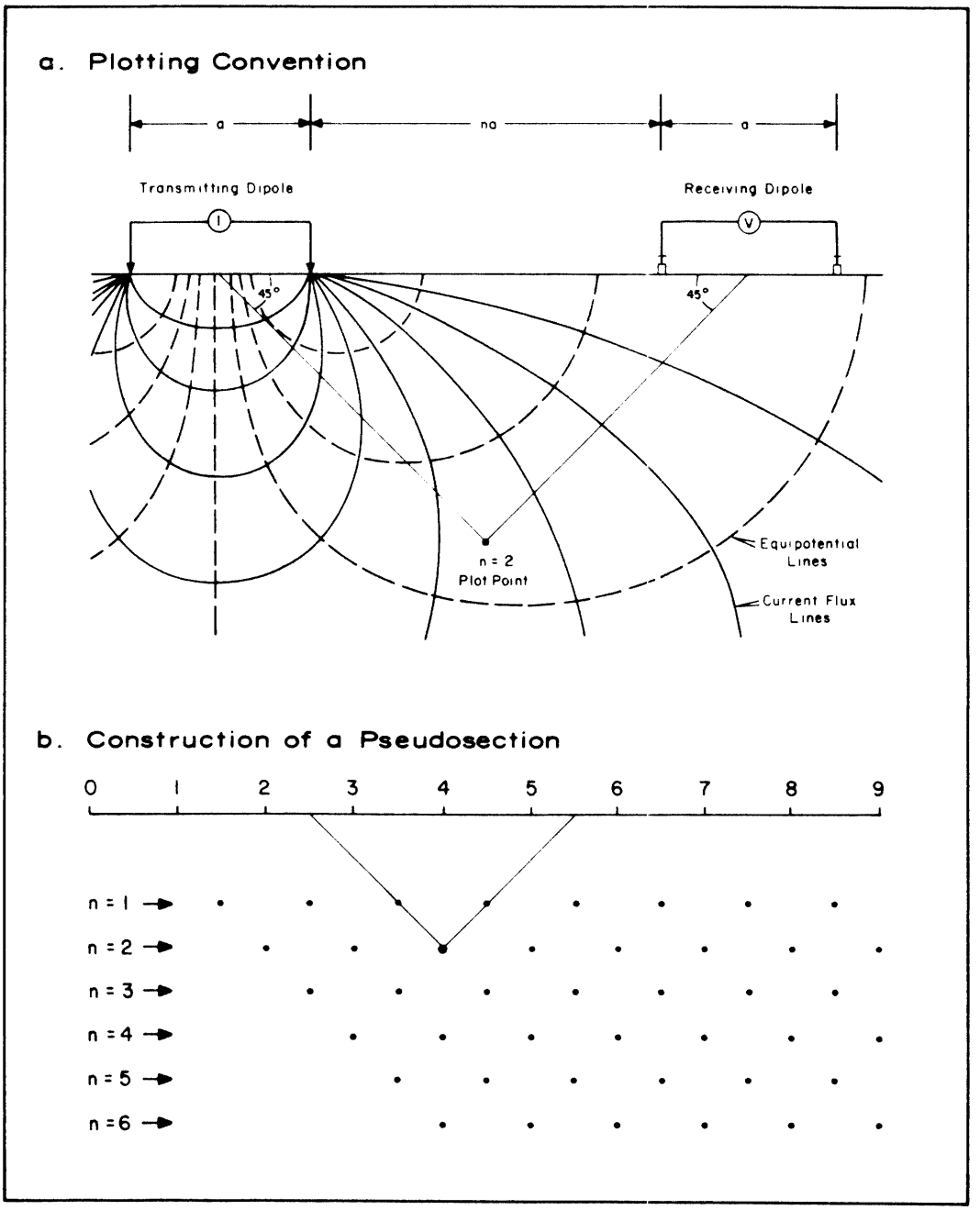

Figure 1.3. Plotting convention for dipole-dipole pseudosections.

Figure 1.4 presents an example of how the appearance of a pseudosection can differ from that of a geologic cross-section. A vertical, conductive, dike-like feature outcrops between stations 0 and 1. Since the dike essentially influences or "casts a shadow" on measurements made from dipoles on either side of it, all apparent resistivity values obtained by measuring through the dike are very low. According to our plotting convention, these low apparent resistivity values will lie along 45 degree diagonals emanating from the vicinity of dipole 0,1. This results in the triangular-shaped anomaly seen in the pseudosection of Figure 1.4. More complicated effects of this nature are also observed, necessitating the use of computer modeling to estimate the shape and magnitudes of anomalies from subsurface features.

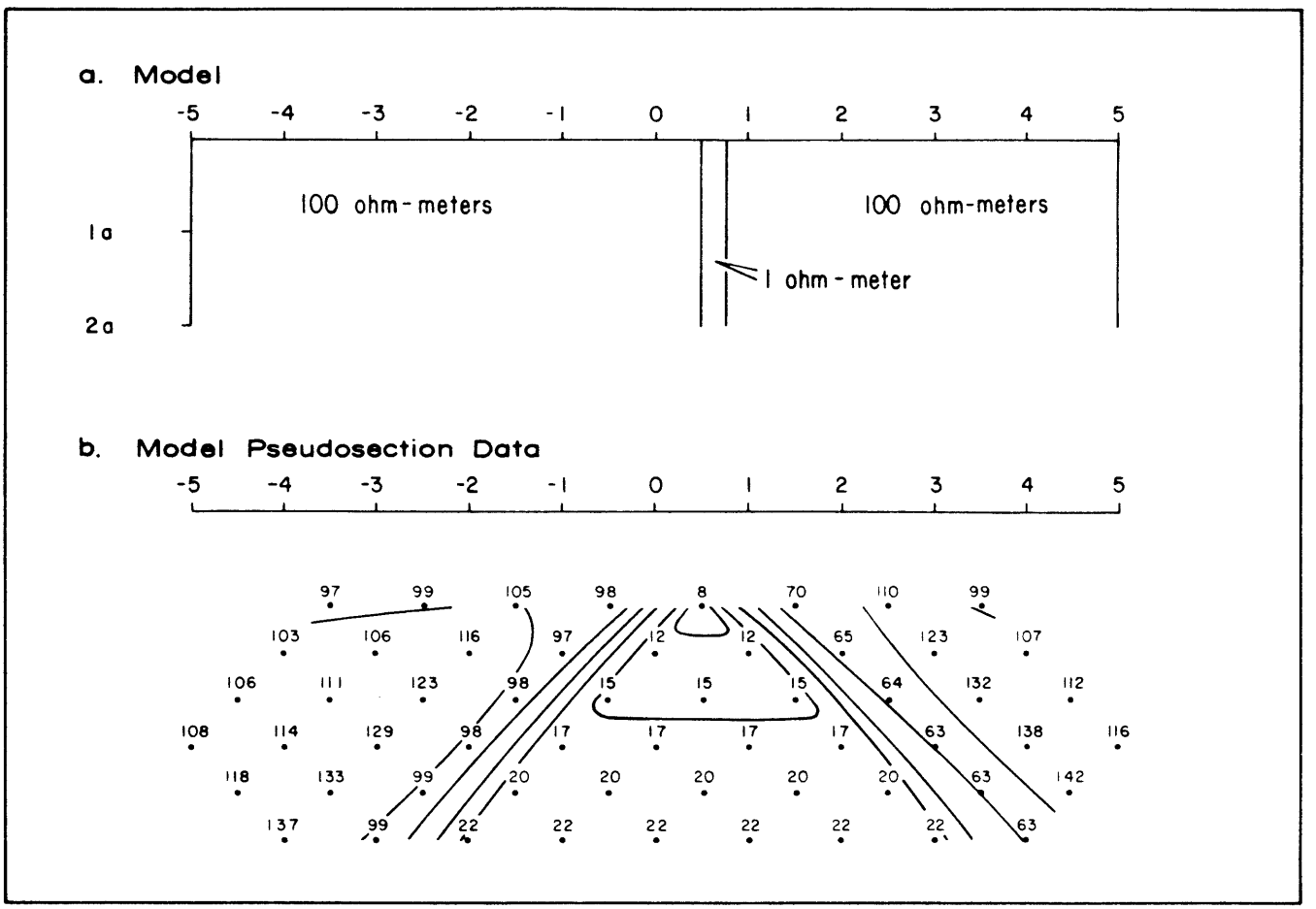

Figure 1.4. Example of a "geometric effect" from a vertical conductive dike. The data are from a two-dimensional computer model called "2DIP," which is explained in Chapter 2. Contour interval: 10.0, 15.9, 25.1, 39.8, 63.1, 100.0, . . . ohm-meters.

In discussing pseudosection data, several specific terms require explanation. In order to identify which diagonals show strong effects, one refers to the dipole from which the diagonal is plotted. For example, one might refer to the "left-plunging diagonal 2,3," or "right-plunging diagonal 3,4," as illustrated in Figure 1.5. Hence, the most strongly effected diagonals of Figure 1.4 are the left-plunging 1,2 diagonal and the right-plunging −1,0 diagonals. A generic term for diagonal and similar features is "geometric effects," so named because it is the specific geometric relationships of the dipole-dipole array and the geology which give the pseudosection its particular appearance.

1.3 ELECTRICAL NOISE

All electrical surveys are affected to some degree by any electrical noise present in the ground, since both the input signal and the noise contribute to the measured signal. Electrical noise measured in geophysical surveys comes from three primary sources: tellurics, atmospherics, and "culture" (man-made conductive features such as powerlines, pipelines, fences, etc.). Most of these signals are detected directly from ground contact, but at frequencies in the kilohertz range, airwave or radiation noise can also be considerable.

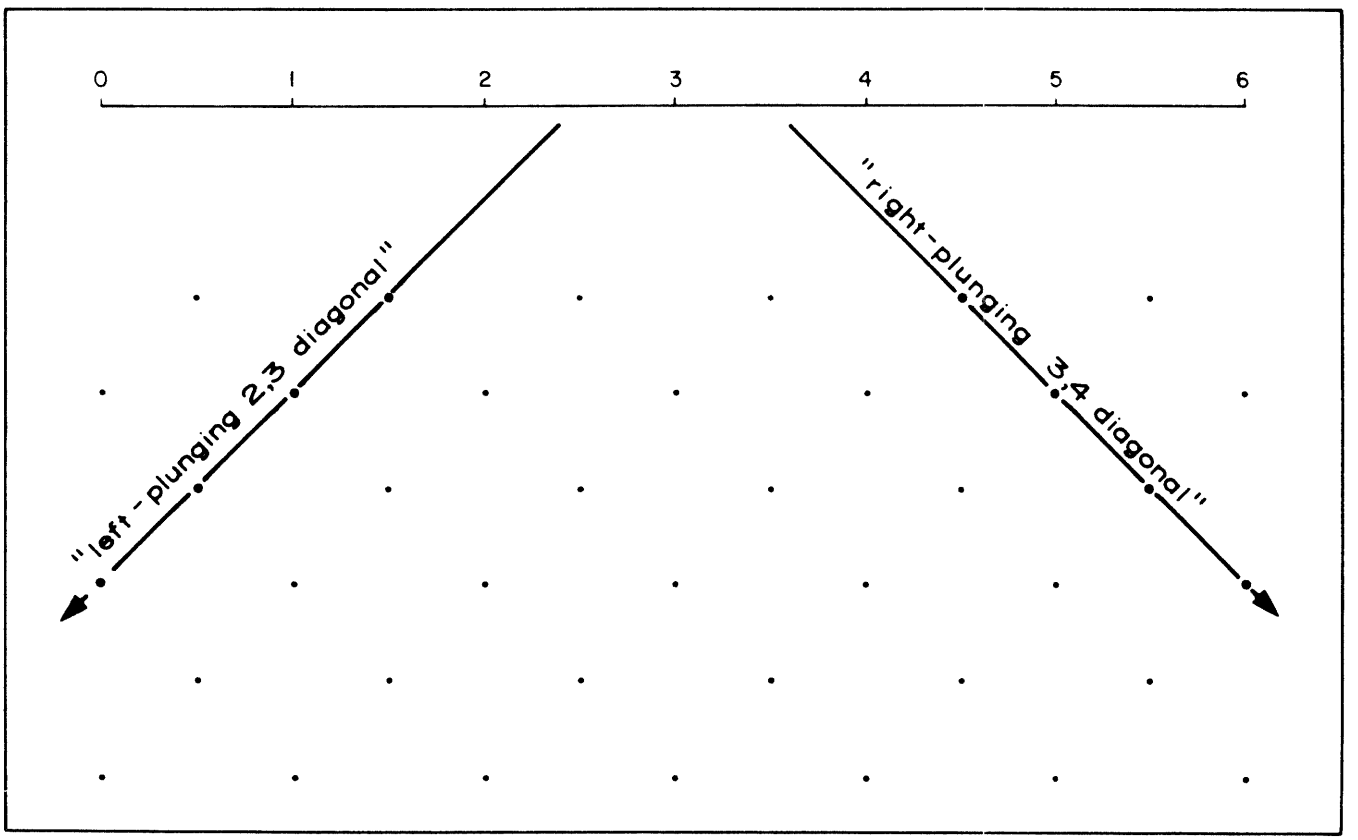

Figure 1.5. Meaning of "left-plunging" and "right-plunging" diagonals.

Tellurics

Tellurics are ground currents whose source is tied to pulsations of the earth's magnetic field and to interactions of the solar wind with it. The solar wind can be thought of as a plasma, composed of positrons and electrons, which is constantly radiated from the sun. The intensity of the solar wind is dependent upon the presence of disturbances in the sun's atmosphere which primarily fluctuate with the 11-year solar activity cycle.

The solar wind streams out from the sun and impinges upon the earth's magnetic field, forcing the field back into a plume-shaped feature. Changes in flux cause the field to pulsate, inducing an electromagnetic current which is transmitted into the earth via hydrodynamic oscillations along plasma-rich magnetic flux lines. Particles which are trapped by the field can be incorporated in the Van Allen radiation belts or can travel down the magnetic field axes near the poles. Interactions in the earth's atmosphere produce a cascade of charged particles, the EM effects of which are transmitted into the ground.

The wave motion of the solar plasma and the pulsations of the magnetic field occur at low to very low frequencies, each of which has higher frequency harmonic pulsations. Particle interactions produce their own range of wave frequencies. Telluric currents coupled into the earth therefore occur at a wide range of frequencies. Not all of these frequencies are observed, however, due to absorption by the ground. Since most telluric noise occurs in the RP/CR frequency range (DC to 100 Hz) and is noncoherent in nature, it cannot be filtered in an easy manner. Smooth, low frequency changes in ground self-potential can be partially removed from the data by digital telluric filters (referred to in this work as "moving average" filters) or

high-pass filters, and by coherent stacking and averaging of the received signal. However, due to the low frequencies used, coherent signal stacking can take an inordinate amount of time to filter out strong telluric signals. Tellurics in the 0.1 to 10 Hz range cause the most damage to data quality, and it is occasionally necessary to shut down a crew during a particularly active solar storm when the noise-to-signal ratio becomes intolerable.

Atmospheric Noise

Noise caused by lightning discharges and atmospheric shear pose the most serious threat to data quality in oilfield projects. The primary energy lies in the middle to higher frequencies (above 100 Hz), but lower-range beat frequencies are observed as well. The problem is both global and local. On a global scale, tropical storms give rise to an ionosphere/troposphere resonant noise called the Schumann resonances. These occur predictably in the RP/CR range, with the larger peak occurring at 8 Hz. On a local scale, storms contribute heavily to high-frequency pulses and tend to dominate global effects. The noise results from intracloud shear, intracloud electrical discharges, and cloud to ground discharges. The higher frequency components can be partially suppressed with low-pass filtering, but a problem arises when lightning strikes are nonrandom in nature. This can occur, for example, when a thunderstorm occurs on the south end of the survey line. Ground current from a lightning strike travels radially outward from the contact point on the ground; hence, the sense of current flow with respect to the survey line is south to north. In this case, the noise is nonrandom and it cannot be properly filtered by digital stacking techniques.

High frequency atmospheric noise has a much greater effect on phase data than on resistivity data, but both sets of data can be rendered practically useless by an especially active storm. Although acceptable data have been obtained in signal to noise ratios worse than 1:100, it is often not economical to do so.

Cultural Noise

The presence of man-made conductors (known as "culture") can introduce a great deal of harmful noise into the measuring process. The worst offender is usually power transmission line noise and its odd harmonics. In the United States, a frequency of 60 Hz is used, hence 60+180+540+ . . . cycle noise is observed, with each harmonic becoming progressively smaller in amplitude. Other frequencies, primarily 50 Hz, are used in other parts of the world. Although a notch filter can be used to remove the powerline frequency and its third harmonic, DC shifts in amplitude (usually related to changes in power load) can drastically reduce data quality.

Cathodic protection of collection pipelines often causes major problems, especially if the frequency regulation is poor. Frequencies are typically 120 Hz (half-wave rectified 60 Hz) but can vary considerably. It is usually advantageous to shut off the cathodic protection circuitry during the duration of a survey, if it is possible to do so.

Carrier signals of 400 Hz, sometimes used for railroad communications, are also encountered occasionally, as are various carrier frequencies on power transmission lines used for automatic load switching. High frequency noise from aircraft navigation signals, broadcast stations, and microwave communication networks is also encountered on occasion. These can usually be filtered by low-pass filters, providing that the signals are not strong enough to cause front-end saturation of the equipment. Front-end saturation can be detected by careful field checks.

Any cultural signal which changes the ground potential in an irregular or DC fashion cannot be filtered. DC shifts due to culture can result from two signals

beating together, from a signal which changes quickly in amplitude (e.g., load switching), from DC pumping equipment, or from underground mine equipment.

Noise-avoidance procedures used on the surveys in this volume are described in section 1.5.

1.4 INSTRUMENTATION

All of the data contained in this volume were acquired with the GDP-12 Geophysical Data Processor instrumentation system. The GDP-12 system has replaced the original Zonge Engineering field system, which consisted of a PDP-8 (registered trademark of Digital Equipment Corporation) computer, a two-channel cassette drive, a teletype, and a Zonge-designed, two-channel analog receiver. This truck-mounted apparatus had been used for complex resistivity measurements since 1972, and it was used to obtain full spectral data (0.1 to 110 Hz) in oilfield work during 1977 and 1978. Once the success of the initial experiments over known oilfields had been established, the PDP-8 system was replaced with the more portable GDP-12 equipment, and the work was advanced to a production basis. The first application of the GDP-12 in oilfield work was for resistivity/phase surveys, using a limited frequency range (0.125 to 1.0 Hz) and multiple receivers in order to boost the rate of data acquisition. Most of the data in this volume came from this phase of the work. By 1980, full complex resistivity programming and instrumentation were completed for the GDP-12, and most oilfield surveys have subsequently been conducted using harmonic analysis complex resistivity.

The GDP-12 is a two-channel, microprocessor-controlled receiver which detects, filters, and amplifies two input signals simultaneously, and which processes the data according to software developed specifically for the particular type of survey desired. Figure 1.6 shows a front panel view of the receiver type used for acquisition of oilfield data during 1979 and 1980. The analog section of the GDP-12 has a 500 megohm input impedance at DC, common-mode noise rejection of better than 60 dB at 2 kHz, and channel separation of better than 80 dB at 2 kHz. The receiver is capable of detecting signals as low as 0.2 microvolts. Amplification can be selected in binary intervals from 1 to 32,768 (2^{15}), allowing full 12-bit digitization of input signals between 300 microvolts and 10 volts.

The filtering system for the receiver consists of alias and notch filters. The alias filter is a four-pole, low-pass Bessel or Butterworth filter which is engaged automatically via software when the operator selects the frequency on the front panel thumbwheel. Notch filtering for standard receivers used in the United States is set for 60 and 180 Hz powerline noise. Rejection of better than 40 dB is provided with a Q factor of 2 to 5.

The analog-to-digital converter is a 12-bit CMOS device whose speed is 16,000 conversions per second. For resistivity/phase frequencies, up to 1,024 sample points are digitized per waveform. The digital section consists of two independent Intersil or Harris 6100 microprocessors utilizing 20k words of 12-bit random access memory.

The GDP-12 can be used either as a truck mounted or portable receiver. The unit is powered by self-contained, rechargeable 12-volt batteries which provide at least 12 hours of continuous operation under field conditions. Timing is controlled by a temperature-controlled quartz crystal oscillator whose stability is one part in 10^{-9} per 24 hours (after warm-up).

The transmitter used in these surveys was a Geotronics FT-20, which transmits a constant-current squarewave signal at up to 18 amperes. Maximum practical output voltage is 800 volts. Power is supplied by a trailer-mounted, 20 kw motor/

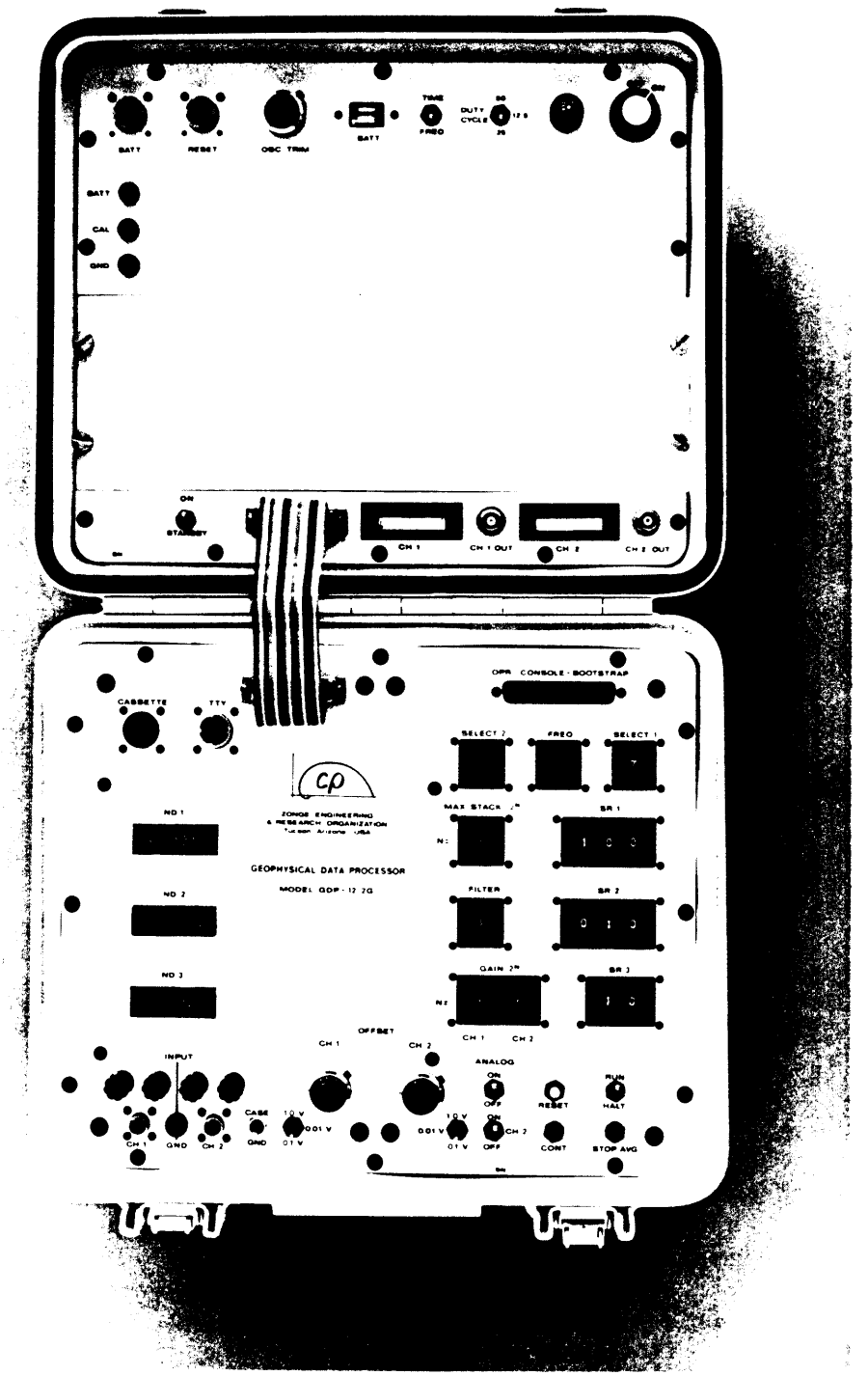

Figure 1.6. Front-panel view of the GDP-12 Geophysical Data Processor. The size of the opened unit is 14.0 x 23.5 inches (36.6 x 59.7 cm).

generator set built by Zonge Engineering. For resistivity/phase work, the timing of the transmitter is controlled by a Zonge Engineering transmitter controller, which has the same crystal oscillator and timing chain as does the GDP-12.

1.5 RESISTIVITY/ PHASE DATA ACQUISITION AND FIELD LOGISTICS

Survey Planning

The dipole length for a resistivity/phase survey is selected upon the basis of two criteria: the expected or known depth to the hydrocarbons, and the expected or known plan-view extent of the field. It is alteration overlying the hydrocarbons which is being measured (not the hydrocarbons themselves). Unfortunately, the depth to the alteration zone is not always predictable, but it often extends up the sedimentary section to about half the depth of the hydrocarbons. Hence, it is desirable to achieve penetration to deeper than half the estimated depth to the hydrocarbons to insure resolution of the overlying alteration. Assuming a depth penetration of REM data to 3 dipole spacings, this consideration suggests that the dipole spacing be greater than or equal to one-sixth that of the depth to the hydrocarbons. This is not a hard-and-fast rule, but it is useful in the planning stages. The areal extent of the hydrocarbons also helps fix the dipole size. Since the lateral resolution of a dipole-dipole survey is at best one-half the a-spacing, the a-spacing should be smaller than the width of the field. If the target is a prospect, a minimum economic field size should be assumed for planning purposes.

As an example, assume that a prospect is to be run in an area in which potential reservoir rocks are expected to be Pennsylvanian to Mississippian in age, at a depth of 7,000 to 9,000 feet (2,100 to 2,700 m). The geologist for the project might suggest that an economically interesting target would probably exceed 2,000 feet (600 m) in plan dimensional width. Hence, one would need to consider both a depth and a lateral size constraint. The depth constraint would fix a minimum a-spacing at around 2,000 feet (600 m), while the lateral size constraint would require that the a-spacing not exceed 1,500 feet (450 m) or so. One would therefore be tempted in this case to make the dipole size around 1,500 feet. This would probably be acceptable, even though the depth constraint is violated, since alteration is usually found well above half the actual depth to the hydrocarbons.

Under normal field conditions, the client provides sufficient information regarding the desired location of survey lines and the geologic nature of the field site to facilitate the permitting of the field site. Actual line location and permitting should be coordinated to minimize the effects of culture on the electrical measurements and lost production time due to restricted line access.

Upon arriving at the field site, the crew normally scouts the area in order to optimize line locations. The criteria which are considered include line access, topography, the location of prime geologic target areas, the location of major faults or steeply dipping geologic contacts, and the presence of culture. Obviously, line access and topography heavily influence the cost of a survey, since these variables can affect production rates. Topography can introduce complications in the interpretation of the data, and while such complications can often be adequately reproduced by computer modeling, it is best to avoid extreme topography if the option exists.

The locations of known major faults or linear contacts in the survey area should be considered when laying out the survey lines, since running directly over and parallel to such features can make interpretation of the data difficult or impossible. A good example of such an effect is found in the case history of Trap Spring, line 2 (Chapter 7).

Culture, in the form of well casings, pipelines, powerlines, and fences, can also have a major impact on the data. Ideally, the dipoles should run perpendicular to cultural features in order to minimize their effects on the data. An electrode should never fall near a cultural feature if such a situation is avoidable. The worst cultural offenders are, in general order of effect: grounded metal pipelines, well casings, grounded metal fences, powerlines, and telephone lines. An example of severe cultural contamination is found in the discussion of Little Buck Creek, line 1 (Chapter 5).

Setting up the Survey Line

Having selected the line locations and dipole spacing, the crew locates one end of the first line via section corners or other reliable landmarks. The line is surveyed with a hand-held Brunton (or equivalent) compass, and checks are continually made against a field topographic map in order to ensure the accurate plotting of the line location, as well as to determine the relative locations of wells and other culture.

The particular type of survey which was used to collect most of the data in this volume requires a crew of eight. Three persons are responsible for acquiring data from the three GDP-12 receivers on line. Two persons lay out the wires, stake electrode positions, and scout access routes for the transmitter truck, all in advance of the receiver stations. Two persons pick up wires behind the rest of the crew, and the eighth person operates the transmitter. Crew members are usually trained for any function on the crew, so that maximum flexibility is maintained in day-to-day operation.

As shown in Figure 1.7, two transmitting dipoles are utilized for a single set-up, with each of the three receivers measuring two potential dipoles. Transmitting electrodes consisting of long steel stakes are driven into the ground. The area surrounding the stakes is doused with saltwater to reduce the ground contact impedance, and the stakes are connected to each other with a medium-grade wire. An insulated, 14-gauge wire leads from each of the three transmitting electrode stations to the transmitter at the truck.

Potential electrodes are ceramic "pots," which consist of a copper electrode inserted into a saturated solution of copper sulfate. The pots are planted in small holes, and the surrounding ground is moistened with fresh water in order to reduce the ground contact impedance. Copper sulfate solution diffuses through the unglazed, porous bottoms of the pots, providing a direct but unpolarizable current path between the ionic conduction in the ground and the electronic conduction in the wires. Insulated wires lead from the potential electrodes to the analog input jacks of the appropriate receivers for measurement of ground potential.

Receiver Synchronization and Calibration

While several crew members are setting up the line, the others bring together the three GDP-12 receivers, a spare receiver, a master transmitter controller and a spare transmitter controller for synchronization of their crystal oscillators (Figure 1.8). Each oscillator has a frequency of 5 MHz, which can be trimmed by up to ± 0.3 Hz by means of an external potentiometer. A timing cable connects the master transmitter controller to a receiver, and the receiver oscillator is trimmed such that its beat frequency is identical to that of the controller's oscillator. This process is

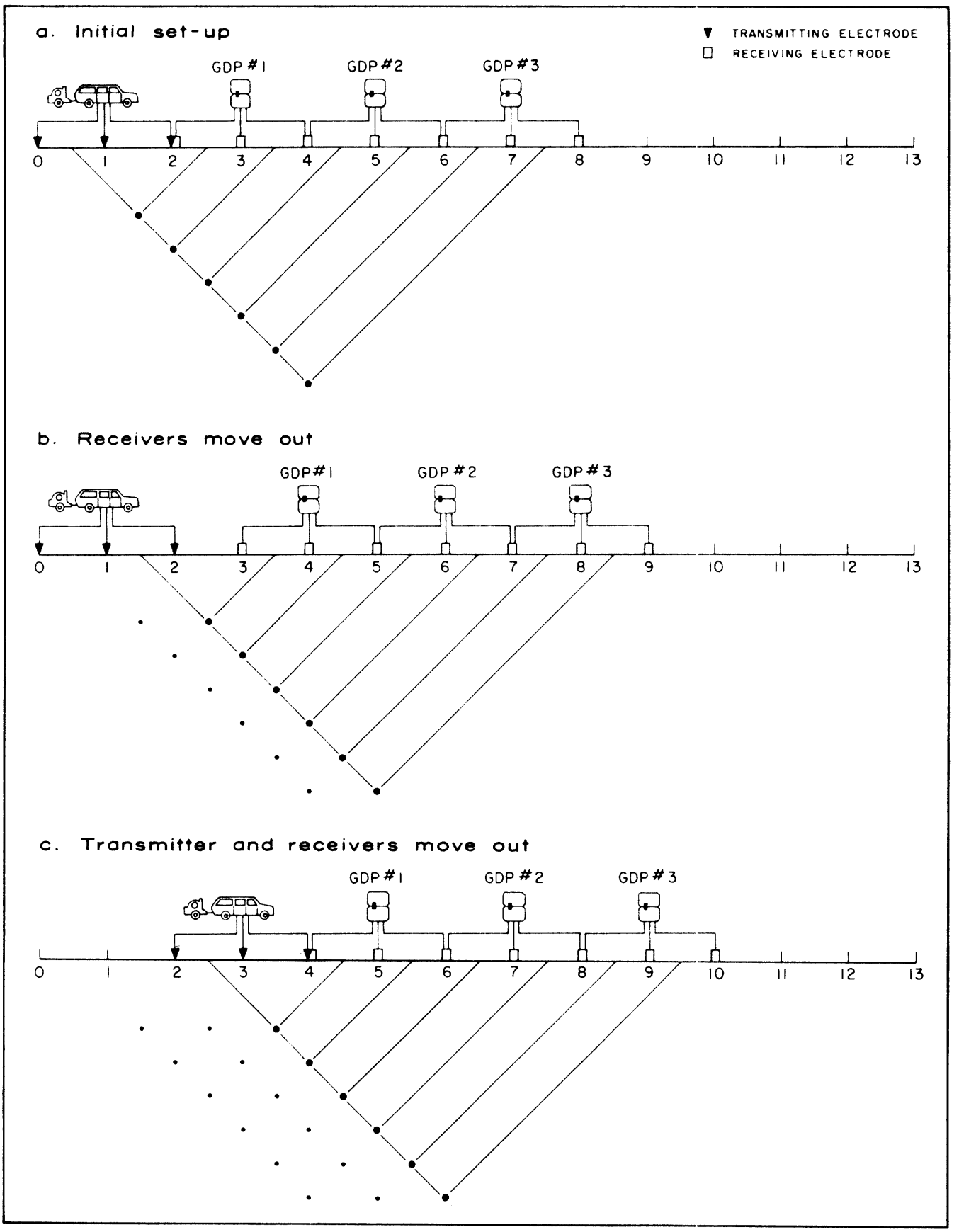

Figure 1.7. Logistical procedure in three-receiver, roll-along, resistivity/phase data acquisition.

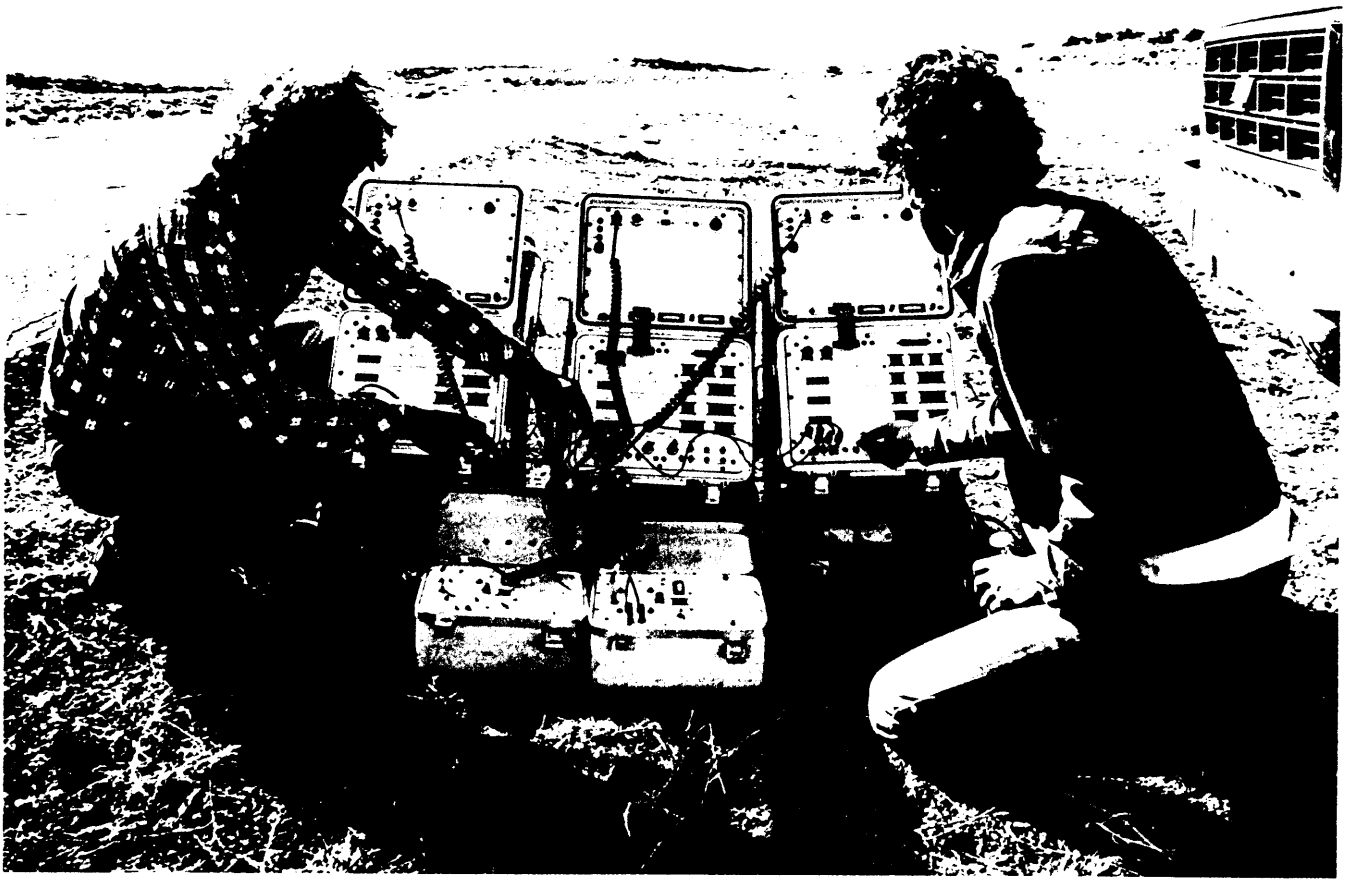

Figure 1.8. Synchronization of receivers at the start of production, Lisbon Field project.

facilitated by a display on the controller's analog meter of the beat frequency between the two oscillators. Each receiver and the spare controller is trimmed in this manner. The oscillator ports of all units are then connected to a junction box, and a reset button is pushed in order to synchronize all oscillators in time. Hence, with all oscillators beating at the same frequency and starting at the same time, they all have the same timing reference for accurate phase angle measurements. The oscillators are all oven-controlled in order to prevent desynchronization due to thermal effects, but other effects, primarily minor impurities in the crystal lattice structures, cause the oscillators to "drift" by up to ±0.2 milliradian at 1 Hz during a normal 10 to 14 hour field day. This lies within acceptable limits.

After the equipment is trimmed and synchronized, the receivers are calibrated using the internal signal of the master transmitter controller. This serves three purposes: it provides a check on the precision of synchronization, it establishes proper functioning of the equipment by repeating calibration values, and it provides an opportunity to store calibration values in memory for later removal from the field data.

Data Collection

After calibration, the three receivers are packed up and moved by truck or foot to the appropriate locations, as shown in Figure 1.7. The receiver nearest the transmitter truck is set up to read the n=1 and n=2 data, the middle receiver is set up to read the n=3 and n=4 data, and the far receiver reads the n=5 and n=6 data. The

n=5/n=6 receiver is the master receiver. Its operator is in charge of coordinating the data acquisition, since his data have the weakest signal and are most strongly affected by noise.

The transmitter operator is instructed to transmit current into dipole 0,1, at a frequency of 0.125 Hz. The current level depends upon the electrode resistance and the power range of the transmitter, but generally the maximum possible current is transmitted. Current linearity checks are done to confirm that the ground is not in a state of current saturation, that is, that it shows a strictly linear or ohmic response. This is done by measuring the voltage at two different currents, for example, at 18 amperes and at 9 amperes. If the ground function is linear, the receiver voltage at 9 amps should be half what it was with 18 amps, and the phase angle should be unchanged.

Examining the received voltage waveform on a portable oscilloscope, each receiver operator determines if noise levels are acceptable, verifies the proper operation of his equipment, determines appropriate gains, and selects the proper n-spacing, a-spacing, receiver station number, filter setting, and current level on the front panel thumbwheel registers. When the reset-continue button is pressed, the receiver begins to collect data automatically. The first waveform is digitized and stored in memory. Subsequent waveforms are digitized and added to memory, and with each successive addition, an averaged phase angle value and a standard error of the mean (SEM) value are displayed for channel 2 in the receiver's liquid crystal display window. This permits the operator to observe how well the data are converging. Data acquisition is stopped manually when convergence has reached an acceptable level, and the receiver proceeds to process the data automatically. A Fast Fourier Transform (FFT) is performed for each channel, apparent resistivity is calculated from the parameters selected on the thumbwheels, and phase angles are decalibrated. The final output is sent to a cassette/printer device, although it can also be recorded by hand. Output for each channel consists of raw magnitude, raw phase angle, apparent resistivity, decalibrated phase angle, and standard error of the mean.

This initial sequence of data collection is called a "stack." Several stacks are often taken to ensure sufficient data repeatability. Once all three receiver operators have obtained acceptable data, the master receiver operator instructs the transmitter operator to increment the frequency to 0.25 Hz. Stacking and averaging proceeds in a similar manner for the 0.25, 0.5, and 1.0 Hz data. Following this, the receivers are moved forward one a-spacing; data are acquired at n=1 to n=6 using dipole 1,2 as a transmitter dipole. The receivers are then moved forward one a-spacing, and the transmitting electrodes are moved forward two a-spacings. This procedure is repeated until adequate coverage has been obtained.

The crew chief is responsible for monitoring the data collection, and he keeps updated field pseudosections. This is done for several reasons. First, subtle problems and errors which have not been detected by the equipment operators can often be detected on pseudosections. Second, the pseudosections can be used to alter survey logistics as needed, depending upon the trends shown in the data. Third, the pseudosections are an invaluable aid to interpretation. Both the apparent resistivity and three-point decoupled phase angle can be used for interpretation in the field. REM data are not generated until after the data are returned to the office.

1.6 HARMONIC COMPLEX RESISTIVITY DATA ACQUISITION AND FIELD LOGISTICS

Data from two of the projects contained in this volume, Desert Springs (Chapter 4) and Garza (section 2.5), were obtained with a harmonic complex resistivity system in which squarewave current at a single frequency is transmitted and data at higher frequencies are calculated from a Fast Fourier Transform (FFT) of the waveform. The instrumentation is somewhat similar to that used for resistivity/phase. The GDP-12 receiver is merely programmed for complex resistivity data acquisition, and the necessary peripheral devices are added to the field set-up. The field data are very similar to the resistivity/phase data; only the frequencies at which they are acquired are different.

The advantages of harmonic data acquisition are two-fold. First, it is much faster, since data are not acquired discretely at every frequency desired, but are calculated from the measured waveform. A complex resistivity system acquiring harmonic data at 0.125, 0.375, 0.625, 0.875, 1.125, and 1.375 Hz on one dipole is about twice as fast as an equivalent, single-receiver resistivity/phase system acquiring discrete frequency data at 0.125, 0.25, 0.5, 1.0, and 2.0 Hz on two dipoles. The second advantage of complex resistivity is that any output irregularities in the transmitted waveform are monitored and deconvolved from the data. This is of crucial importance; many of the resistivity/phase surveys run in the past have been plagued by current instabilities from the effects of geology on the transmitter electrodes, resulting in peculiar diagonal effects. Such effects may be hand-corrected at times, but this process is tedious and injects unwanted elements of ambiguity into the data.

Instead of reading data with a receiver placed directly at the receiving dipole, as in resistivity/phase, the receiver and transmitter are mounted in a recording truck for complex resistivity work. The voltage drop across a remote receiving dipole is sensed by a small preamplifier, which also provides some noise rejection; the signal is sent down a communications cable (the analogue of a seismic cable) to the receiver in the recording truck. The cable replaces the crystal oscillator for purposes of synchronization of transmitted and received signals.

Setting Up the Survey Line

As with resistivity/phase work, a dipole-dipole array is used for complex resistivity. There are two modes of operation, and which one is used depends upon terrain, truck access to the line, etc. The two methods of operation are shown in Figures 1.9 and 1.10. The "roll-along" mode (Figure 1.9) involves a set-up similar to roll-along resistivity/phase. Three to seven transmitting electrodes are set out, and data are obtained one dipole at a time in a forward direction. After the receiver dipole has been advanced sufficiently to obtain the first "spread" of pseudosection data, the transmitting electrode array is advanced, and the survey continues in this fashion. The second mode (Figure 1.10) is called the "center-spread" mode. This involves setting up seven to ten transmitting electrodes, with the transmitting truck at the center of the spread. Data are obtained first on one side of the spread by advancing the receiving dipole from the center to well past the last transmitting electrode; the receiving dipole is then flipped to the other side and data are obtained by moving the receiving dipole in a reverse direction. Suitable repeat points are obtained to check the effects of reversing the relative positions of transmitting and receiving dipoles (this is called a reciprocity check).

As a matter of convenience, the center-spread mode is described in detail in this discussion, although the same principles apply almost universally to the roll-along mode. The field layout is illustrated in Figure 1.11.

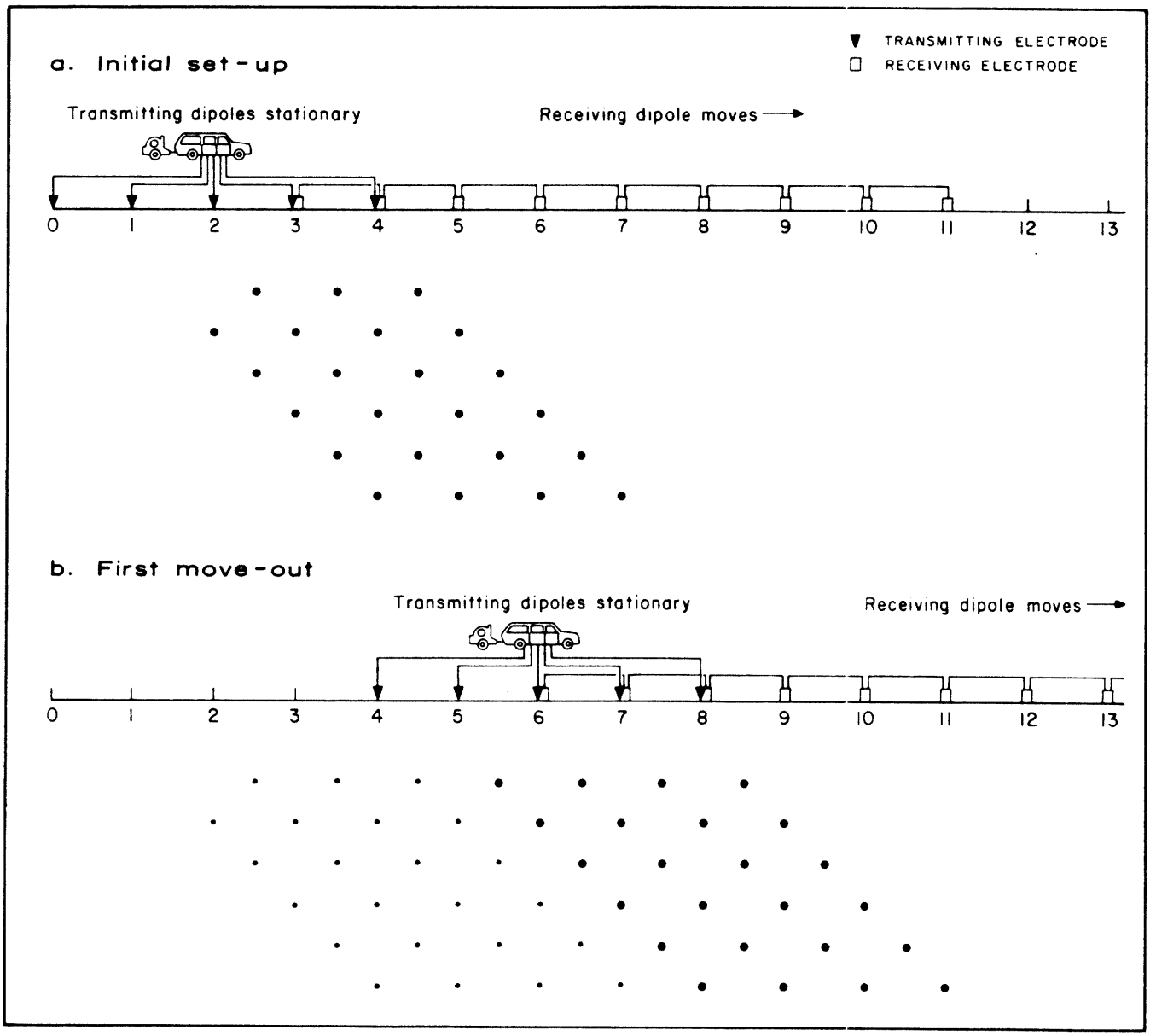

Figure 1.9. Logistical procedure in roll-along complex resistivity data acquisition.

Receiver Calibration

While the wires are being set out by the line crew, the crew chief assembles the GDP-12 instrumentation for a system calibration. This is done to confirm proper system operation and is performed every day prior to data acquisition. The goal in this procedure is to measure the resistance and phase shifts of the system for later removal from the data. A low-current squarewave signal, obtained from the GDP-12 receiver lid, is split into a single-ended and double-ended output via a voltage divider box. The double-ended (differential) signal is fed through a field preamplifier and isolation amplifier combination into channel one of the GDP-12 (this is the side that monitors the field signal). The single-ended source is fed through the isolation amplifier and into channel two of the GDP-12 (this is the side that monitors the transmitted signal). The two waveforms thus pass through similar electronic paths and through the same array of amplification and filtering devices into the GDP-12. In

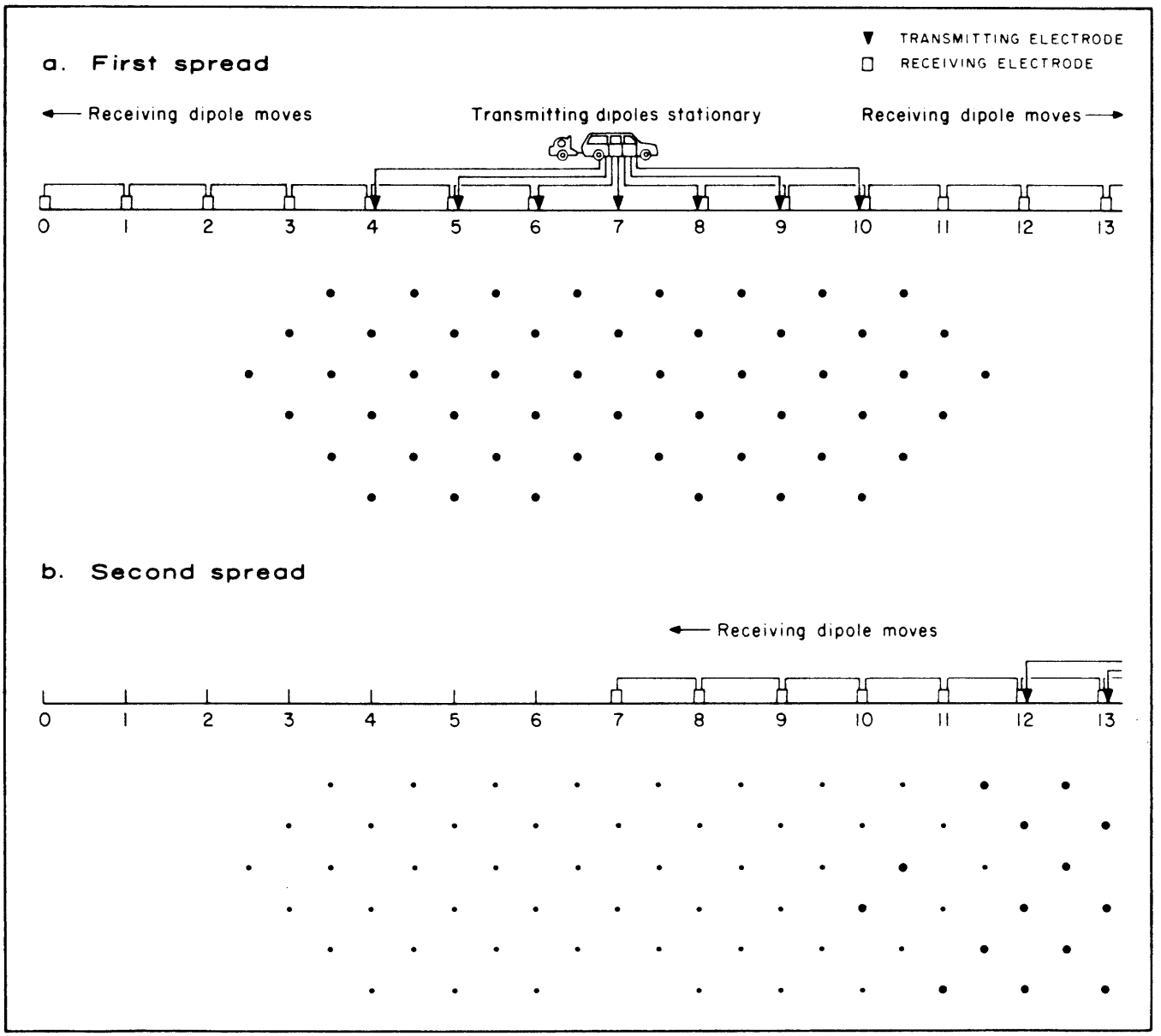

Figure 1.10. Logistical procedure in center-spread complex resistivity data acquisition. Several data points are often repeated between multiple spreads in order to provide a check of data continuity and reciprocity.

order to find the minor differences in the two paths (due to filtering in the field preamplifier and slight differences in electronic components), the two waveforms are deconvolved, as they are in the field measurements, with voltages being divided and phase angles subtracted. The deconvolved magnitude/phase data are known as the final system calibration, and are stored and later removed from the field data.

Field Processing Techniques

Two standard signal processing techniques are used in data acquisition: the Fast Fourier Transform (FFT), and deconvolution. While both of these are described in standard electrical engineering texts, a brief treatment is provided here for the benefit of the reader.

The FFT is a method by which a periodic signal may be represented by the sum of a series of sinusoids. A squarewave, which is normally used in complex

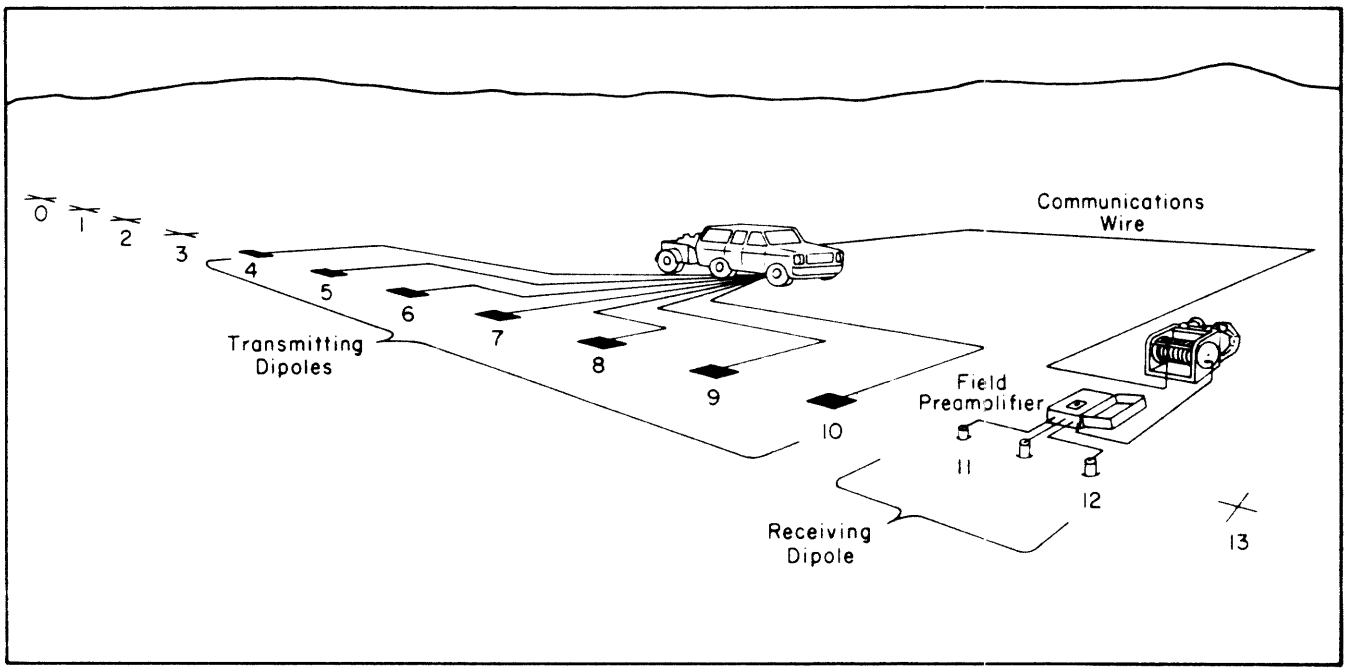

Figure 1.11. Field layout of a center-spread complex resistivity survey.

resistivity work, can be represented by the sum of a series of odd Fourier harmonics:

$$V = A \sin \omega t + \frac{A}{3} \sin 3\omega t + \frac{A}{5} \sin 5\omega t + \cdots \frac{A}{n} \sin n\omega t + \cdots \qquad (1.1)$$

(n odd)

in which V is the voltage or amplitude of the squarewave, $A=4/\pi$ is the amplitude of the first Fourier harmonic (i.e., the first term in the equation), ω is the angular frequency, and t is some arbitrary point in time. The first term is the first Fourier harmonic, or fundamental; the second term is the third harmonic, the next term is the fifth harmonic, and so forth. The even harmonics are zero for an ideal squarewave. Note that each successive harmonic is decreased in amplitude by the inverse of its harmonic number. Figure 1.12 shows the squarewave and its first few odd harmonics; if all harmonics are added together, their sum takes on the appearance of the original squarewave.

Since the nth harmonic has a frequency of n times the fundamental frequency, one can see that, by transmitting a squarewave with a frequency of f, one can use the FFT to obtain amplitude and phase data for frequencies f, 3f, 5f, . . . nf. In other words, instead of transmitting and receiving data at every frequency desired, a single frequency is transmitted and a suite of data at higher frequencies is obtained automatically. The only limitation to this approach is that, since harmonic amplitudes decrease according to their harmonic number, the signal to noise ratio becomes much worse for the higher harmonics. In practical applications, harmonics 1 through 11 are normally obtained; harmonics higher than the 11th are too noisy to be obtained economically.

The lowest frequency normally used in complex resistivity work is 0.125 Hz. From this, data at frequencies of 0.125 to 1.375 Hz are obtained. In order to extend this range to higher frequencies, fundamental frequencies of 1.0 Hz and 8.0 Hz are

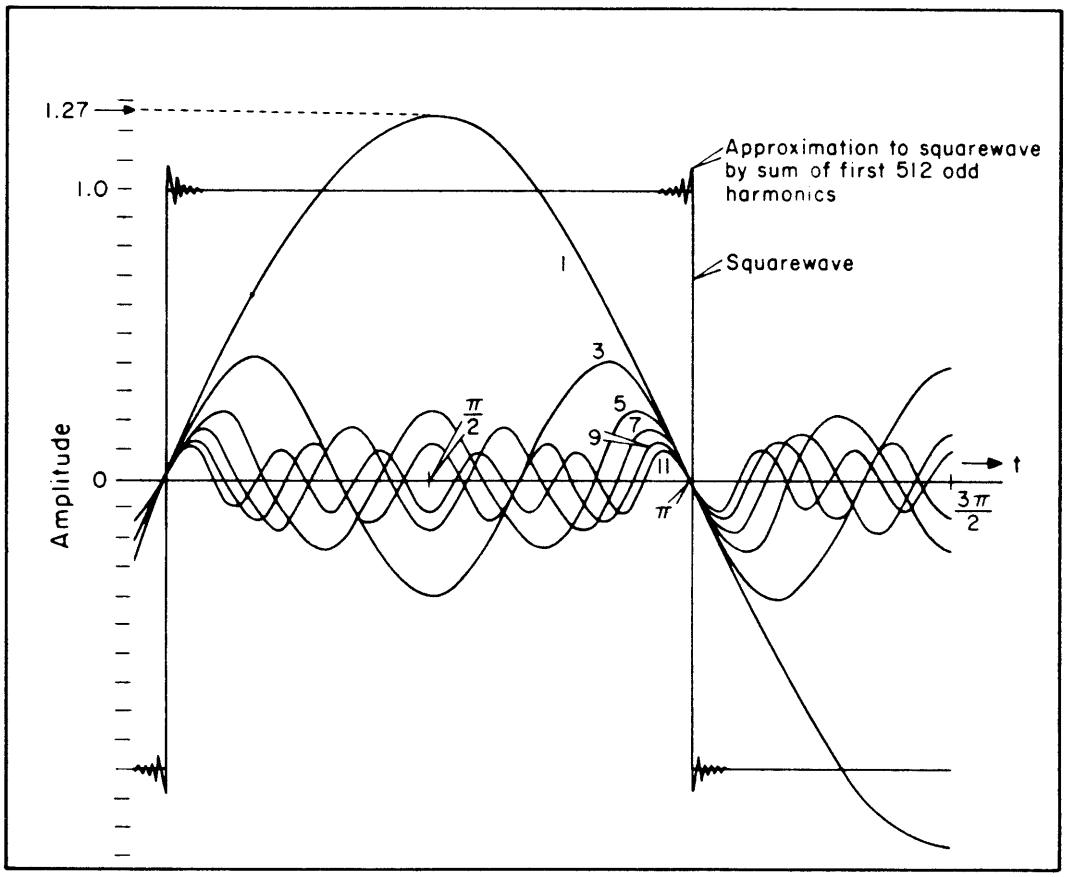

Figure 1.12. Representation of a squarewave by a series of odd Fourier harmonics.

also used, and non-zero odd harmonics from 1 to 11 are obtained for each of these. The result is a discrete frequency spectrum from 0.125 to 88 Hz, composed of three "blocks" of data (Table 1.1). The overlap between these "blocks" allows for a check of data quality through "bracketing."

Deconvolution is a process by which a given effect present in two Fourier transformed signals is removed from them by division. In complex resistivity, the squarewave signal transmitted into the ground is measured on channel 2 of the receiver, and the squarewave voltage which has been modified by the ground's electrical characteristics is measured on channel 1. While the original squarewave is needed to initiate a ground response, this waveform itself is of no interest to us, and

TABLE 1.1: COMPLEX RESISTIVITY FREQUENCIES

	0.125 Hz Data Block	1.0 Hz Data Block	8.0 Hz Data Block
Fundamental frequency	0.125 Hz	1.0 Hz	8.0 Hz
3rd harmonic	0.375	3.0	24.0
5th harmonic	0.625	5.0	40.0
7th harmonic	0.875	7.0	56.0
9th harmonic	1.125	9.0	72.0
11th harmonic	1.375	11.0	88.0

it must be removed from the total received response. This is accomplished by deconvolution, in which the Fourier transform of the received voltage is divided by the Fourier transform of the transmitted current, and the transmitted phase angle is subtracted from the received phase angle. The result of this is what we want: the ground response, or transfer impedance, for a given frequency.

Deconvolution serves another very important purpose. Any current or phasing instabilities due to the transmitter or due to peculiar electrode effects will be reflected in the received data; they will also be present in the data from the transmitted waveform. By deconvolving received and transmitted data, these effects will be removed. In making milliradian-accuracy measurements, this process is indispensable.

Data Collection

Following calibration, the field preamplifier is moved to the center of the receiving dipole. Three porous pots, planted at the ends and the center of the dipole, are connected to the preamplifier input. The signal is measured across the end pots; the center pot is used for common mode noise rejection. The crew checks proper preamplifier operation, selects a gain of 1 or 10, and determines the pot contact resistance. The communications cable, which has been laid out between the recording truck and the receiving dipole, is connected to the preamplifier.

Setting up the equipment in the recording truck, the crew chief disengages all filtering at the GDP-12 and examines the natural ground noise via a two-channel portable oscilloscope. This provides a check on types of noise present and provides information necessary to avoid signal saturation. Next, current is transmitted into one of the transmitting dipoles at the highest fundamental frequency being used on the survey, which typically is 1 or 8 Hz. After both the received and transmitted waveforms are carefully examined on the oscilloscope, appropriate filtering, gains, current level, n-spacing, a-spacing, and receiver station number are selected on the front-panel thumbwheels of the GDP-12. Stacking and averaging is then commenced by pressing the reset and continue buttons. Each successively measured waveform is digitized and is added to memory, and real-time raw phase angle and standard error of the mean values are calculated and displayed on the GDP-12's liquid crystal displays. These values are used to determine proper convergence of the data; stacking and averaging is terminated manually by the crew chief when data of the required precision have been acquired. The data set obtained from this process is called a "stack."

After termination of data collection, the GDP-12 begins processing the data. The digitized, summed waveforms are divided by the number of stacks in order to determine the averaged waveform, and a fast Fourier Transform is performed to obtain the harmonic data. The harmonics for the received and transmitted waveforms are then deconvolved, harmonic-for-harmonic, in order to derive the ground response, which is independent of the type of waveform. The apparent resistivity is calculated and all the input parameters and harmonic data are recorded on a minicassette and on paper by an electrostatic printer. The operator determines the quality of the data by examining the smoothness of the data changes and by examining the bracketing between data blocks, and by monitoring the real-time standard of the mean calculation provided for 0.125 and 1.0 Hz. At the outset of the project, a second stack is usually taken in order to relate absolute repeatability to the smoothness, bracketing, and standard of the mean checks.

Once acceptable data have been obtained, the next-lowest fundamental frequency is selected. Data are taken as before, and once data at all the required

frequencies have been obtained, the next transmitting dipole is selected. The process is continued until the desired pseudosection coverage has been obtained.

The crew chief keeps an updated data inventory list and updated pseudosections as the data are acquired in order to identify problems, and to provide preliminary in-the-field interpretation of the results.

1.7 CONTROLLED SOURCE AMT DATA ACQUISITION AND FIELD LOGISTICS

Description of the Technique

Having been used in massive sulfide detection for more than five years, the controlled source audiofrequency magnetotellurics (CSAMT) technique was applied to petroleum exploration in 1982. This technique is substantially different from resistivity/phase or complex resistivity.

While it is beyond the scope of this project to describe the CSAMT technique in detail, a brief discussion is provided in order to familiarize the reader with the basic principles. As shown in Figure 1.13, a long transmitting dipole is laid out on the ground several miles away from the site to be investigated. Four quantities are measured: 1) the potential drop across a grounded electric dipole which is oriented parallel to the transmitting dipole, 2) the magnetic field pickup in an antenna which is oriented perpendicular to the transmitting dipole, 3) the phase lag of the electric field waveform with respect to the transmitted waveform, and 4) the phase lag of the magnetic field waveform. The ratio of the horizontal electric field

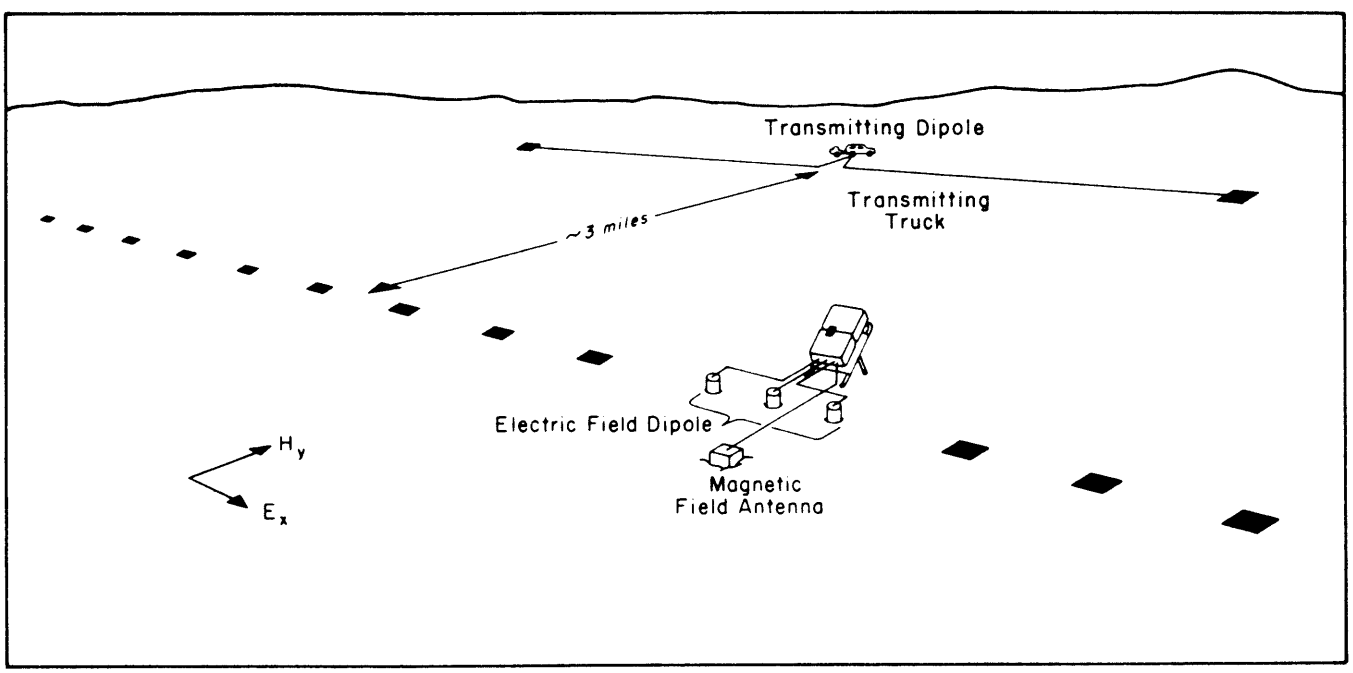

Figure 1.13. Field layout of a CSAMT survey.

voltage (E_x) and the perpendicular, horizontal magnetic field strength (H_y) is related to the apparent resistivity (ρ) of the ground at a given signal frequency (f):

$$\rho = \frac{1}{2\pi f \mu_0}\left(\frac{E_x}{H_y}\right)^2 \tag{1.2}$$

The depth of penetration is related to skin depth (δ), which is given by equation (9.87):

$$\delta = 503\sqrt{\frac{\rho}{f}} \quad \text{(meters)} \tag{1.3}$$

Equation (1.3) shows that signal penetration increases with lower frequency signals and with higher resistivity ground. In contrast with resistivity/phase and complex resistivity techniques, penetration is not affected by geometric factors (i.e , dipole sizes or separations), since the ground sensed by the dipole-antenna combination is being subjected to a near-plane wave from the distant transmitter. As a result, the CSAMT pseudosection is not affected by diagonally-controlled geometric effects which are seen in dipole-dipole pseudosections.

CSAMT has a distinct advantage in that lateral resolution across a traverse is approximately equal to the size of the electric dipole. By using a sufficiently small dipole, the boundaries of a buried conductive or resistive feature can be determined to within a few feet. The chief disadvantage of CSAMT is that, at this time, it is difficult to determine accurate depth to a responsive zone when it falls within the "near-field" or "transition" frequency zones of CSAMT data acquisition. Computer modeling may eventually help resolve this problem.

Controlled source AMT differs in several respects from natural source MT methods, which have been used with mixed success in structure mapping for petroleum applications over the past three or four decades. The chief difference is that CSAMT has a dependable fixed signal source, while MT does not. This accounts for the enormous cost difference between the two systems: while a single MT station may require up to a day of data collection, CSAMT stations typically require less than 45 minutes. The CSAMT method also has a shallower penetration—typically less than 10,000 feet (3,000 m)—while MT penetrates up to many miles. Hence CSAMT is better suited to examining the alteration patterns which exist in sediments overlying hydrocarbon traps. CSAMT also requires a far less sophisticated and less expensive data acquisition system. The GDP-12 system is used for all data acquisition.

CSAMT Pseudosections

Apparent resistivity is the primary parameter of interest in CSAMT work. This is plotted as a function of signal frequency versus station number in pseudosection form, as shown in Figure 1.14. The rationale behind this approach is found in equation (1.3): higher frequencies result in shallower penetration, so the pseudosection is plotted with high frequency data at the top and low frequency data at the bottom.

Further Information

More detailed information on CSAMT can be found in the work of Goldstein and Strangway (1975), Zonge, Emer, and Ostrander (1980), Ostrander (1981), Bartel (1982), and Sandberg and Hohman (1982). An informational brochure (Zonge Engineering, 1981) describes the field logistics used by Zonge Engineering.

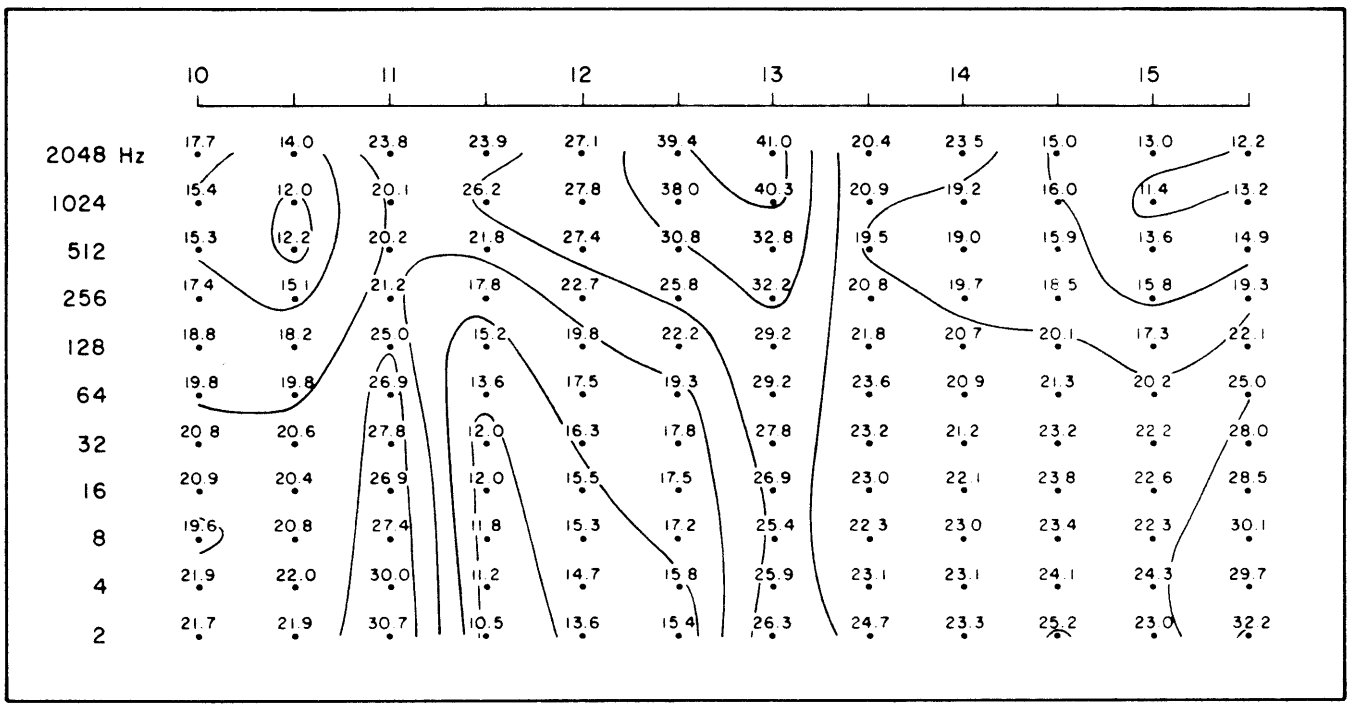

Figure 1.14. Apparent resistivity data from CSAMT data over Cowboy Field, San Juan County, Utah. Contour interval: 10.0, 12.6, 15.9, 20.0, 25.1, 31.6, 39.8 ohm-meters.

1.8 DATA PROCESSING TECHNIQUES, RESISTIVITY/ PHASE AND COMPLEX RESISTIVITY DATA

Interfacing with the PRIME 750

Data are sent to the office by registered mail on a biweekly basis. The field data are stored on cassette tapes and electrosensitive paper; "inventory sheets" are kept as notes on acquisition of the data.

Cassette data are read into the memory of Zonge Engineering's PRIME 750 by means of a cassette reader device. A number of checks are made to ensure the proper transfer of the data. The bulk of the resistivity/phase data presented in this volume was obtained during the development of the CAP-12 Cassette/Printer, and consequently these data were recorded by hand. This required manual entry of the data into the computer.

Editing and Pre-Processing

Upon transfer of the raw data to the PRIME, a thorough check of data quality is made by data processing personnel. Data glitches and inconsistencies are corrected, incompletely transferred data blocks are identified, and the magnitude and phase data are averaged to produce a final set of raw data. These data are then decalibrated, and, if the data were acquired by means of complex resistivity, a correction factor is made for the resistance of the communications wire.

The apparent resistivity at 0.125 Hz is calculated for the dipole-dipole array data from equation (9.55):

$$\rho_a = \frac{V}{I} \pi an\ (n+1)\ (n+2) \qquad (1.4)$$

in which V is the voltage measured across the receiving dipole, I is the transmitted current, a is the dipole size, and n is the dipole separation. Corrections for gain settings are made automatically.

Decoupling the Field Data

At this point, the data consist of magnitude and raw phase angle measurements for each frequency obtained on the survey. The raw phase angle data consist of two distinct responses: induced polarization and electromagnetic coupling. In order to make use of these two responses in interpretation, they must be separated from each other. The processing required for this separation is called "decoupling."

As explained in section 9.8, decoupling is a very difficult process. The exact solution of the complex impedance equation is essentially untenable, so the normal approach is to make a few initial assumptions about the response of the earth and to invert the data iteratively by means of theoretical and empirical constraints. One of two types of solutions are normally obtained for Zonge Engineering data. The first is a "quick solution," which employs a quadratic extrapolation approach of the type developed by Kennecott and published by Hallof (1974). The second is a more exact solution developed and held proprietary by Zonge Engineering (Wynn and Zonge, 1975). All data which are presented in this volume have been decoupled by means of the latter technique.

QUADRATIC EXTRAPOLATION SOLUTION

The quadratic extrapolation technique is an arbitrary graphical approach which makes use of three assumptions: 1) induced polarization phase response is constant (independent of frequency) and is defined at DC; 2) electromagnetic coupling varies smoothly with frequency and is exactly zero at DC; 3) the two effects are additive. A fourth, implied assumption is that the extrapolation occurs over a relatively unchanging portion of the complex plane curve, and that the total coupling phase shift is relatively small (e.g., less than 100 milliradians).

Figure 1.15 shows the basic approach. A quadratic fit is made using data at three low frequencies on the curve, and an extrapolation is made to DC. If the extrapolated value is zero, the curve is assumed to be generated by electromagnetic coupling exclusively. If the extrapolated value is non-zero, the curve is assumed to be generated by both electromagnetic coupling and polarization, and the DC extrapolated value is supposed to represent the polarization response at DC. The equations used for the extrapolation are developed in section 9.8. For the resistivity/phase frequencies, which differ by binary intervals, the 3-point extrapolation equation is:

$$\phi_c = \frac{8}{3}\phi_{.125} - 2\phi_{.25} + \frac{1}{3}\phi_{.50} \qquad (1.5)$$

in which:

ϕ_c is the three-point phase angle
$\phi_{.125}$ is the phase angle at 0.125 Hz
$\phi_{.25}$ is the phase angle at 0.25 Hz
$\phi_{.50}$ is the phase angle at 0.50 Hz

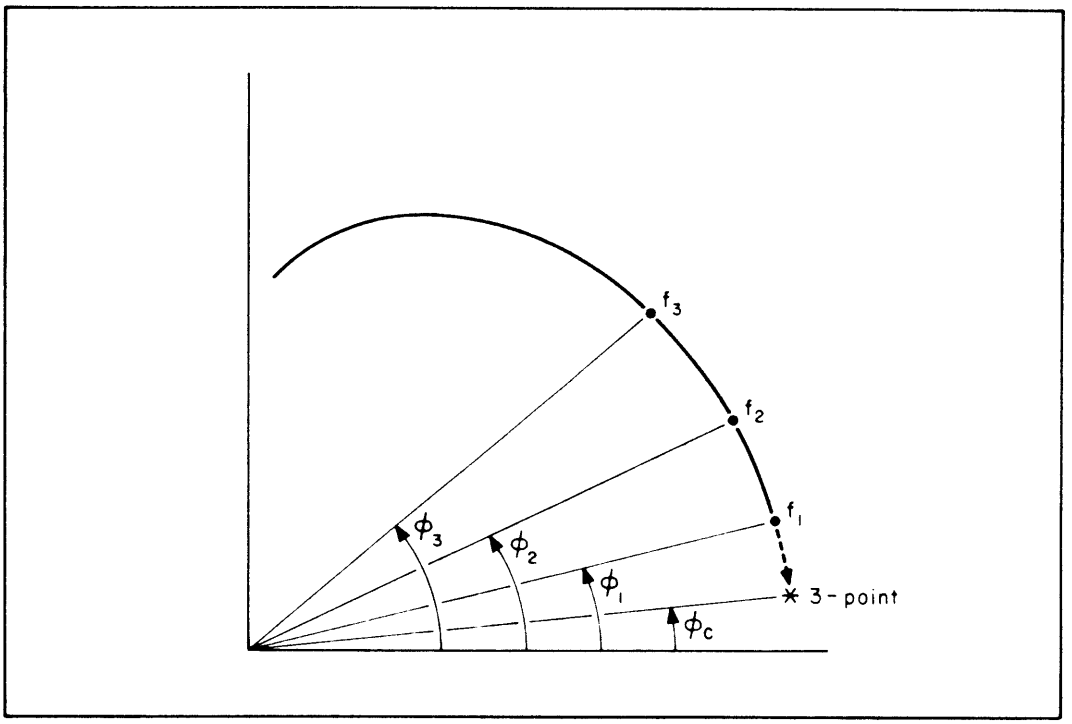

Figure 1.15. Three-point quadratic extrapolation.

In order to determine the separate polarization and coupling values at all frequencies, the polarization value is assumed to be independent of frequency, and the three-point value is subtracted from coupling values at each frequency. This approach has obvious drawbacks, since the inherent frequency response of polarization is ignored.

While the quadratic extrapolation technique is useful for a quick look at gross changes in polarization effects at a single frequency, it almost always produces either an artificial undercorrection or overcorrection to the data. An example of this is provided by examining the coupling for a dipole-dipole array over a homogeneous earth. An electromagnetic coupling routine called "TWOLAY" was used for this purpose, using a standard dipole spacing of 2,000 feet (610 m) and a ground resistivity of 30 ohm-meters. Only electromagnetic coupling effects were included; the ground was assumed to be nonpolarizable and homogeneous.

Three-point extrapolations of data at 0.125, 0.375, and 0.625 Hz were made for coupling curves at n-spacings of 1 through 6. Now, if the three-point extrapolation were correcting properly for coupling, we would expect all extrapolated values to be zero, since no polarization is assigned to the homogeneous half-space. However, the three-point data calculated from the model results are all non-zero, increasing in value from 0.4 milliradians at n=1 to 21.8 milliradians at n=6. This produces an artificially layered effect when plotted in pseudosection form, an effect which would artificially enhance an isolated polarization anomaly, as well as making it appear to be lower in the pseudosection than it really is. The reason for the failure of three-point calculations to match expected values is related to the non-validity of the fourth assumption behind the technique, i.e., the phase shifts are too large to be valid for a small angle approximation. Figure 1.16 illustrates the difference between the n=1 and n=6 extrapolations. For n=1, the coupling curve is small since the geometric separation is small (refer to section 9.8), and extrapolation occurs along

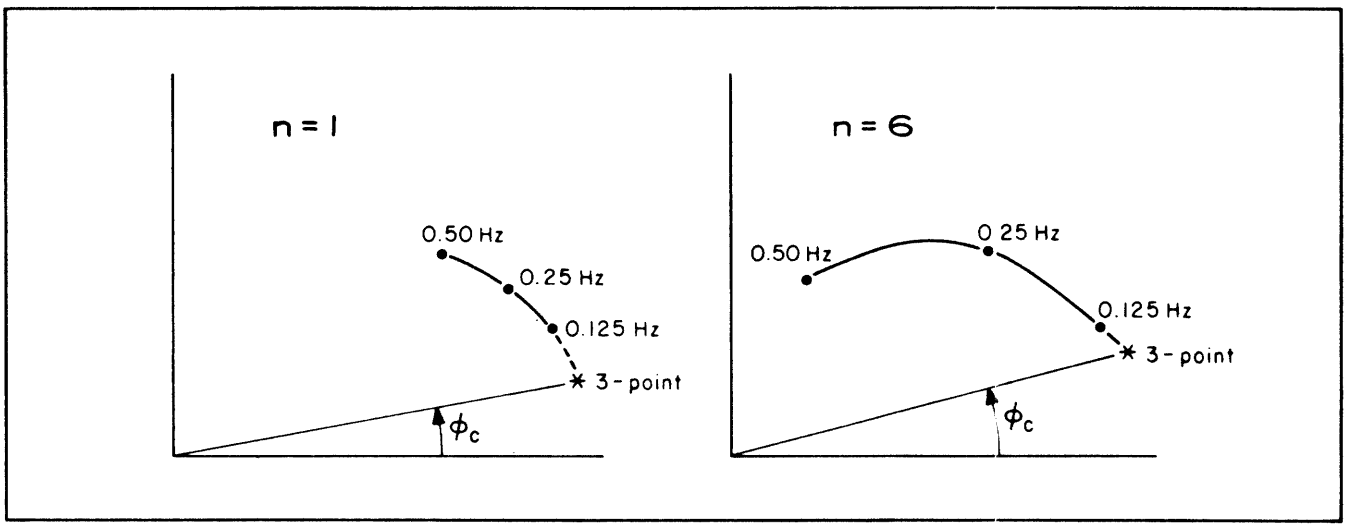

Figure 1.16. Comparison of the extrapolated 3-point phase angles for n=1 and n=6 on an arbitrary coupling curve.

the more linear portion of the curve. However, at n=6, the coupling curve is greatly extended due to the larger geometric separation, and the extrapolation is made from data points on the strongly curved portion of the coupling curve, resulting in an "undercorrection" or stronger residual phase calculation. The situation is even worse in high-over-low resistivity layering, where the coupling curve is even more strongly curved.

In-house research has shown that many subtle, polarizable anomalies over oil and gas fields can be lost in the three-point layering effect, especially in geologically complicated environments. As a result, it is advisable to use the more exact technique for decoupling the field data. Additional frequencies are usually required for this approach.

ZONGE ENGINEERING DECOUPLING TECHNIQUE

At this point, it would be useful for the reader to review the discussion of electromagnetic coupling in section 9.8. The following approach was developed by Ken Zonge in early 1973, and has been used successfully for mining and petroleum applications. The descriptions and explanations of the decoupling technique are provided solely for the understanding of the reader and are considered to be held under the proprietary agreement under which this volume has been distributed.

The sequence of decoupling is: 1) establish starting parameters of magnitude and phase angle, 2) select the number of levels or resistivity layers upon which to iterate, 3) curve-match the starting parameters with the field data until an acceptable decoupled response curve has been established.

The first step in decoupling is to establish initial IP parameters. The magnitude (M) and phase (ϕ) are determined by:

$$M = e^{-\frac{2\phi}{\pi} \ln \omega} \tag{1.6}$$

$$\phi = \phi_c \tag{1.7}$$

in which ω is the angular frequency and ϕ_c is the three-point extrapolated phase angle.

A layered-earth model is run in order to establish the minimum number of major resistivity layers which fit the apparent resistivity and electromagnetic coupling data. Usually the number of layers (i) is kept to one or two for the initial iterations, and is expanded to more than two if needed. The so-called coupling coefficients (CCi) for each layer (i) are roughly correlatable to resistivity contrast at each interface. The first coupling coefficient (CC1) determines the first level of layering:

CC1 > 1	low-over-high interface
CC1 $= 1$	homogeneous earth
CC1 < 1	high-over-high interface

The second through fifth coupling coefficients determine additional levels of layering:

CC2-5 > 0	low-over-high interface
CC2-5 < 0	high-over-low interface

The extension of the coupling curve (θ) which results from each layer is given by

$$\theta = 8.564 \times 10^{-4}\, a\sqrt{\frac{f}{\rho_i}} \tag{1.8}$$

in which a is the dipole spacing and ρ_i is the resistivity of the ith-level layer. The magnitude and phase angle are given by

$$M = e^{-x} \qquad X = \frac{2\phi_c}{\pi}\left[\ln \omega + \frac{A}{1+q}\left(\ln \frac{\omega}{\omega_{.125}}\right)^{1+q}\right] \tag{1.9}$$

$$\phi = \phi_c\left[1 + A\left(\ln \frac{\omega}{\omega_{.125}}\right)^{q}\right] \tag{1.10}$$

in which $\omega_{.125}$ is the angular frequency at 0.125 Hz. The quantities "A" and "q" are the Hilbert transform slopes, which are empirically determined. These quantities specify the shape of the iterated polarization curve.

Decoupling consists of an inversion routine which fits the starting data (layered-earth coupling plus Hilbert transform) to the raw field data in an iterative fashion. The success of the iterative process is determined by comparing the results to empirical observations of responses observed in field and laboratory measurements. The simplest initial assumptions which yield a successful inversion are adopted as the final solution. If an acceptable polarization response curve is not obtained, the complexity of the initial assumptions is increased until a proper inversion is achieved. Hence, decoupling results are not unique in a strict sense, but they represent the simplest possible solution which adequately fits the field data.

Calculation of REM Data

Following the decoupling process, four parameters are available for interpretation: apparent resistivity, apparent polarization as a function of frequency (spectral type), coupling coefficients, and total electromagnetic coupling data. In typical petroleum projects, the coupling data make up most of the response. The bulk of this response is simply the general response one would see using a large dipole array over a homogeneous earth with low resistivities. Hence, it would be useful to remove the homogeneous response from the total response in order to yield a residual response which is indicative of inhomogeneities in the ground—which are the things we want to detect. This is the logic behind the calculation of residual electromagnetic (REM) data.

The process is essentially a matter of straight algebraic subtraction and normalization. Pure electromagnetic coupling data are calculated for a homogeneous earth of the measured apparent resistivity and for the a and n-spacings. These data are subtracted on a frequency-by-frequency basis from the total coupling data to yield the unnormalized REM data. Since coupling is proportional to frequency, the frequency at which each data point is obtained is normalized to the highest frequency which has been obtained in field surveys (110 Hz). Next, since coupling is proportional to n-spacing, it must be normalized according to n-spacing in order to generate inter-comparable pseudosection data. The n-spacing normalizing factors are empirically determined, and are based upon the deepest data normally obtained (n=6).

The final, normalized REM data consist of real ("in-phase") and imaginary ("quadrature") components. Both contain valuable information, but usually the quadrature component is the most diagnostic in terms of detecting lateral effects in the earth. Only the quadrature components are presented in this volume. A brief description of these data is offered in the following section.

1.9 PARAMETERS USED IN RESISTIVITY/ PHASE AND COMPLEX RESISTIVITY INTERPRETATION

As noted earlier, three parameters are normally used for resistivity/phase interpretation: apparent resistivity, apparent polarization, and residual electromagnetic or REM. Other, additional parameters, such as raw phase angle, spectral type, and coupling coefficients are used in high resolution complex resistivity work, but they are not discussed here.

Apparent Resistivity

Apparent resistivity is a measurement of how well the earth conducts electricity. The dipole-dipole equation for apparent resistivity is derived in section 9.6, and the equation most useful for field work is given in equation (1.4):

$$\rho_a = \frac{V}{I} \pi an\,(n+1)\,(n+2)$$

in which "a" is the dipole size (meters), "n" is the separation between receiving and transmitting dipoles (expressed as a multiple of "a"), I is the transmitted current (amperes), and V is the voltage drop measured across the receiving dipole (volts). The units for apparent resistivity are ohm-meters. Apparent resistivity is the direct inverse of apparent conductivity, whose units are mhos per meter or siemens per meter.

Apparent resistivity data are most sensitive to a conductive object lying in a resistive environment. The data are normally plotted in pseudosection form at 0.125 Hz. Modeling and field experience show that the depth of penetration of apparent resistivity data, obtained from n=1 to n=6 by means of the dipole-dipole array, is about twice the a-spacing. Given typical a-spacings of some 1,000 to 2,000 feet (300-600 m) for hydrocarbon surveys, it can be seen that apparent resistivity data typically respond to features whose depth of burial is less than 2,000 to 4,000 feet (600-1,200 m).

Apparent Polarization

Apparent polarization data represent the ability of the ground to store electrical charge in a capacitive way. Ground capacitance can result from any interface in which the mode of current transport changes from electronic to electrolytic or

when certain ions are restricted in motion by electrical or mechanical forces (see Chapter 8 for a more complete discussion of polarization). The most common sources of polarization in the earth are metallic minerals such as pyrite and chalcopyrite, or clays and graphitic shales.

Apparent polarization is usually plotted in pseudosection form. If the data have been decoupled, as is the case with all the data in this volume, the plotted values are called "decoupled phase angle"; they are plotted at 0.125 Hz. If a quadratic extrapolation has been used, the plotted values are called "three-point phase angle" and they represent extrapolated DC (0 Hz) values. Apparent polarization penetration is about the same as that for apparent resistivity—roughly twice the a-spacing.

Residual Electromagnetic (REM)

As seen in the previous section, REM data represent how much the electromagnetic coupling in the ground differs from the calculated homogeneous earth coupling. In practical terms, REM data sense lateral resistivity changes in the ground, usually at depths greater than those probed by apparent resistivity and apparent polarization data. Due to the complex nature of the coupling observed for a dipole-dipole array, it is not possible to establish a firm, theoretically-derived value for the depth penetration of REM data. Modeling would help greatly in this effort, and a three-dimensional electromagnetic algorithm is currently under development. On a strictly empirical level, it has been observed that REM penetration is about 2 to 3 a-spacings, or up to 50 percent greater than the penetration of standard galvanic data. Several of the case histories illustrate this observation. Theoretical calculations show that the effective depth of penetration can be extended past 4 a-spacings with proper estimation of the inductive coupling term.

Only the imaginary or quadrature component of REM is presented in this volume. The numbers are normalized and hence do not have any physical units associated with them. The numbers are not normalized to a-spacing, so data taken with 1,000-foot (305 m) dipoles (for an example) will be lower in magnitude by a factor of 4 than data taken with 2,000-foot (610-m) dipoles. In these data, numbers vary from positive to negative, according to whether the homogeneous earth coupling curve is larger or smaller than the field coupling curve, respectively. Numbers near zero indicate the two curves are nearly identical (i.e., the response resembles a homogeneous earth). Positive numbers indicate a low-over-high resistivity layering, while negative numbers indicate high-over-low layering. Since negative REM values indicate low resistivities at depth, they may be specifically indicative of hydrocarbon-induced alteration, which is typically conductive.

REFERENCES

Bartel, L.C., 1982, Evaluation of the CSAMT technique for mapping enhanced oil recovery processes (abs.): Geophysics, v. 47, p. 452.

Goldstein, M.A., and Strangway, D.W., 1975, Audio-frequency magnetotellurics with a grounded electric dipole source: Geophysics, v. 40, p. 669-683.

Hallof, P.G., 1974, The IP phase measurement and inductive coupling: Geophysics, v. 39, p. 650-665.

Ostrander, A.G., 1981, Controlled source AMT—application and advantage (unpublished): 87th Annual Northwest Mining Association Convention, Spokane, Dec. 4. Reprints available from Zonge Engineering.

Sandberg, S.K., and Hohmann, G.W., 1982, Controlled-source audiomagnetotellurics in geothermal exploration: Geophysics, v. 47, p. 100-116.

Wynn, J.C., and Zonge, K.L., 1975, EM coupling, its intrinsic value, its removal and the cultural coupling problem: Geophysics, v. 40, p. 831-850.

Zonge, K.L., Emer, D.F., and Ostrander, A.G., 1980, Controlled source audiofrequency magnetotelluric measurements: Technical papers, 50th Annual International Meeting and Exposition, SEG, Houston, v. 5, p. 2491-2521.

Zonge Engineering, 1981, Controlled source AMT: information brochure.

Chapter 2
Interpreting Hydrocarbon Anomalies

2.1 INTRODUCTION

This chapter is dedicated to analyzing the characteristics of electrical anomalies measured over known hydrocarbons, to determining an explanation for them, and to demonstrating how the data are interpreted. The discussion will be confined primarily to resistivity/phase and complex resistivity measurements.

It shall be simply stated that the measurements themselves are both valid and repeatable. The validity of the induced polarization technique in general has been well demonstrated in a number of spectacular exploration successes in the mining industry since the 1950s, and by extensive theoretical investigations over the past 50 years. The utility of Zonge Engineering complex resistivity and resistivity/phase surveys has been firmly established in exploration programs over the last 10 years of contract field services. Repeatability of field measurements over periods of months and years has also been established on a number of projects by re-occupying lines for experimental or developmental projects. Quality control over the data is maintained by techniques outlined in Chapter 1.

2.2 STATISTICAL ANALYSIS OF ZONGE ENGINEERING HYDROCARBON SURVEYS, 1977-1982

This section summarizes all Zonge Engineering hydrocarbon projects conducted during the past five years, ending December 31, 1982. The current study involves 879 surface line-miles (1,414 line-km) of data, or 561 subsurface line-miles (903 line-km), obtained over 57.1 crew-months. The total cost of these surveys was $2.6 million, with the resulting average cost of just under $3,000 per surface line-mile. As shown in Figure 2.1, the surveys have been conducted in 10 states and two provinces, all in the western and midwestern area of the North American continent. A total of 55 lines have been run over 29 oil and gas fields, which vary in size from very small (less than 8 barrels of oil per day) to gas giants. Production varies from heavy oils to gas, at depths from 200 to over 16,000 feet (60-4,900 m). About 45% of the fields are structural traps, and 55% are stratigraphic; 20% involve primarily gas production, 60% primarily oil, and 20% have both oil and gas. In addition, 101 lines of data have been run over 49 prospects, 20 of which have been or are currently being drilled.

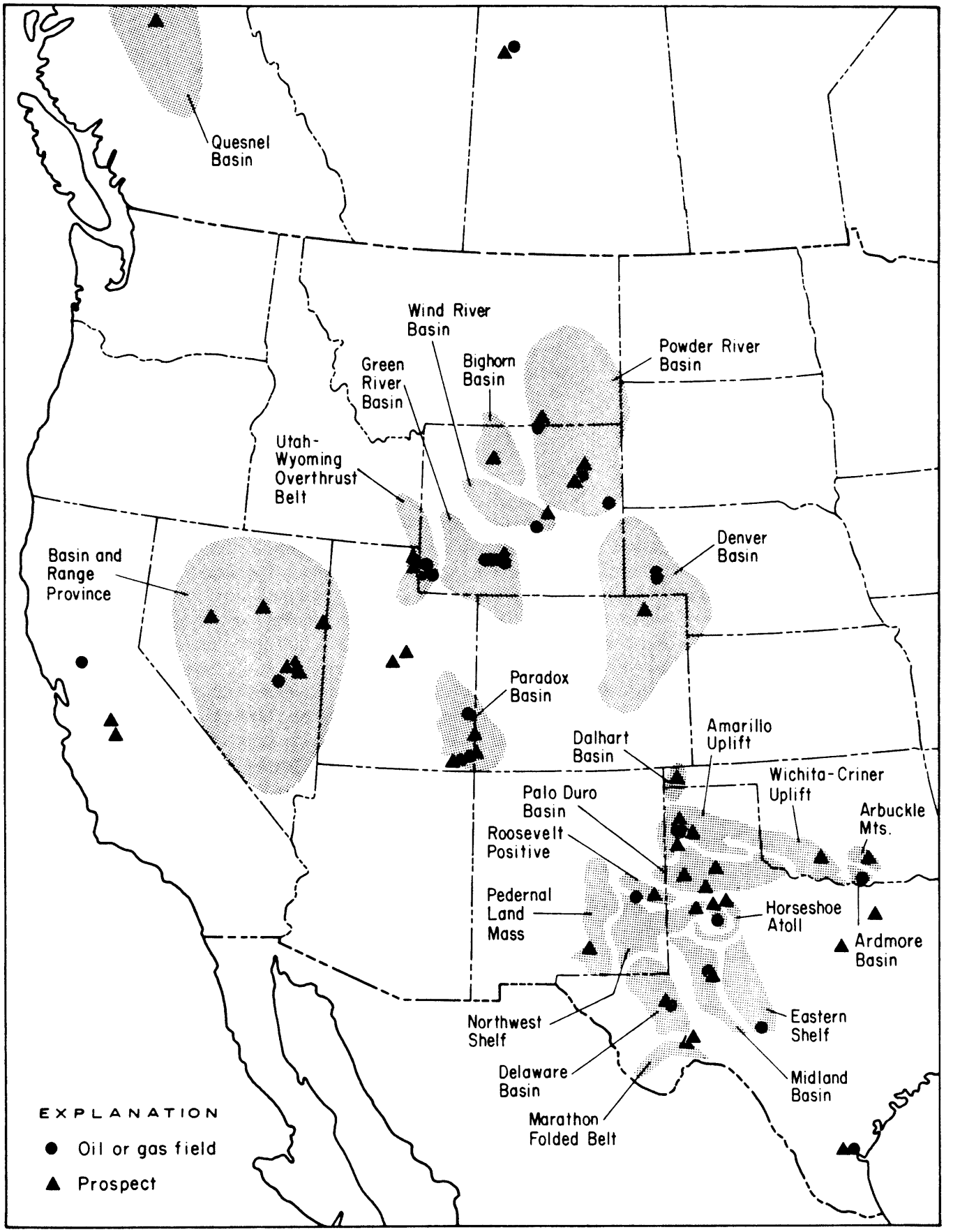

Figure 2.1. Locations of Zonge Engineering petroleum projects. 1977-1982.

Statistical Analysis of the Data

Almost all surveys run to date have used the dipole-dipole array to obtain either discrete-frequency resistivity/phase data or harmonic-frequency complex resistivity data. Frequencies as low as 0.01 Hz and as high as 110 Hz were used on some surveys, but the most commonly obtained frequencies are generally 0.125 to 1.375 Hz.

Three interpretational parameters—apparent resistivity, apparent polarization, and residual electromagnetic (REM) data—were analyzed in early 1983 for patterns in the data which resemble bonafide hydrocarbon responses. The data from existing oil and gas fields were specifically examined for the correlation of conductive apparent resistivity and REM anomalies, and of high polarization anomalies, with the lateral extent of the hydrocarbons. The anomalies were classified as follows:

1. Fair to excellent: moderately well-defined to classically shaped anomaly, well-correlated in plan view to the lateral extent of the hydrocarbons; would be recommended as a favorable drilling target if it were a prospect.
2. Absent to poor: poorly defined or poorly correlated anomaly, or one in which the definition is severely complicated by cultural, topographic, or structural effects; would not generally be recommended as a favorable drilling target, even though it may show subtly favorable trends.
3. Negatively correlated: distinct high resistivity, low polarization, or positive REM anomaly associated with the lateral extent of the hydrocarbons.
4. Data uninterpretable: severe cultural, structural, topographic, or other effects contaminating data.

Data from rank prospects were evaluated in a similar manner, with the obvious exception that correlation considerations were omitted. All statistics were compiled on a line-by-line basis; the statistics compiled on a field-by-field basis were quite similar. All lines run up through December, 1982 are included.

It should be stressed that the following statistics are to be regarded with some degree of caution, since any statistical summary of such widely varying field projects is subject to considerable ambiguity. Evaluations of a given anomaly are based upon interpretation, which is highly dependent upon the proper recognition of effects due to well casings, surface culture, topography, surface high resistivity materials, structure, etc. While care has to be taken to distinguish these spurious effects from true hydrocarbon alteration responses, it is not always possible to make the differentiation with absolute assurance. Hence, it is possible that some of the so-called "favorable" anomalies are merely unrecognized cultural or other spurious anomalies; conversely, it is also possible that some anomalies which were attributed to spurious effects may actually be partly due to bonafide hydrocarbon alteration responses. Great care has been taken to minimize the uncertainty in these regards. It is also important to recognize that the statistical sample in these compilations is rather small. In general, however, the statistics of Tables 2.1, 2.2, and 2.3 represent in a *qualitative* way the results of Zonge Engineering work to date.

An additional statement must be made in regard to these statistics: they merely represent a *statistical correlation* between electrical anomalies and hydrocarbons, prospects, and drilling. In no way can it be assumed *a priori* that a causal link exists; causality must be established by evidence which is independent of a simple statistical summary. For the present, we present these statistics merely for observation. Later sections will attempt to explain the origin of these anomalies.

Table 2.1 shows the correlation of electrical anomalies with the location of established hydrocarbon production. The parameters of apparent resistivity and REM are statistically correlated with hydrocarbons about one-half to two-thirds of

TABLE 2.1: CORRELATION OF ANOMALIES TO OIL AND GAS FIELDS

ALL PROJECTS (55 lines, 29 fields)

	Apparent Resistivity	Apparent Polarization	REM	At Least One Parameter
Fair to excellent	58%	24%	65%	66%
Absent to poor	31	58	24	27
Negative correlation	0	0	0	0
Uninterpretable or ambiguous	11	18	11	7

CASE HISTORIES (14 lines, 9 fields)

	Apparent Resistivity	Apparent Polarization	REM	At Least One Parameter
Fair to excellent	58%	29%	64%	64%
Absent to poor	21	64	15	29
Negative correlation	0	0	0	0
Uninterpretable or ambiguous	21	7	21	7

the time and are non-correlated about one-fourth of the time. In many cases, lack of correlation occurred over fields which had minimal production, spotty lateral production (e.g., discontinuous channel sand facies), or which produced only heavy oil. However, in several other cases, lack of correlation could not be readily associated with any particular field characteristics.

About one-tenth of the resistivity and REM data sets were rendered uninterpretable by cultural or structural effects, and at least half of the projects showed some signs of such contamination. Apparent polarization shows a lower statistical correlation with hydrocarbons; in fact, it is more often uncorrelated than it is correlated. Many of the incidences of non-correlation cannot be related to field characteristics, a fact which will be discussed later in regard to proposed anomaly mechanisms. At least one of the three interpretational parameters was correlated to producing fields in two-thirds of the projects.

Several items are of interest here. First, while apparent resistivity and REM show roughly similar correlations with oil and gas fields, it was noted that REM almost always provides better definition and lateral correlation to the producing field than does the resistivity parameter. Several examples of this are presented in the case histories. Second, all anomalous responses are low in resistivity, high in polarization, and negative (conductive) in REM; none of the fields show distinct negative correlations, i.e., high resistivity, low polarization, or positive (resistive) REM.

Table 2.1 also contains statistics for the case histories contained specifically in this volume: Garza, Ryckman Creek, Whitney Canyon, Desert Springs, Playa-Lewis, Desert Springs West, Little Buck Creek, Lisbon, and Trap Spring. The statistics for these fields show a very similar "success rate" to that of the larger group of 29 fields.

A useful supplement to this information is the results of work done over undeveloped prospects, summarized in Table 2.2. These statistics show similarities with results obtained over known fields. Some 20% of the prospects surveyed show some sort of an anomaly. Note that apparent resistivity and REM parameters show anomalies at roughly three times the rate of the polarization anomaly, comparing

TABLE 2.2: ANOMALIES OBSERVED OVER UNDEVELOPED PROSPECTS

	Apparent Resistivity	Apparent Polarization	REM	At Least One Parameter
Fair to excellent	16%	6%	19%	22%
Absent to poor	72	80	68	67
Uninterpretable or ambiguous	12	14	13	11

favorably with the results of Table 2.1. Most of the "uninterpretable" anomalies occurred on the ends of survey lines, where proper interpretation is not possible. Only about 5% of the projects were severely contaminated by cultural or structural effects.

A total of 35 wells have been drilled within one dipole length of Zonge Engineering survey lines, and the production results are tabulated in Table 2.3. The numbers represent the original interpretation prior to drilling. The drilling results from non-anomalous projects essentially reflect numbers just a bit better than those one might expect from grid-drilling a petroliferous basin, so one should be careful not to overinterpret them. However, the drilling results over previously established anomalies are really quite encouraging, despite the low statistical sample. These results also provide an early indication that a *perfect* success record is not necessarily guaranteed by using this technique; success is greatly enhanced by judicious use of information from other sources. For example, two dry holes were drilled on apparently favorable anomalies; computer modeling later showed the anomalies were probably artifacts of discontinuous high resistivities at the surface.

TABLE 2.3: PROSPECTS SUBSEQUENTLY DRILLED

	Producing Wells	Shows, Uneconomic	Dry Holes, No Shows
Drillholes on favorable anomalies (14)	79%	7%	14%
Drillholes on questionable anomalies (6)	33	50	17
Drillholes on non-anomalous areas (15)	0	0	100

The Origin of the Anomalies

It is important to recognize that the statistics of Table 2.1 merely point out an apparent correlation between electrical anomalies and the presence of hydrocarbons. There is considerable debate at present as to whether this is a matter of coincidence or whether there is an actual causal link between the anomalies and the hydrocarbons. The resolution of this issue will help determine whether or not electrical techniques can be used as a viable exploration tool in the petroleum industry.

There have been a number of ideas suggested to explain the anomalies observed by electrical contractors in general. These ideas generally fall into four categories:

1. Hydrocarbons are being detected directly by virtue of their high electrical resistivity.
2. Anomalies are partly or totally due to the presence of saline waters and zones of electrochemical alteration caused by upward migration from deep hydrocarbon accumulations.

3. Conductive and polarizable anomalies measured over established hydrocarbon production are due (at least in part) to spurious effects arising from the presence of conductive well casings, pipelines, or other cultural features.
4. Anomalies are partly or totally due to topography or subsurface structure effects.

The following discussion will deal with each of these four categories as possible sources of the anomalous responses reported in the literature and in this study.

2.3 THE DIRECT DETECTION OF HYDROCARBONS

Introduction

As is discussed in Chapter 10, the search for oil and gas by electrical methods has long concentrated on attempts at direct detection of the hydrocarbons at depth. A number of groups have claimed success in this effort, but invariably the evidence for these claims has been clouded by vagueness or misapplication of the fundamental laws of electromagnetism. As a result, electrical methods in general, and direct detection methods in particular, have earned a rather poor reputation with the petroleum industry.

This discussion briefly outlines the reasons why most claims of direct detection in the past have almost certainly been misdirected, and why direct detection in the near future is rather unlikely.

Oil as an Insulator

Many of the proponents of direct detection have claimed that oil, whose resistivity is some 3×10^{11} ohm-meters, should be distinguished quite easily by electrical data from sedimentary rocks, whose resistivities are typically less than 100 ohm-meters. These proponents claim that gas, as a nearly perfect insulator, should be an even better target.

This argument suffers from several rather substantial problems. A surface electrical measurement technique responds not only to oil and gas, but also to lithology, mineralogy, and especially pore fluid content. In a trap, interstitial pore spaces in the reservoir rock are typically filled not only with hydrocarbons but with saline (and therefore conductive) waters. As a result, the resistivity of a trap can be much lower than the resistivity of oil or gas, varying according to pore water salinity, pore space saturation, and type of permeability. Resistivity logs often show highly variable responses in hydrocarbon reservoirs, and it is not uncommon for the reservoir to actually show up as conductive due to the influence of pore fluids. Therefore, it is difficult to see the validity in searching for oil and gas as insulators, if their insulating properties are often overridden by the dominant effects of more conductive materials.

Detection of an Insulator with DC Resistivity

Assuming for the sake of argument that a given reservoir rock is much more resistive where hydrocarbons are present than where only pore fluids are found, what are the chances that the hydrocarbon-producing zone can be detected by means of DC resistivity measurements? In order to answer this question, a computer modeling routine known as "2DIP" (described in section 2.7) was used to model the dipole-dipole response to a buried insulator. The results, illustrated in Figure 2.2,

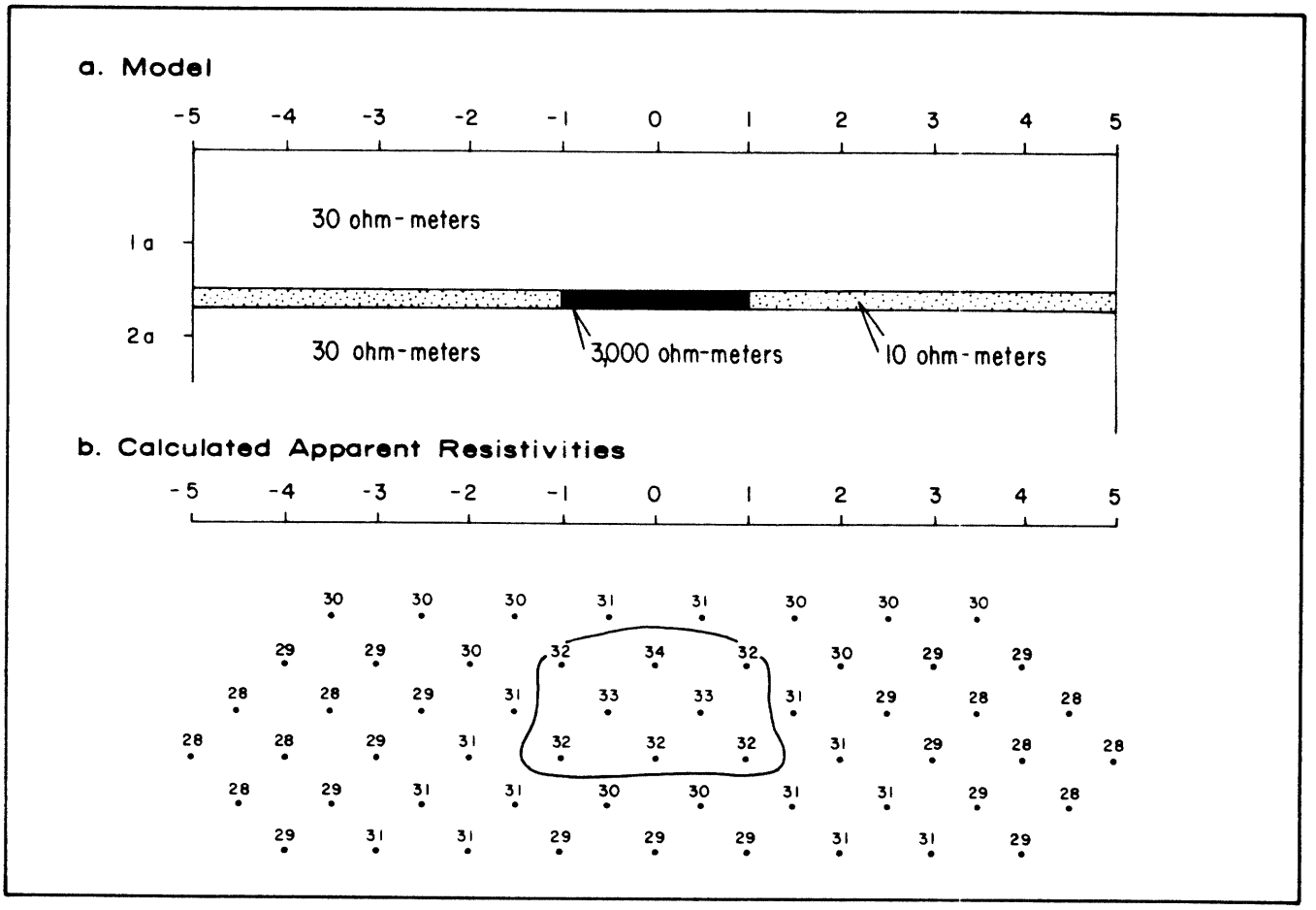

Figure 2.2. Two-dimensional resistivity model of a shallow resistive body. The model simulates the DC effects of an oil-saturated zone in a thin, porous reservoir sand. Contour interval: 10.0, 12.6, 15.9, 20.0, 25.1, 31.6, 39.8, 50.1, 63.1, 79.4, 100.0, . . . ohm-meters.

show that a resistive body could be identified as a subtle feature in a homogeneous earth environment, providing that the body is shallow and has sufficient thickness and lateral extent. This, unfortunately, is not a typical hydrocarbon exploration target, but is the exception. Further, the response from even such a shallow target as this would be obliterated by the mildest of effects from variations in surface and subsurface geology. Therefore, the direct detection of a hydrocarbon reservoir, even if it happens to be highly resistive as a whole, is unlikely using the dipole-dipole array.

The rather pessimistic conclusion regarding direct detection with resistivity measurements should not be too surprising. Since the strength of a measured electrical signal is determined by the flow of current through the path of least resistance, i.e., through the conductive portions of the ground, it seems reasonable that a conductor in a homogeneous half-space would show a much stronger effect than an equivalent resistor. This is demonstrated by the "2DIP" models of Figure 2.3, in which the resistivity of a thin, buried body is varied from conductive to resistive to *very* resistive. When conductive, the body produces an anomaly whose maximum strength differs from background by a factor of 1:5; when resistive, it produces a maximum anomaly of less than 2:1. As pointed out some 50 years ago (Hedstrom, 1930), making the resistor even more resistive does not change the strength of the

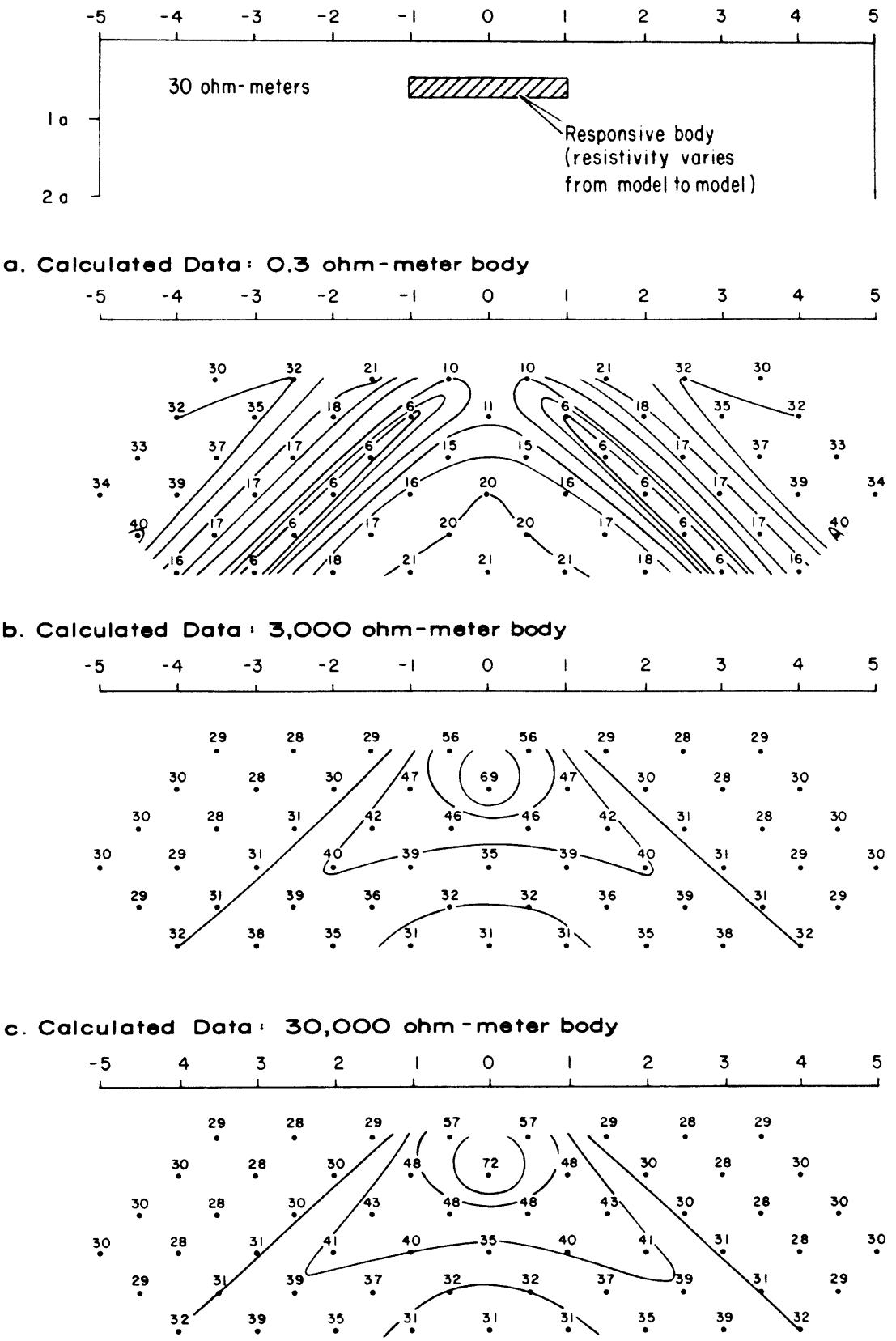

Figure 2.3. Two-dimensional resistivity model of a shallow body: a) a conductive body, with 1:100 resistivity contrast with respect to background; b) a resistive body, with 100:1 resistivity contrast; c) a resistive body, with 1,000:1 resistivity contrast. Contour interval: same as in Figure 2.2.

resistive anomaly significantly. This fact can be appreciated by comparing the model of Figure 2.3b to that of Figure 2.3c. Hence, the absolute value of the resistivity of oil and gas is irrelevant in regard to resistivity measurements, as long as the contrast is at least 100:1 with respect to background.

Detection of an Insulator with Magnetotellurics

Not only are insulators difficult to detect with resistivity methods, they are also difficult to detect with magnetotellurics (MT). The MT method represents a parametric sounding technique in which penetration is a function of signal frequency, as opposed to the dipole-dipole induced polarization method, in which penetration is a function of array dimensions. An MT modeling routine ("EMCDC") was used to compute the theoretical effects of the resistive slab of Figure 2.2. The results (Figure 2.4) again show a subtle anomaly which would be easily lost in a normal geologic environment. Hence, MT does not appear to offer significant advantages over resistivity methods in regard to direct detection of hydrocarbons.

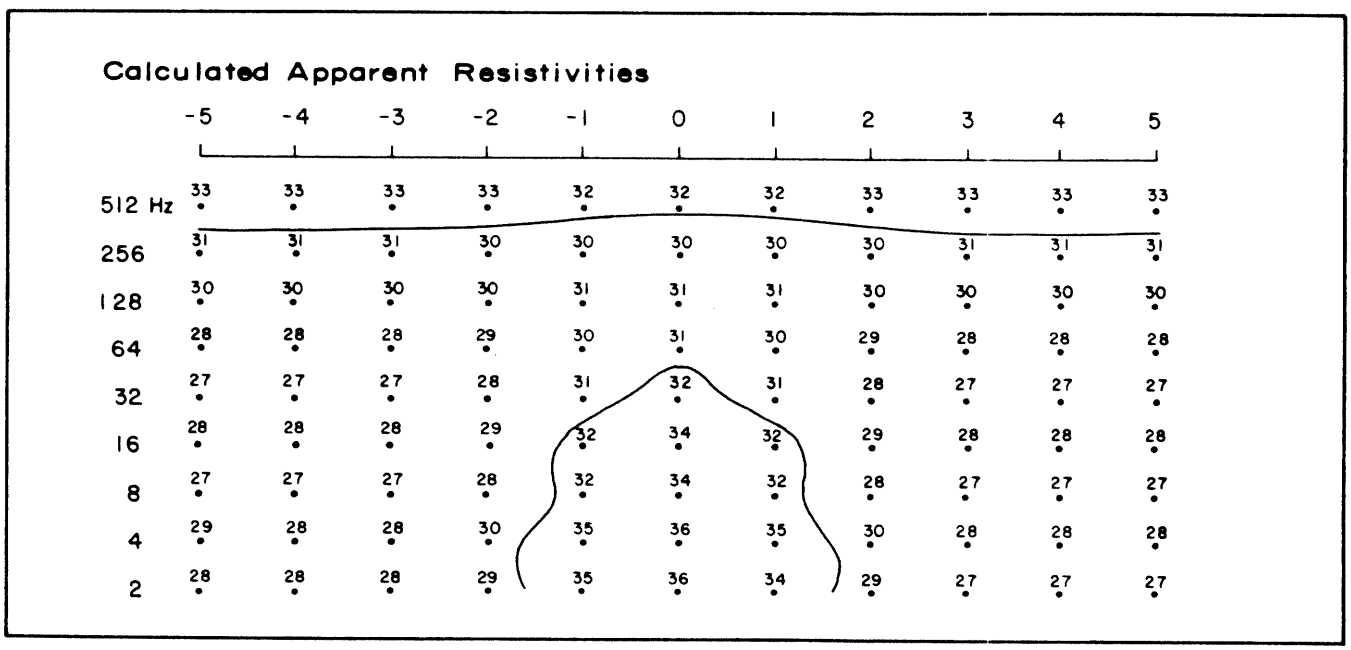

Figure 2.4. Two-dimensional MT resistivity model of a shallow resistive body. The model parameters and contour interval are the same as shown in Figure 2.2.

Transient "Reflections" from an Insulator

The preceding discussion has shown qualitatively some of the problems in the direct detection of hydrocarbons by processes which rely on measurement of the electric field at DC or low AC frequencies. There are also strong quantitative arguments against direct detection of "reflections" from the surface of an insulator.

An example of "transient reflection" methods is provided in the work by Electraflex, which is discussed briefly in Chapter 10. Electraflex uses a Schlumberger array, whose transmitting dipole is 2,640 feet (805 m) long and whose receiving dipole is 500 feet (152 m) long. In his numerous discussions of the technique, Jamil Azad states that a time-domain waveform of the type illustrated in Figure 2.5 is used for the measurements. The decay waveform during the "off" cycle is measured following a gap time; although it is never said what that gap time is, it is understood that measurements commence after 0.05 cycle has elapsed from the time of signal shut-off.

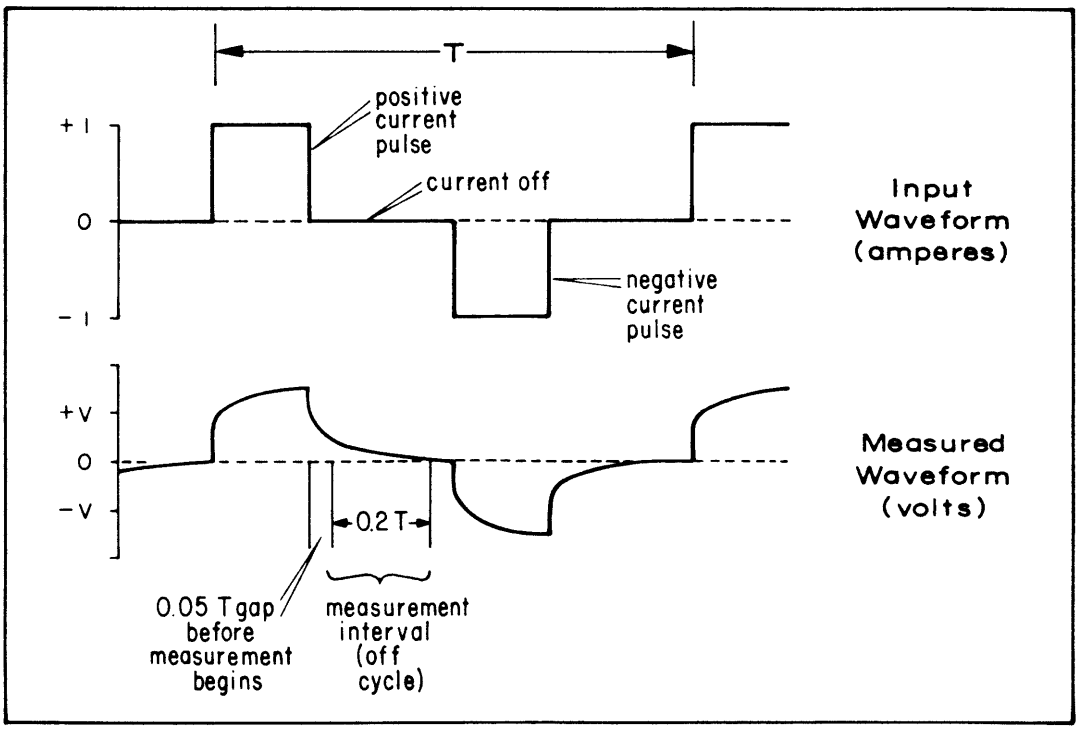

Figure 2.5. Typical Electraflex time-domain signal. Measurements are made after both positive and negative pulses.

Azad (1973) states that the gap is necessary to allow time for the IP response and near surface reflections ("first break") to decay, allowing deep electromagnetic effects to come through. However, Newmont scientists (Dolan, 1967), working with an almost identical waveform for some 30 years, have experimentally determined that a 0.055 cycle gap rejects most of the rapidly decaying electromagnetic effects and permits optimum measurement of the induced polarization effect. Also, note that the fixed dimensions of the Electraflex array dictate the penetration depth of the surveys in regard to induced polarization effects. That depth is not much greater than half the transmitting dipole length, or about 1,300 feet (400 m). Hence, it is likely that Electraflex measurements are not responding to deep "transient reflections" from hydrocarbons, as claimed by Azad, but are primarily measuring shallower induced polarization effects. This conclusion has recently been reached by Elflex (Powell, 1981), which had previously claimed to make transient measurements similar to those made by Electraflex.

Theoretical Problems with Reflection Measurements

Is it possible to measure the electromagnetic reflections from a buried insulator? In order to determine the answer to this question, consider the effects of a plane wave which is propagating through the earth in the z-direction, a subject which is treated in Chapter 9. Ignoring sinusoidal variations, the electric field amplitude E_x for a plane wave traveling downward in the earth (the z-direction) is related to the maximum field strength E_o by equation (9.82):

$$E_x = E_o\, e^{-kz} \tag{2.1}$$

in which k is the so-called propagation constant:

$$k = \alpha + i\beta \tag{2.2}$$

The quantities α and β are, respectively, the phase constant and the attenuation constant, which for conductive materials are given by equation (9.80):

$$\alpha = \beta = \sqrt{\mu\sigma\omega/2} \tag{2.3}$$

in which ω is the angular frequency, σ is the ground conductivity, and μ is the magnetic permeability. The effective depth of penetration, δ, from equation (9.85) is

$$\delta = 1/\alpha = \sqrt{2/\mu\sigma\omega} \tag{2.4}$$

and the wavelength of the plane wave is, from equation (9.88):

$$\lambda = 2\pi\delta \tag{2.5}$$

The attenuation of a downward travelling plane wave, expressed as a function of wavelength, can be rewritten from equation (2.1) as

$$E_x/E_o = e^{-\alpha\lambda} \tag{2.6}$$

which reduces to

$$E_x/E_o = e^{-2\pi} = 0.001867 \tag{2.7}$$

This can be expressed in terms of db by

$$20 \log_{10} (0.001867) = -54.6 \text{ db} \tag{2.8}$$

In other words, a plane wave is attenuated by a factor of about 55db per wavelength.

Now, consider the fact that, in order for a reflection to be resolved by a correlation-type receiver system, the object being measured must be separated from the receiving dipole by at least one and preferably two wavelengths. This immediately implies that the receiver system must have a dynamic range better than 100 db in order to resolve an electromagnetic reflection from an object one wavelength deep. However, it is doubtful that the Electraflex equipment has a dynamic range much better than 80 db. Hence, true transient reflections would be missed no matter what the depth of the target is: at large depths, attenuation would exceed the 80 db dynamic range and the receiver could not detect the minimal signal level, while at small depths, the target would be too shallow with respect to wavelength to be resolved. Given considerations of layering and subsurface structure, a dynamic range of at least 150 db would be required to reliably detect transients from a hydrocarbon layer at depth. Such a receiver system has yet to be built.

We can conclude from this discussion that resistivity soundings for direct detection of oil and gas are unlikely to succeed except for very shallow, thick targets. We can also conclude that detection of transient reflections from a hydrocarbon interface using currently available equipment is extremely unlikely.

Zonge Engineering Data

There is not the slightest chance that the Zonge Engineering data are responding to hydrocarbons directly. This can be stated not only for the arguments just outlined, but also for two other reasons. First, all anomalies which have been linked statistically to the presence of hydrocarbons at depth are electrically conductive. None are resistive, as might be expected at least part of the time if hydro-

carbons were being directly detected. Secondly, nearly all the hydrocarbon deposits measured to date have been much deeper than the galvanic penetration depth of the surveys. What is being measured are clearly conductive and occasionally polarizable effects which are much shallower than the hydrocarbons themselves.

2.4 THE ORIGIN OF ELECTRICAL ANOMALIES OVER HYDROCARBONS

Introduction

There is little doubt that light hydrocarbons migrate in meager amounts from their traps at depth to the surface of the earth. The evidence for vertical migration is provided by a number of studies over the past 50 years by geochemists, microbiologists, hydrologists, engineers, and geologists.

A general, intensive investigation of "tertiary migration," or leakage from hydrocarbon traps, has yet to be undertaken. Very little is understood about the mechanics and electrochemical results of migration through a complex sedimentary section. It is the purpose of this discussion to present some of the ideas currently in circulation and to relate these ideas to the origin of electrical anomalies over hydrocarbon deposits.

Evidence for Vertical Migration

The first evidence of hydrocarbon migration from depth was the observations of tar seeps, which go back several thousand years. A number of seeps are known throughout the world, although they probably occur over only a fraction of the known oil and gas fields. Color alteration of sediments (Donovan, 1974), vegetation changes (Richers, et al., 1982), and other effects are sometimes related to seepage areas.

Geochemists have presented convincing evidence of vertical migration in direct measurements of hydrocarbons in near-surface soils and in measurements of isotopic carbon ratios of near-surface, methane-altered carbonates. Horvitz (1969, 1982) and Duchscherer (1980, 1981) provide some general discussions and reading lists on geochemical methods. Pirson (1969, 1980) also contributes some interesting ideas from an electrochemical point of view. Roberts (1982) discusses vertical migration of helium from hydrocarbon traps. Davis (1969) presents evidence of hydrocarbon migration through a study of bacterial activity, which causes the precipitation of metallic sulfides in the overlying sediments. Ferguson (1979) outlines a number of near-surface mineralogic changes which appear to result from vertical migration.

Roberts (1980b) summarizes numerous observations of high-temperature anomalies over hydrocarbons, which he attributes to vertical migration processes. Roberts (1980a) also advocates some hydrodynamic theories which are designed to explain primary migration processes but which relate to tertiary migration as well.

Theory of Electrical Anomaly Generation

Due to the paucity of work on the mechanisms which result in the electrical anomalies observed over oil and gas fields, this discussion is by nature incomplete. However, the more likely possibilities in regard to induced polarization work will be discussed in this section.

As noted in section 2.2, the work conducted by Zonge Engineering shows

relatively consistent conductive anomalies but variable polarization anomalies in data obtained over hydrocarbon traps. Some of these anomalies are believed to be enhanced or caused by cultural, topographic, or structural interferences, as will be discussed in later sections of this chapter. However, many of these anomalies cannot be attributed to these effects, and instead are believed to arise from alteration of the sediments and changes in the pore fluids above the traps. The alteration patterns are highly variable in terms of their origin and magnitude, judging by the variability of the electrical anomalies. This should not be surprising, considering the complexities of hydrologic, mineralogic, chemical, and physical conditions present in the ground.

Anomalies measured by Zonge Engineering can often be placed in two categories: "deep" and "shallow." The "deep anomaly" is believed to be due to migration of saline water vertically out of the trap. It is detected as a deep, conductive zone by means of REM and apparent resistivity data. The "shallow anomaly" is probably due to mineralization and alteration which result from vertical migration of lighter hydrocarbons and possibly connate waters from the trap at depth. It is detectable as a shallow, polarizable anomaly with variable resistivites.

The "Deep Anomaly"

The "deep anomaly" is the most consistently observed feature in electrical surveys over existing oil and gas fields. Only a few characteristics of the "deep anomaly" can be stated unequivocably. When it exists, it is always electrically conductive, showing an apparent resistivity contrast of roughly 1 to 2 with respect to background. No deep resistive feature has yet been seen directly over a hydrocarbon trap, although, as noted in section 2.2, the conductive feature is occasionally absent. The "deep anomaly" rarely has an associated polarization response. It appears to be quite deep in extent, possibly extending to the depth of the trap itself. It does not often extend shallower than 1,000 feet (300 m) or so.

Due to resolution limitations of dipole-dipole data, not much can be said regarding the vertical or lateral structure of the "deep anomaly." It is roughly in the shape of a cylindrical column or plume which is, in general, reasonably well correlated with the lateral extent of the hydrocarbons. Computer modeling has suggested that the column is most conductive at depth, decreasing to nonanomalous values closer to the surface. This conclusion is only a preliminary one at this time, due to the small number of fields analyzed with high-resolution techniques such as controlled source AMT. Lateral structure is even less well-known. Computer modeling shows that it is difficult to distinguish between a solid cylindrical conductor and a hollow-cylinder conductor in typical dipole-dipole field data. Again, the detailing of structure in the "deep anomaly" is best left to techniques with better resolution.

THE "DEEP ANOMALY" MECHANISM

The "deep anomaly" is believed to be a direct result of brine discharge from hydrocarbon traps. As summarized by Meinhold (1971), Tóth (1980), and Roberts (1980a), the accumulation of many oil and gas deposits in traps in mature sedimentary basins may have been controlled by hydrodynamic factors which are often still active today. Roberts (Figure 2.6) views hydrocarbon traps as a "forced-draft" system in which organic material is carried from compacting shales (the source beds) to the ultimate trap by waters whose flow characteristics are controlled primarily by regional patterns of recharge and discharge. When water nears a trap with some vertical extent, its essentially horizontal movement is changed to vertical movement by the hydraulic gradient in the vicinity of the trap. If the trap is an effective one, Roberts argues that it acts as a filtering mechanism, discharging water but retaining the organic material or hydrocarbons as well as much of the dissolved salts. Whether

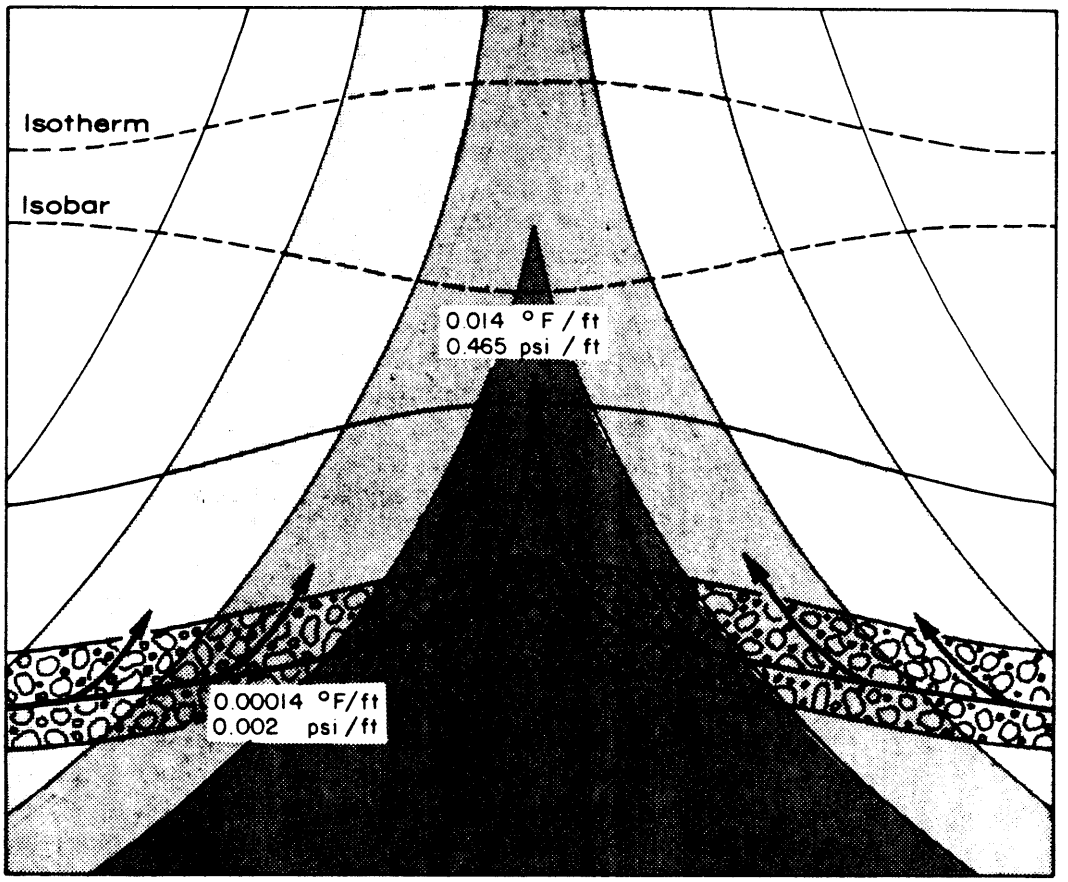

Fig. 2.6. Temperature, pressure, and salinity changes imposed upon convergent, upward-moving waters and their contents. Shaded zones show areas of higher salinity. Composite drawing from Roberts (1980a).

or not the hydrodynamic theory of hydrocarbon accumulation is correct is currently a matter of debate (Magara, 1981), but it is an idea which might help explain the origin of electrical anomalies. Other theories of petroleum migration may be equally compatible with the electrical data.

It is likely that any "impermeable" seal above the hydrocarbons will allow a small percentage of brine to be passed vertically out of the trap, especially in systems which have strong hydraulic gradients. Since the water originates from depth, it will have a higher temperature than the surrounding waters (Meinhold, 1971; Roberts, 1980b) and will therefore retain salts in solution more readily than the cooler waters which surround it. The volume of brine will be forced upwards by the continuous discharge from the trap beneath it, by virtue of its higher temperature, by decreased local pressure directly over the trap, and because of hydrostatic pressure considerations. Eventually, a decrease in temperature and pressure will cause salts to precipitate out of the water. The salts are subject to four competing influences: movement by horizontal groundwater flow, statistical diffusion, gravitational sink, and hydraulic lift from the discharge area of the trap. The relative importance of these four influences is not known and may vary considerably. However, in a dynamic system, brine is continually supplied through the trap, replacing the dispersing column above. Therefore, the "deep anomaly" might only be present in a dynamic system: as soon as the hydraulic water flow (and the supply of

hydrocarbons) through the trap ceases, the brine supply is terminated, the saline zone dissipates, and no anomaly can be measured.

Several substantial problems are associated with the brine discharge theory. First, it is an open question as to whether or not typical capping sediments are partly permeable to saline water. Neglia (1979) notes that no rock unit is completely impermeable, with the exception of evaporites and salts, but the relative permeability of the trap seal must allow enough brine to be discharged in order to supply the overlying sediments with salts faster than they are being dispersed. No studies into this matter have been found. Questions closely related to this involve the expected transport speed of the brines and the relative strengths of forces which tend to increase or decrease the salinities. For example, it might be argued that horizontal groundwater movement would tend to carry salts away faster than they could be resupplied. One encouraging bit of evidence in this regard comes from Bredehoeft and Papadopulos (1965) who note that the *minimum* vertical movement of water needed to support the lowest-level observed geothermal anomalies would be about one foot (0.3 m) per year. This is roughly the same magnitude as the flow rate through compacted sedimentary units, indicating that *total* dispersion of vertically migrating brines is unlikely.

A significant problem with the observation of conductive material at depth is that insufficient work has been done to compare the field measurements to borehole resistivity logs. If a preferentially conductive zone often existed over hydrocarbon traps, one would think that fact would have been noted in well logs long ago (unless clays have complicated the well log data). The problem here is that ground resistivity measurements are made at around 0.1 Hz, and resistivity logs are made at frequencies above 1 kHz, hence, the two measurements differ in frequency by four to five orders of magnitude. Work by Clavier, Heim, and Scala (1976) suggests that a frequency difference of this magnitude would significantly influence the measurements. However, one would need to determine whether such a difference would result in a preferential insensitivity of well logs to changes in pore fluid salinity or clay alteration, a point which is currently hard to accept.

There are alternatives to the brine discharge theory which may be important in some or all environments. The main alternative involves alteration of clays at depth due to preferential cation exchange from waters rich in calcium or sodium. This possibility involves a number of questions and very few answers at present. However, ion exchange involves an influx of water-borne ions, and that almost certainly relates to the "forced-draft" ideas just considered; hence, the clay-alteration theory may have a driving force similar to the brine-discharge theory.

EXPLORATION LIMITATIONS

If the brine-discharge theory is substantively correct, what would the resulting anomaly be expected to look like? A roughly vertical column of brine, becoming more diffuse toward the edges and upward, would be expected. Maximum dissolved salts would be contained in regions of highest pressure and temperature, i.e., at depth near the discharge area. This is consistent with the interpretation of field data.

It is useful to engage in a few "thought experiments" in order to evaluate several possible limitations of the "deep anomaly" mechanism theory, as shown in the following discussion.

1) *Possibility of "false" anomalies.* An anomaly would be expected wherever a zone of brine is subject to upward movement. Presumably this would include zones in which hydrocarbons are just beginning to accumulate or even those in

which hydrocarbons will never accumulate due to the lack of organic material or a suitable trap. In other words, "false" anomalies might be measured in areas of discharge, regardless of whether or not hydrocarbons are present. In order to test this possibility, a large number of electrical anomalies would have to be drilled. Drilling to date has not favored the "false" anomaly hypothesis, but the small number of wells actually drilled prevents any firm conclusion to be made in this matter.

2) *Limitation as a function of trap design*. Whether or not the proposed mechanism would be similar for both stratigraphic and structural traps cannot be determined at this point. A difference in the magnitude of the conductive effect might be expected; however, since both types of traps involve changes in porosity and permeability, vertically as well as horizontally, both would be expected to produce some sort of anomaly. Indeed,"deep"anomalies have been measured over both types of traps.

3) *Depressurized reservoirs*. An anomaly over a depressurized reservoir might be expected to be weaker than an anomaly over a fully pressurized reservoir, due to solubility considerations. Lower pressures would mean lower solubility of salts; hence, waters migrating out of the trap would contain less total dissolved solids, and their resistivity would be higher than if the reservoir were more highly pressurized. The case histories of Desert Springs (Chapter 4) and Little Buck Creek (Chapter 5) tend to support this idea. In addition, low reservoir pressures would certainly have an effect upon flow velocity in and near the trap, but it is difficult to say what this effect would be.

4) *Depletion of hydrocarbons*. The role of upward-migrating hydrocarbons upon the "deep anomaly" is extremely difficult to understand at this point. It is possible that the invasion of clays and shales by low molecular weight hydrocarbons might alter the electrochemical characteristics of these sediments in some appreciable manner. Physical changes, such as evaporation of interstitial waters (Nisle, 1941), should also be considered, but again it is difficult to say what the electrical effects of these changes would be. Fortunately, depleted reservoirs are of no direct relevance to the use of electrical techniques in rank exploration, so the question is of academic interest.

5) *Cessation of hydrodynamic flow*. If the primary control on hydrocarbon accumulation is hydrodynamic, as Roberts (1980a) suggests, an anomaly might not be expected if the hydrodynamic flow of meteoric waters into the trap has ceased due to age. Hence, anomalies might be measured preferentially as a function of age: young traps, which might statistically involve gas more often than oil (Meinhold, 1971), would be more commonly detected than older traps on a statistical basis. Insufficient information is available to evaluate this possibility. Indeed, at this stage it is not even possible to judge the validity of the hydrodynamic hypothesis itself.

6) *Impermeable barrier above trap*. As suggested by Neglia (1979), shales and evaporites often pose permeability barriers to the cross-formational movement of waters and gases. In fact, shale layers may act as "filters" above the trap, retaining salts and organic material while passing water (Roberts, 1980a). It might be expected, then, that a thick shale or evaporite sequence might limit the strength of the "deep anomaly" by diminishing the amount of brine which passes through it. The almost universal presence of shales in petroliferous areas makes this hypothesis difficult to test, but some of the field data obtained by Zonge Engineering may support the idea. It is interesting to note that a strong conductive anomaly was measured at Lisbon Field (Chapter 6) in the shallow sediments despite a 3,000-foot (900 m) layer of salts which lie between these sediments and the hydrocarbon trap at depth.

7) *Contrast effects*. The relative effect of a buried body upon the apparent resistivity data depends partly upon the resistivity contrast of the body with respect to background. Hence, the invasion of highly saline waters into high resistivity ground will, by virtue of a high resistivity contrast, result in a pronounced anomaly. Conversely, the invasion of only moderately saline waters into low resistivity ground will result in a much weaker anomaly.

8) *Dipole size*. When the conductive zone is small with respect to the dipole size, the anomaly will be weakened (regardless of contrast) because the large dipole measures a bulk resistivity, averaging the conductive anomaly with resistive host rock. When the dipole is too small relative to target depth, the penetration will be insufficient and only the top of the column may be sensed, resulting in a weakened anomaly. Hence, it is fairly important to select a dipole size which is compatible with the target size and depth, as discussed in more detail in section 2.5.

The "Shallow Anomaly"

The "shallow anomaly" is found less consistently than the "deep anomaly", and its characteristics are more variable. When it is well defined, it is highly polarizable, but this occurs over only about one-fourth of the fields surveyed to date. It may involve high or low apparent resistivities near the surface, depending upon a number of specific geologic circumstances. The "shallow anomaly" is usually near the surface, but it can also extend to considerable depths.

THE "SHALLOW ANOMALY" MECHANISM

While the character of the "shallow anomaly" is inconsistent, its origin is probably better understood than is the origin of the "deep anomaly." The mechanisms for both are believed to have the same initial drive: vertical, hydraulic transport of material from the trap into the overlying sediments. However, the "shallow anomaly" is probably determined more by migration of light hydrocarbons than by migration of water.

When saline waters are discharged from the trap, light hydrocarbons (predominantly methane through propane) are also discharged, either in solution or in separate phases. It seems likely that these hydrocarbons, if they are ever in solution, come out of solution before they emerge from the trap. One of the reasons for this assumption is that hydrocarbons are usually detected in surface soils *directly above* the trap; hydrocarbons dissolved in water would move partly by diffusion, moving horizontally as well as vertically and hence resulting in a broad, diffuse anomaly, whereas hydrocarbons in a separate phase would migrate primarily in a vertical direction as a result of the hydrostatic pressure gradient, resulting in the more focused anomalies seen in geochemical surveys. Another way of looking at this question is to consider that, if "salting out" caused deposition of hydrocarbons in the trap in the first place, these hydrocarbons would probably not go back into a brine solution above the trap, especially considering the decreased aqueous solubility of hydrocarbons in the much lower pressures above the trap. Although the light hydrocarbons might pass through the seal in solution, this decreased aqueous solubility and the lower pressures would soon result in the separation of phases above the trap. The slight increase in solubility with the lower temperatures above the trap would probably not offset the opposite effect of lower pressure and sustained salinity, but, as pointed out by Barker (1980), studies of the solubility of methane in brines at commonly encountered subsurface temperatures, pressures, and salinities are not available.

In any case, hydrocarbons are probably in separate-phase migration while rising through the sedimentary column. As such, they have higher mobilities than

water. Their migration rate is subject to considerable debate. The close plan-view correlation of hydrocarbons in near-surface soils and traps at depth argues for a fairly rapid ascent. The fact that hydrocarbons make it to the surface at all also argues for a rapid ascent, since bacterial degradation from mircoorganisms in the sedimentary column would destroy any slow-moving hydrocarbons. Duchscherer (1980) quotes an AEC study in which vertical methane movement of rates of over 70 feet (20 m) per day were noted, but he provides no bibliographic reference.

Bacterial Degradation

As methane and small quantities of ethane and propane rise through the sedimentary column, they are usually subjected to biodegradation by anaerobic bacteria. The characteristics of these bacteria vary widely, but in general the result is the reduction of sulfatic waters through the action of *Desulfovibrio desulfuricans*:

$$CaSO_4 + (C+4H) \rightarrow H_2S + CaCO_3 + H_2O$$

The sensitivity of bacteria to hydrocarbons depends upon various factors, including the level of hydrocarbons present. If a certain threshold level of hydrocarbons is not present in the ground, microbial action will be of minimal importance. Hence, over the center of the field, where methane concentration would be expected to be highest, microbial activity would be most intense; somewhere toward the edge of the field, the sensitivity threshold would be reached, and hydrocarbons would continue up the sedimentary column unaltered, albeit in greatly diminished quantity. Mogilevskii (1940) and Soli (1957) suggested that this may explain the geochemical halos, in which surface hydrocarbons form a ring or halo around the producing field—a halo which is observed quite frequently, according to Horvitz (1969) and Duchscherer (1980). This explanation seems much more plausible than the one favored by Duchscherer, who proposes that carbonate precipitation causes an impermeable blockage to the hydrocarbons, which bypass the blockage, forming a halo. This writer sees no reason why the blockage would not continue to grow ever larger in lateral extent, eventually sealing off hydrocarbon migration completely.

Davis (1969), in a very interesting discussion of effects due to bacteria, describes a number of species which utilize straight-chain paraffinic hydrocarbons. Most of these consume methane; others have a preference for ethane or propane. This is useful since methane is both consumed and produced biogenically, but the presence of, say, ethane-oxidizing bacteria indicates the presence of an ethane source, which is normally a hydrocarbon trap at depth.

In general, anaerobic bacteria are found at temperatures less than about 140°F (60°C). The maximum practical depth limit is around 4,500 feet (1,500 m), and they often extend up the entire sedimentary column. Aerobic bacteria may be found near the surface or where the dissolved oxygen content of the waters is greater than about 8 milligrams per liter (Harwood, 1973); they typically inhabit sediments within the 68° to 122°F (20° to 50°C) range.

Hydrocarbons which survive bacterial degradation migrate up the sedimentary column and escape from the surface into the atmosphere. The concentration of hydrocarbons in surface soils is usually very low, indicating either a low rate of supply or a high rate of dissipation. It is widely believed that hydrocarbon accumulation in subsurface soils is a rather slow process. Transport is aided by microfractures and faults, but it is very possible that vertical transport through an unfractured, unfaulted section can also occur.

Near-Surface Mineralization

Within the top few thousand feet of sediments, the by-products of bacterial degradation—chiefly hydrogen sulfide, carbon dioxide, and calcium carbonates—interact with the sedimentary materials or meteoric waters to precipitate metallic sulfides and other substances. Chemical reactions account for much of this activity, but precipitation due to low temperature and pressure also occurs.

Pyrite is commonly found in sediments directly above some oil and gas fields. Ferguson (1979) shows a good correlation of pyrite with the planar extent of three fields in southwestern Oklahoma, and many other workers have noted pyrite over other fields as well. The mechanism which creates pyrite involves the reaction of hydrogen sulfide with iron. Hydrogen sulfide is derived either through microbial degradation of hydrocarbons or through upward migration of hydrogen sulfide from sour gases or oils in the trap at depth. Iron may be derived from two primary sources. One source is hematitic grain coatings and bonding agents in sandstones, in which case the following action may occur:

$$2H_2S + Fe_2O_3 \rightarrow FeS_2 + FeO + 2H_2O$$

The stability of the results of this reaction is quite variable, since oxidation of pyrite can occur in the oxidizing zones near the surface or in the environments of oxygenated water recharge. A second source of iron is from meteoric waters, but this is probably not of primary importance.

Snyder, et al. (1981), Oehler and Sternberg (1982), and a number of other researchers attribute induced polarization anomalies measured over hydrocarbon traps to pyrite generation. This is a natural assumption because of the inherent electrical response of disseminated pyrite and its relative abundance in the earth. Oehler and Sternberg showed a strong correlation between in-hole polarization responses and concentrations of pyrite over Ashland Field in southeastern Oklahoma. However, work by Carlson, Hughes, and Zonge (1982) shows that polarization responses over oilfields are quite variable, suggesting that the pyrite precipitation process is strongly affected by localized conditions.

It is interesting to note that, while micron-sized, unconnected pyrite grains will normally produce a strong polarization effect, the effect on apparent resistivities is quite variable. It is true that pyrite, as a metallic sulfide, is an efficient conductor of electrical current, but the effective conduction in a water-saturated rock usually occurs through pore fluids, not through disseminated metals. Unless the pyrite occurs in truly massive quantities, with interconnected grains, it will not usually supplant pore fluids as the chief conductive mechanism in the rock. Massive pyrite in a petroliferous environment is extremely rare; hence, pyrite probably has minimal effect on resistivities in most oilfield environments. Indeed, work by Duckworth (1981) at the University of Calgary indicates that, for pyrite quantities normally found in sedimentary environments (0 to 5%), interfacial impedance overwhelms the high conductivity of pyrite grains, yielding a *higher* resistivity for the rock as a whole. Laboratory measurements of artificial rocks (Ostrander and Zonge, 1979) show that the presence of disseminated pyrite has little effect on overall rock resistivity, although overall rock resistivity does have an effect on the polarization response of pyrite. Hence, one should not specifically expect either high or low apparent resistivities in the disseminated pyritic zones occasionally found over hydrocarbon deposits.

Resistivity anomalies can, however, result from carbonate cementation in near-surface sediments. It was noted earlier that organic reduction processes may

yield calcium carbonate, but calcite and dolomite can also result from inorganic processes. Oehler and Sternberg (1982) show high resistivities at the surface over hydrocarbon traps, and they attribute this to carbonate cementation. Note that this is a *very* near-surface effect; it has little to do with the "deep anomaly" unless calcification forms a physical barrier to salt discharge from the trap. Surface high-resistivity anomalies are not normally observed in Zonge Engineering surveys, since they tend to be overwhelmed by more conductive features and "averaged out" by the large dipole sizes used to achieve deep penetration.

Many other minerals are found over hydrocarbons and are attributed to leakage or migration processes. Most of these minerals occur in such meager amounts that they have little effect upon electrical measurements, so they are mentioned here only briefly as further evidence of migration. Sulfur may be found in oxidizing environments due to the instability of hydrogen sulfide there:

$$2H_2S + \tfrac{1}{2}O_2 \rightarrow 2S + 2H_2O$$

Ferguson (1979) found sulfur over three Oklahoma Fields, and many others have also noted the correlation of sulfur mineralization and petroleum. Donovan, Forgey, and Roberts (1979) have noted the presence of magnetite over some fields. They envision the production of magnetite to be related to reduction of hydrated iron oxides, which are found as grain coatings and bonding agents in sandstones. Other metallic minerals noted over oil and gas fields are lead, zinc, uranium, vanadium, manganese, nickel, chromium, and cobalt. In addition to these metal precipitates, rare gases, especially helium (Roberts, 1982), have been associated with some fields.

Clay Effects

One process which has not been mentioned in the literature in regard to resistivity and polarization anomalies is the role of clays. This is surprising in one sense, as clays are an extremely common source of low resistivity and high polarization anomalies in many areas of the world. In another sense, the lack of research into clay effects is not surprising due to the apparent unpredictability of clay responses. The properties of cation exchange, membrane polarization, and surface conduction in clays may be a major, but as yet unrecognized contributor to anomalies measured in sediments overlying hydrocarbons. If this is so, understanding the reaction of clay to an ascending column of hydrocarbons, biodegraded materials, and ion-filled waters may be of crucial importance to the successful use of electrical methods as a hydrocarbon exploration technique.

EXPLORATION LIMITATIONS

If the hydrocarbon migration mechanism is essentially correct, what might we expect "shallow" anomalies to look like? First, we would expect the maximum polarization effect to occur where the maximum iron and hydrogen sulfide supplies coincide. In a symmetrical anticline, maximum hydrocarbon leakage would occur from the center of the trap; microbial action would also be highest in the center of the migration column, and so would the produced hydrogen sulfide. Hence, anomalies in such a situation would be symmetrically centered over the oilfield. In addition, if clay alteration plays a significant role, one might expect a maximum anomaly where clays are present and where ion-rich waters and reducing hydrocarbons are found.

Some of the possible limitations noted earlier in conjunction with the discussion of the "deep anomaly" also apply to the "shallow anomaly." The possibility of "false" anomalies is not to be ignored, since the precipitation of pyrite and the

alteration of clays can be attributed to a number of sources separate from vertical migration from hydrocarbon traps. This problem is illustrated by the work by Oehler and Sternberg (1982), who present an example of a "false anomaly."

1) *Absence of iron or clays.* If the sediments through which the hydrocarbons and waters rise contain no available iron or clays for mineralization or alteration, no "shallow anomaly" will occur. While it is rare for a thick sedimentary sequence to lack both iron and clays, these materials may be poorly configured to produce an electrical response. For example, the iron may not be free to combine with hydrogen sulfide, or the clays may have a low cation-exchange capacity or peculiar geometry-pore fluid dynamics. Clays in particular are an infamous source of unpredictable electrical responses, largely because conductive and polarizable effects are so heavily dependent upon membrane and surface effects. This topic is treated in more detail in Chapter 8, and by Sumner (1967) and Madden and Cantwell (1967).

2) *Impermeable barrier above trap.* The smaller size and greater buoyancy of hydrocarbon gases allows them to pass through low-permeability layers such as shales and evaporites more effectively than saline waters. However, the upward migration process is probably considerably impeded by such layers. This has led many geochemists to the conclusion that hydrocarbons migrate upward by means of interconnected micro-fractures, faults, and geologic contacts. However, if this fracture-dependence is true, it is difficult to explain why geochemical and electrical anomalies are so well correlated in plan view with the lateral location of the hydrocarbons at depth, unless micro-fractures are so pervasive that faults and contacts provide only minor impedances to the migration. Hence, it is likely that most commonly encountered sedimentary units are, to one degree or another, significantly permeable to hydrocarbons of low molecular weight, regardless of fracturing.

3) *Depletion of hydrocarbons.* The low levels of hydrocarbons which migrate to the surface may decrease significantly as the trap is depleted of hydrocarbons, perhaps to the point of indetectability. Such an effect appears to have been observed by Horvitz (1969), who documented the disappearance of a geochemical anomaly over Hastings Field in Texas as the reserves were slowly diminished. Depletion of hydrocarbon reserves would slow the refueling process for the "shallow anomaly." It should then remain as a "fossil" anomaly or would disappear due to disruptive effects.

4) *Anomaly disruptive effects.* As noted earlier, hydrogen sulfide is unstable in an oxidizing environment, precipitating sulfur. If hydrogen sulfide oxidizes before it encounters a source of iron, no pyrite will be precipitated. Further, pyrite may also be unstable in an oxidizing zone, degenerating to iron oxide. Clay alteration is similarly sensitive to local conditions, especially to ion content of the waters and the degree of pore-fluid saturation.

A number of other limitations to the presence of "shallow" anomalies can also be raised. Therefore, a rather unpredictable anomaly of varying size, depth, and magnitude might be expected. This is precisely what is observed in the field. Hence, it is important to evaluate the absence or presence of the "shallow anomaly" in the light of the absence or presence of the "deep anomaly."

Conclusions on Mechanisms

It is clear from the preceding discussion that, while there is ample evidence for the existence of vertical migration and its effects on the sedimentary column, a great deal of work remains to be done. Therefore, any generalized theory of the origin of observed electrical anomalies must be largely speculative in terms of details. It is useful, however, to summarize the more important aspects of the problem.

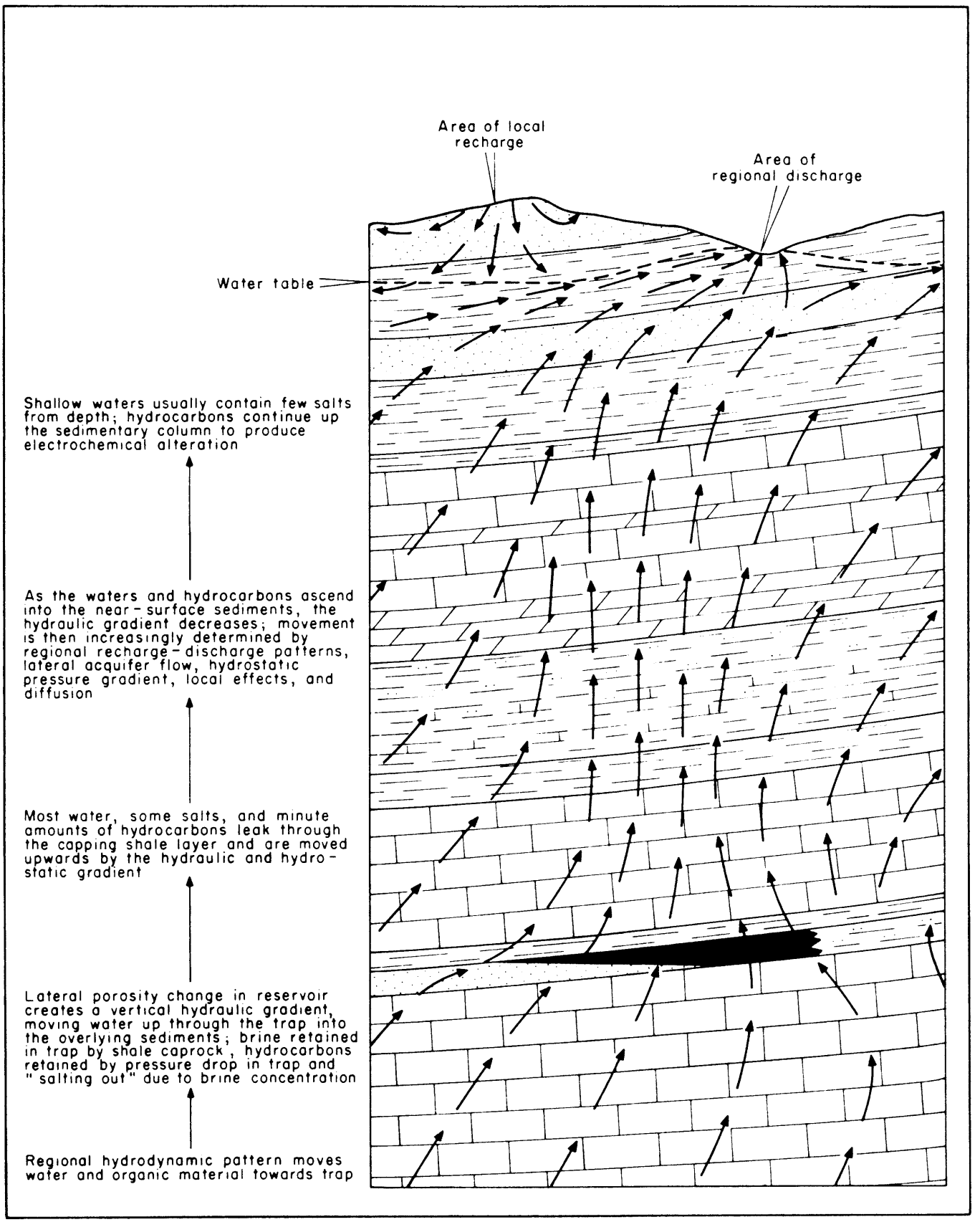

Figure 2.7. Hydrodynamic considerations in the origin of electrical anomalies. The figure is highly idealized for purposes of illustration. Figure 2.8 shows how the anomalies result from this pattern of water flow.

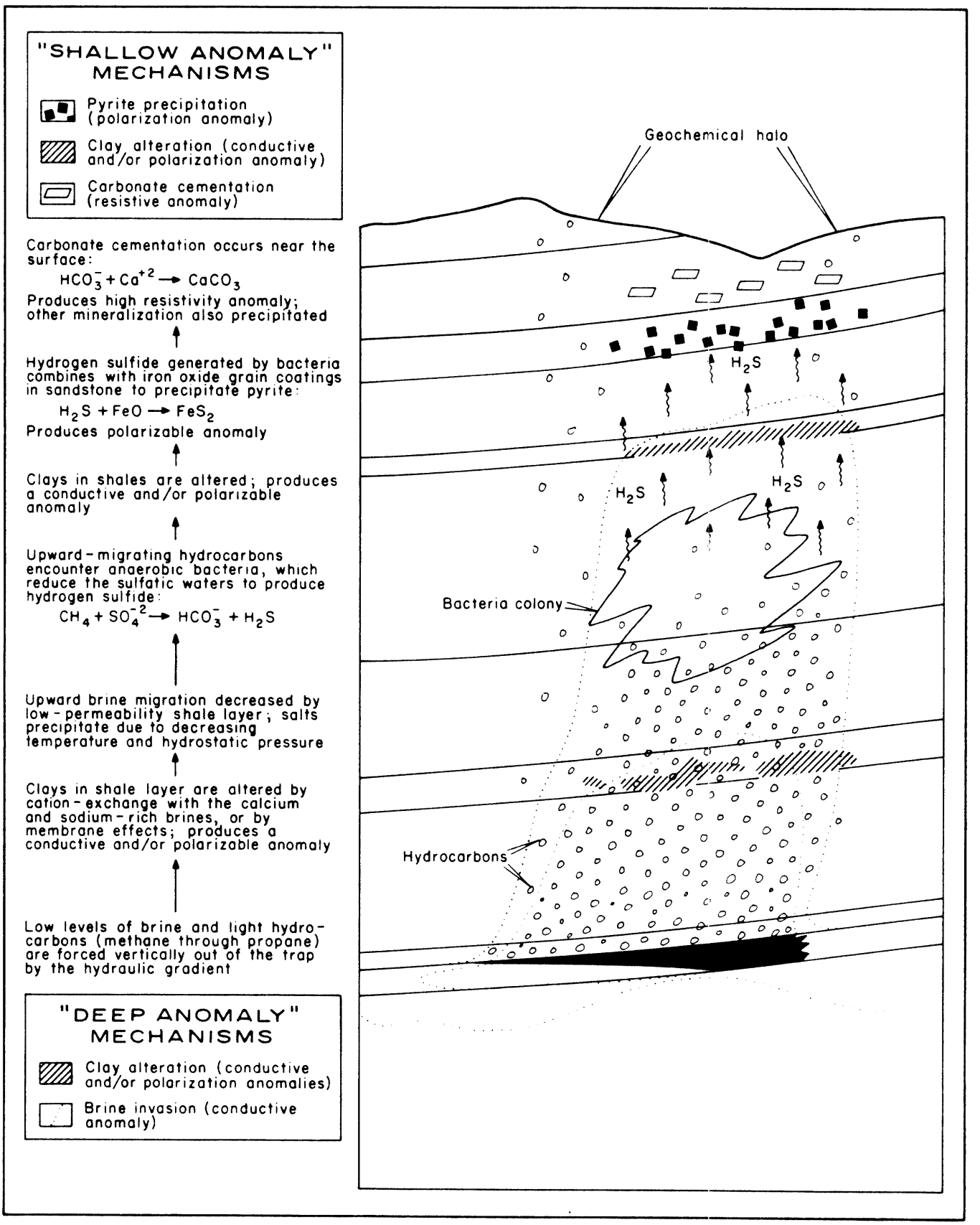

Figure 2.8. Proposed origin of the "deep" and "shallow" anomalies based upon the hydrodynamic considerations of Figure 2.7. The circumstances under which the proposed anomaly mechanisms are effective depend heavily upon geology; hence, the figure is highly idealized for purposes of illustration.

The theory presented in this chapter is based upon the upward migration of both saline waters and hydrocarbons from their trap at depth, both by hydraulic/hydrostatic means and by high-angle faults and fractures in the sedimentary column. Figure 2.7 shows a schematic representation of possible water flow patterns suggested by the theory, with specific reference to hydrodynamic processes (which may or may not be applicable in any given area). Figure 2.8 shows the resultant anomaly processes.

The theory helps explain two common types of electrical anomalies which are frequently encountered over oil and gas fields. The so-called "deep anomaly," a conductive, usually nonpolarizable feature, is attributed to vertical hydraulic discharge of brine from the top of the trap. The increased temperature of the discharged water enables it to retain a higher level of dissolved salts than surrounding waters, making it more electrically conductive. As the brine rises, cools, and enters areas of lower hydrostatic pressure, the salts are precipitated. Hence, the conductivity is greatest at depth, decreasing towards the surface. The so-called "shallow anomaly," a highly variable, polarizable feature, is probably related to pyrite or clay alteration. Pyrite is formed by the combination of hydrogen sulfide and iron in sediments at medium and shallow depths. The hydrogen sulfide is derived from leakage from sour hydrocarbon accumulations or through microbial degradation of lighter hydrocarbons; iron is derived from cementing material in sandstones or from free iron in meteoric waters. Clay alteration may have major effects on the data in some areas, due to ion exchange or membrane polarization effects. It remains to be seen how rising hydrocarbons in a reducing environment can affect the electrical properties of clays, but the subject should not be neglected. Minor resistivity anomalies near the surface may be due to mineralization, clays, or clastic cementation.

Future work in understanding the anomaly mechanisms is strongly advised, since this knowledge may eventually enable the geologist to extract more information from electrical data, such as depth and economic potential (two quantities which cannot be ascertained today). Research should be multidisciplinary, involving studies of geology, hydrology, fluid mechanics, geochemistry, and electrochemistry.

2.5 WELL-CASING EFFECTS

Introduction

In 1980 and 1981, Educational Data Consultants (EDCON) (Snyder et al., 1981) and Zonge Engineering (Zonge and Hughes, 1981) disclosed that they had measured apparent resistivity, apparent polarization, and electromagnetic coupling anomalies over several known hydrocarbon-producing fields. They claimed that these results indicated the presence of an alteration zone in the sediments above the hydrocarbons, a conclusion which suggested the induced polarization technique as a viable exploration tool in the search for oil and gas.

Almost immediately, Scott Holladay and Gordon West (1982) argued that the anomalies were not necessarily caused by true ground effects, but could very well be due to current channeling due to cased production wells. Using a modeling routine ("PIPE") developed at the University of Toronto, Holladay and West successfully simulated an apparent resistivity anomaly measured by EDCON over Lambert Field in Texas.

The well-casing problem can be illustrated by comparing the modeling results from a two-dimensional model of a "deep anomaly" to the results of a three-

dimensional model of well-casing effects. Figure 2.9 shows such a comparison for an idealized, elliptical-shaped oil field in which the producing wells are placed at regularly spaced locations. The first set of data (Figure 2.9a) was calculated for an idealized, cylindrical conductor extending vertically from the trap to 0.8 a-spacing of the surface. The results show a pronounced anomaly centered about the field. The second set of data (Figure 2.9b) was calculated for 7 well-casings placed symmetrically about the center of the field. The strong similarity in the results of these two widely differing models shows that, in this particular case, it would be difficult to distinguish well-casing effects from alteration effects. Obviously, then, one would be ill-advised to ignore well-casing effects in interpreting field data.

The issue of well-casing effects versus ground-alteration effects is still wide open to debate, and the applicability of the "PIPE" algorithm to field data figures prominently in the discussion of the case histories in this volume. Therefore, it is appropriate to describe the model, and to demonstrate some possible problems in its application.

Description of the Model

"PIPE" is an integral equation technique which calculates the effects at DC of infinitely long, hollow, cylindrical conductors lying vertically in a homogeneous half-space. The effects of each conductor are summed, and the net apparent resistivity and induced polarization effects are calculated as a function of field position for any four-electrode array. The details of the algorithm are scheduled for publication in an upcoming issue of *Geophysics.*

The input parameters for "PIPE" are: inner casing diameter, outer casing diameter, longitudinal conductance of the casing, wave number, complex impedance at the surface of the casing, planar location of the casings with respect to the survey line electrodes, and homogeneous half-space resistivity. Output consists of apparent resistivity and apparent polarization. For purposes of this volume, data are plotted in pseudosection form for the dipole-dipole array.

A number of tests were undertaken to ensure logical self-consistency of the model and to determine its limitations. The material presented in this volume represents modeling within those limitations.

Problems with Using "PIPE"

There are some significant limitations to applying "PIPE" to data measured in the field, limitations which must be borne in mind when evaluating data calculated by the model. The object here is not to discredit the model, but to qualify its use in this volume. The work of Holladay and West is an achievement of fundamental importance in understanding induced polarization data, and those who seek to understand those data are indebted to these workers for their pioneering achievement. This section sets the context in which the model results can be used most successfully.

VARIABILITY OF WELL-CASING RESPONSE: A CASE HISTORY

The main problem with "PIPE" is not related to the algorithm at all, but is really a problem with the unpredictability of well-casing effects. It has been observed in field work that drill stem, which from an electrical standpoint should behave similarly to well casings, has usually (but not always) failed to produce any noticeable effects in the data. It has also been observed that many cased wells which lie close to receiving electrodes often show no strong effects. On the other hand, some cased wells cause extreme effects (see, for example, the Desert Springs case history of Chapter 4). In some field studies, wells of the same diameter, depth, and age respond in a radically different manner along the same survey line. This recalls

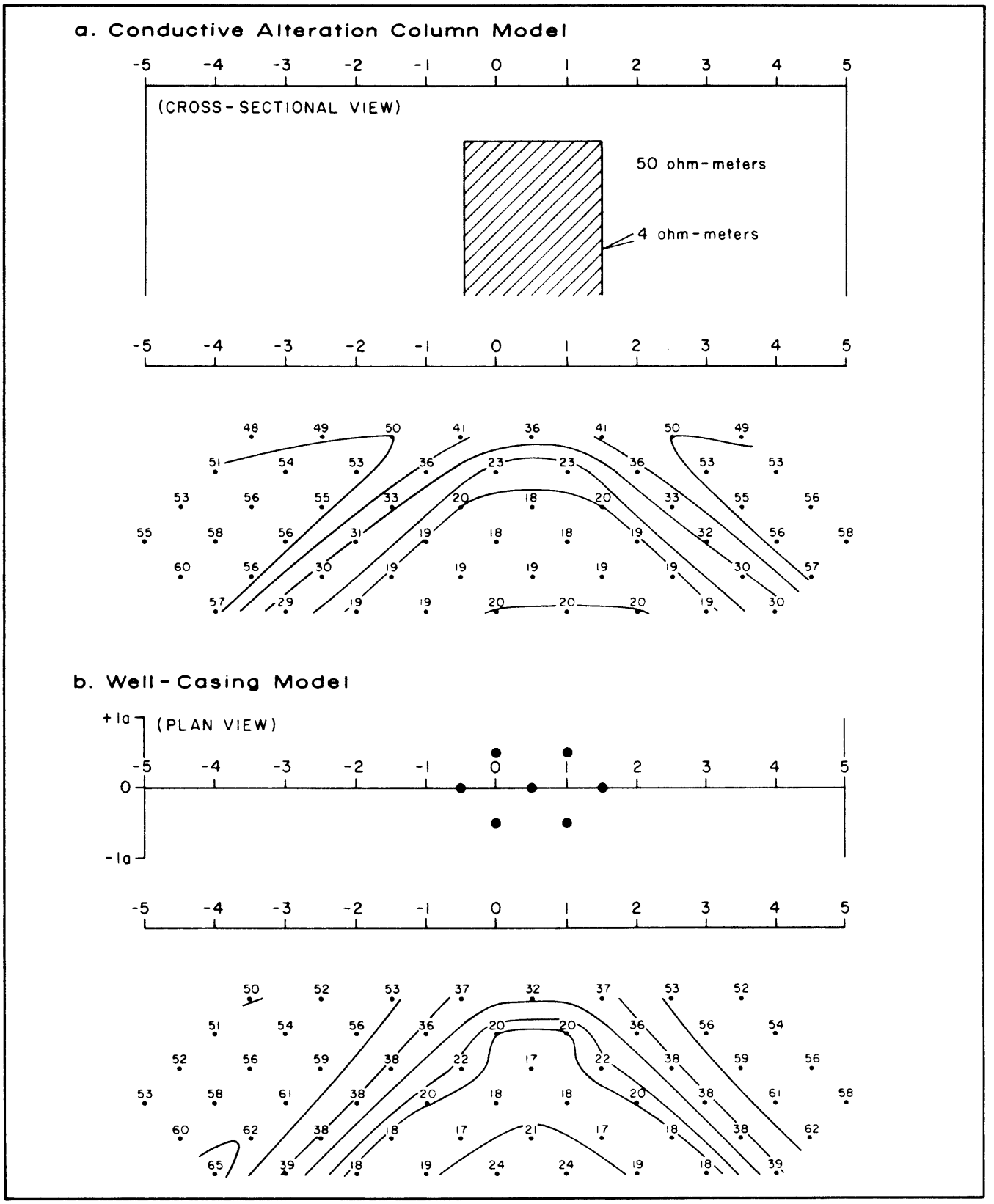

Figure 2.9. Results of computer modeling of apparent resistivity which compare the effects of a conductive alteration column over a hydrocarbon trap to the effects of well casings. a) Location of the conductive column (cross-sectional view), and results of the two-dimensional IP model "2DIP." Background resistivity = 50 ohm-meters. b) Location of the well casings (plan view), and results of the well-casing model "PIPE". Model parameters: well-casing diameter = 5.5 inches (14.0 cm), casing resistivity = 2.0×10^{-7} ohm-meters, surface impedance = $0 + 0i$, background resistivity = 50 ohm-meters. Refer to the text for an explanation of these parameters.

the extreme variability of responses from other grounded metal features such as pipelines, fences, and powerlines. If well-casing responses are unpredictable, it is impossible to model them successfully with confidence.

An example of the variability of well-casing response is provided by complex resistivity data obtained over Garza Field, located just east of the town of Post, in Garza County, Texas. The field has been producing oil from the San Andres and Glorieta formations of the lower Permian since the discovery well was drilled in 1935 (Myres, 1977). Drilling has continued up to the present. The field produces 36° API gravity oil primarily from the fine-grained, crystalline dolomites of the San Andres Formation between 2,910 and 3,260 feet (887-994 m). The trap is stratigraphic in nature; permeability is primarily intercrystalline.

Three lines of complex resistivity were obtained over Garza Field, using an a-spacing of 1,000 feet (304 m). Line 1, whose location is shown in Figure 2.10, is of particular interest in that data were obtained over it on three separate occasions. The first work involved a standard center-spread arrangement using nine transmitting electrodes. The second set of data was obtained over line 1, but with all dipoles shifted by 0.5 a-spacing. After these data were collected, four new producing wells were drilled in the vicinity of the line. About one month after drilling, line 1 was reoccupied in order to provide a check on well-casing effects. In order to distinguish the three sets of data, the following terminology will be used in this discussion.

1. Original data set: electrodes at integral-numbered stations.
2. Second data set: electrodes shifted half a dipole spacing to non-integral numbered stations.
3. Third data set: after drilling, electrodes at integral-numbered stations.

Apparent resistivities are about 10 ohm-meters on the line (Figure 2.11). A distinctive but low-amplitude conductive anomaly is superposed upon the low-over-high resistivity layering. This anomaly is well correlated with the producing zone; modeling strongly indicates that it is not due to well-casing effects, although some question remains about the effects of surface pipelines and powerlines. The low overall resistivities in the area make it difficult to perform a before-and-after well casing comparison for the apparent resistivity parameter, but the high phase response measured over the field shows more diagnostic effects.

Figure 2.12 shows both the field data and well-casing model data for apparent polarization, plotted at 0.125 Hz. The field data (Figure 2.12a) show a very strong polarization anomaly which is well correlated with the location of oil production. The peak response has the appearance of an inverted chevron centered on station 6, with a weaker response zone flanking it towards the southeast. The diagonal effects within this anomalous zone suggest the possibility of cultural contamination. The well-casing model of Figure 2.12b shows a similar chevron-shaped anomaly, with two substantial differences: first, the model anomaly is shifted with respect to the field anomaly by about 1,000 feet (300 m), and second, the strong polarization increases at depth which are evident in the field data are not reproduced by the model. However, the model does reproduce the general outline of the anomaly.

After the initial phase of field work was completed, four new wells were spudded near the line. All four were completed in the San Andres. In order to provide a direct before-and-after study of well casing effects, the Zonge Engineering crew returned to Garza Field, re-occupied the original stations exactly, and re-ran part of the original line. The data are compared to the original data set in Figure 2.13.

A comparison of the before-drilling and after-drilling data is very interesting. Most of the phase values compare relatively well. Some phases in the after-drilling

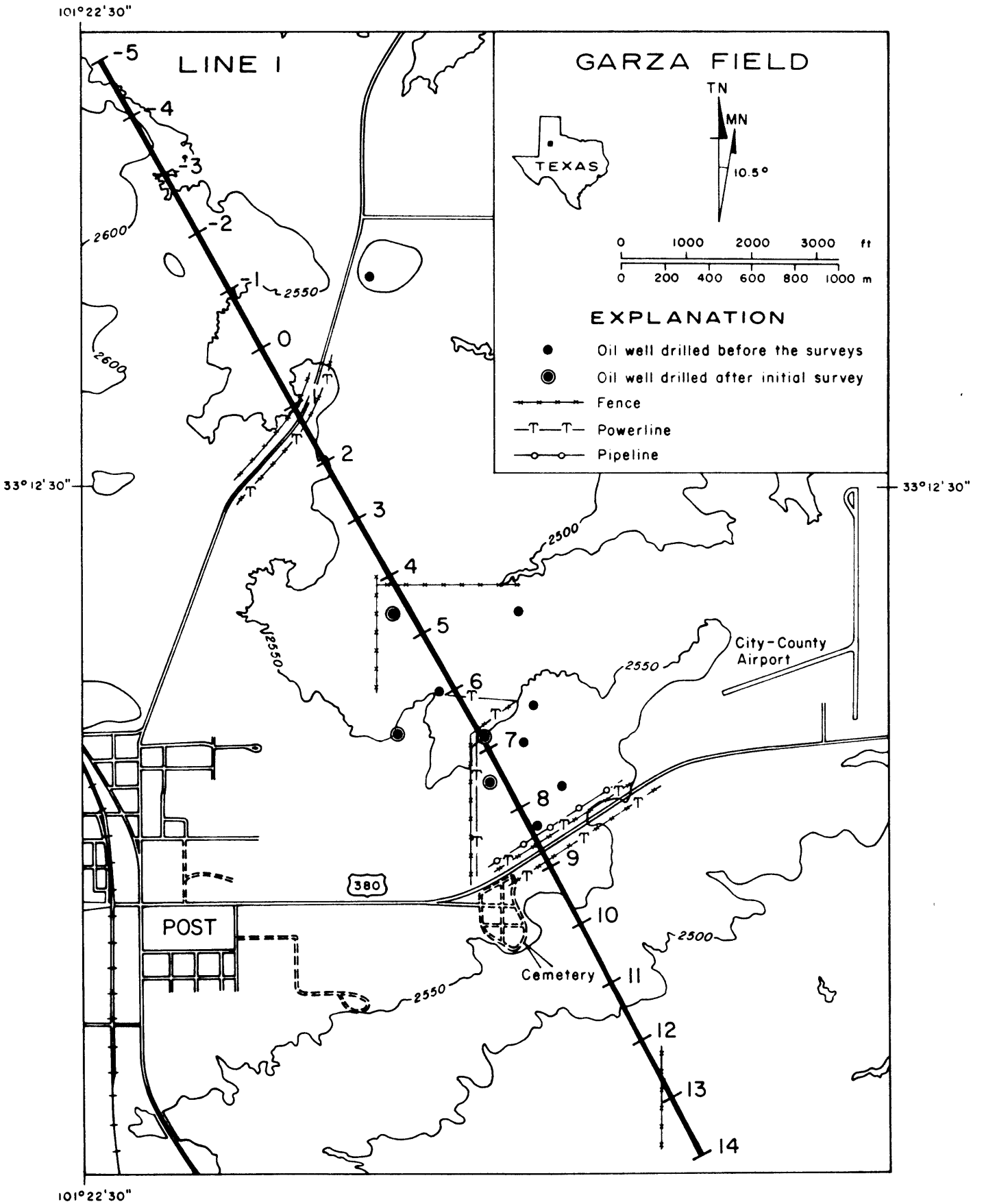

Figure 2.10. Location map of line 1, Garza Field, Garza County, Texas.

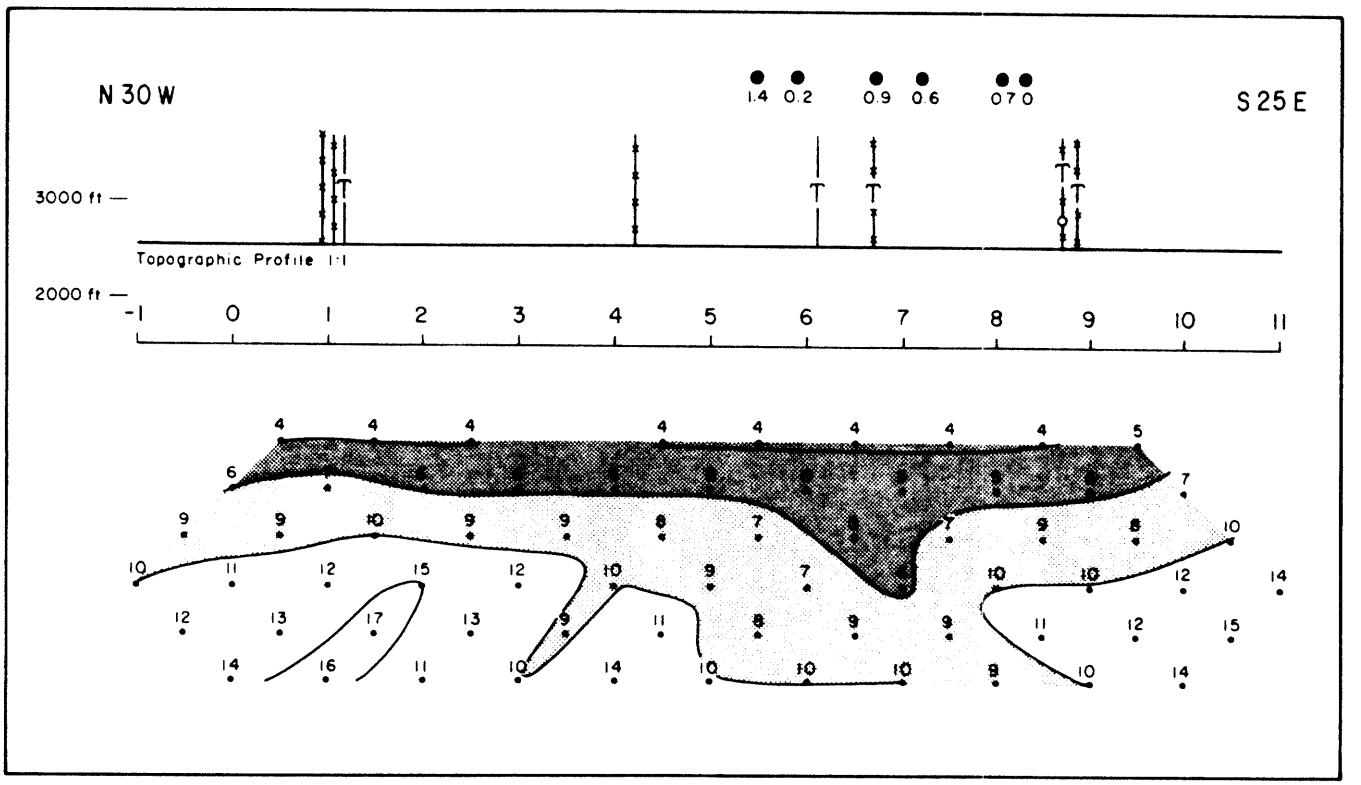

Figure 2.11. Apparent resistivity field data, Garza Field, for the original data set (see text). Contour interval: 1.0, 1.6, 2.5, 4.0, 6.3, 10.0, . . . ohm-meters. For explanation of symbols, see Figure 2.10.

survey are lower, but none are significantly higher. Now compare these data to the before-and-after well-casing model simulation of Figure 2.13b. These model data predict strong near-surface responses from the new well casings, especially at the n=1 position beneath station 4.5 and along the left-plunging 7,8 diagonal. None of these predicted changes are evident in the field data, however.

At this point, we are faced with three possibilities: 1) the polarization response at Garza is primarily due to the well casings, but they respond in an erratic and unpredictable manner; 2) the response has very little to do with well casings, but is due to surface culture and alteration of the sediments overlying the oilfield; 3) the response is a combination of both the above. In examining the first possibility, we would initially suspect that the well casing near station 5.9 is easily the strongest responder; yet, well-casing modeling shows much too strong a surface response and too weak a deep response to support such a conclusion. Clearly, the data are affected by more than well-casing effects, since the character of the data and the character of well-casing effects are fundamentally different. The second possibility, i.e., that well-casing effects have no effect on the data, is also unlikely, since modeling does resemble some of the trends seen in the data. It is therefore believed that non-casing effects are more important than casing effects, although both are present in the field data.

Additional evidence that well casings do not produce the bulk of the anomaly is provided in Figure 2.14, which compares the original set of resistivity data with the second set of data, in which the line was shifted by exactly half a dipole spacing. It is known that when electrodes are moved with respect to a surface feature, the character of the anomaly changes substantially (see, for example, the apparent resistivity changes in Figures 2.15a and 2.15b in section 2.6). However, the only major change between the original and the shifted data at Garza Field is the elevation of mid-pseudosection phases beneath station 8.5 and the drastic lowering

of the left-plunging 8,9 diagonal; otherwise, the two sets of data merge quite satisfactorily. Modeling indicates that the intense powerline-pipeline-fence cluster at station 8.5 is responsible for the variations between the two data sets. Note, however, that the well casings do not produce a similar change. This suggests that well casings do not cause the majority of the response at Garza Field.

The conclusion to this investigation is that extreme variability in individual casing responses makes modeling very difficult. Therefore, one should be cautious in drawing unwarranted conclusions based upon the "PIPE" modeling alone.

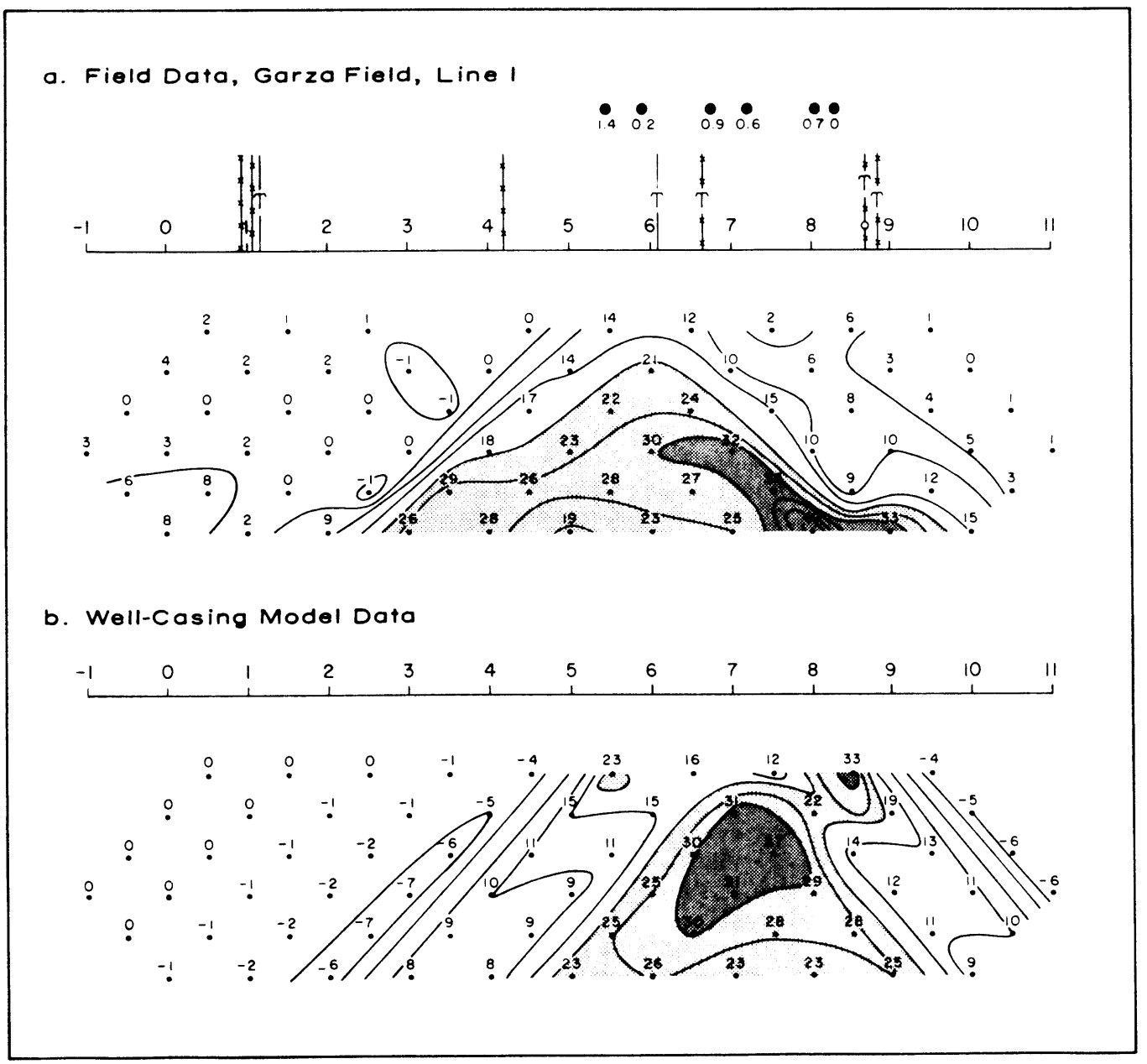

Figure 2.12. Apparent polarization field and well-casing model data, Garza Field, for the original data set (see text). Contour interval: 0, 5, 10, . . . milliradians. Model parameters: 6 well-casings, casing diameter = 4-1/2 inches (11.4 cm), casing resistivity = 2×10^{-7} ohm-meters, surface impedance = $1.0 + 1.8i$, background resistivity = 10 ohm-meters. For explanation of symbols, see Figure 2.10.

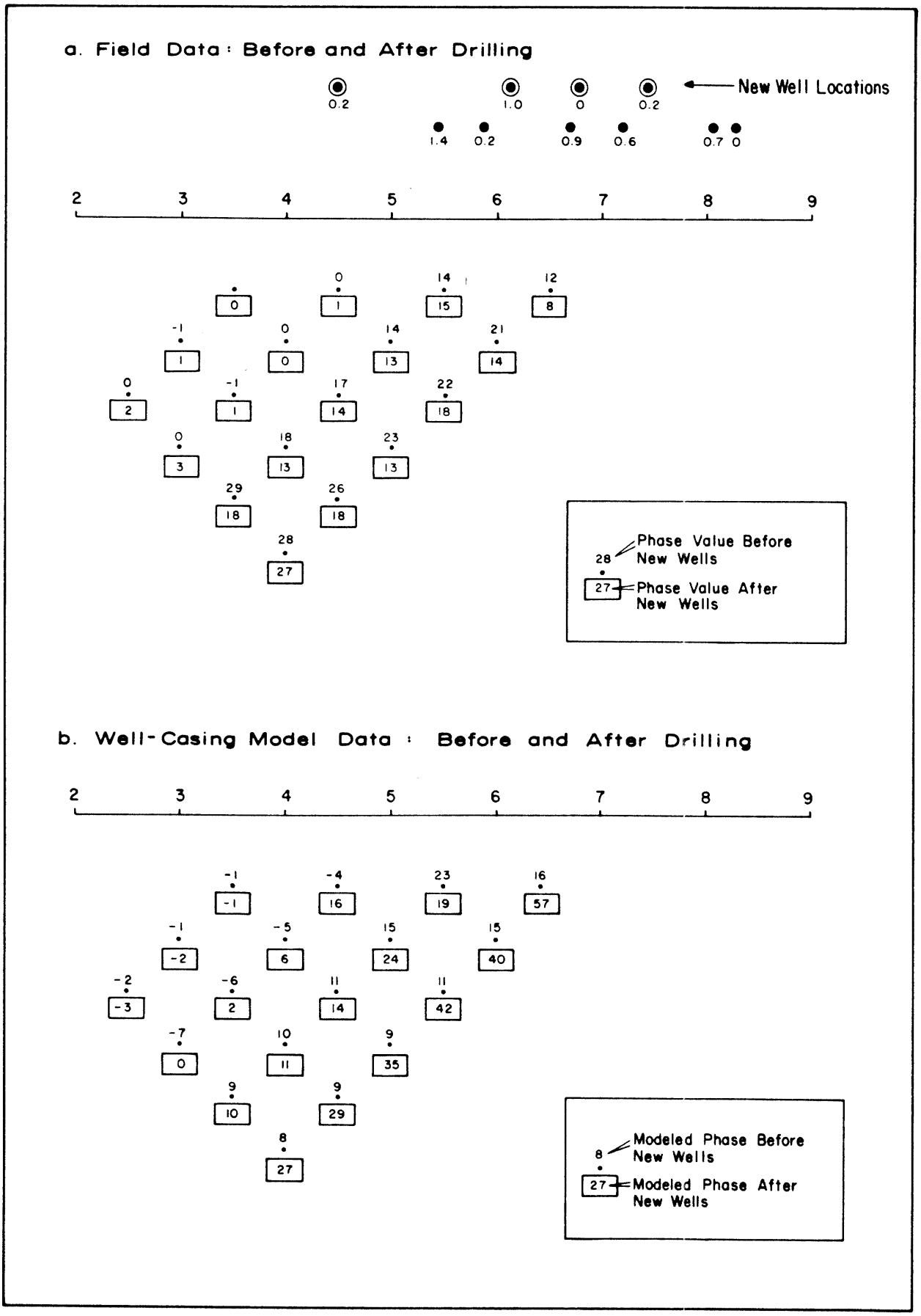

Figure 2.13. Apparent polarization for field and well-casing model data, Garza Field, comparing the original data set to the third data set, which was obtained after development drilling (see text). Contour interval: 0, 5, 10, . . . milliradians. Model parameters: 10 well-casings; other parameters same as in Figure 2.12. For explanation of symbols, see Figure 2.10.

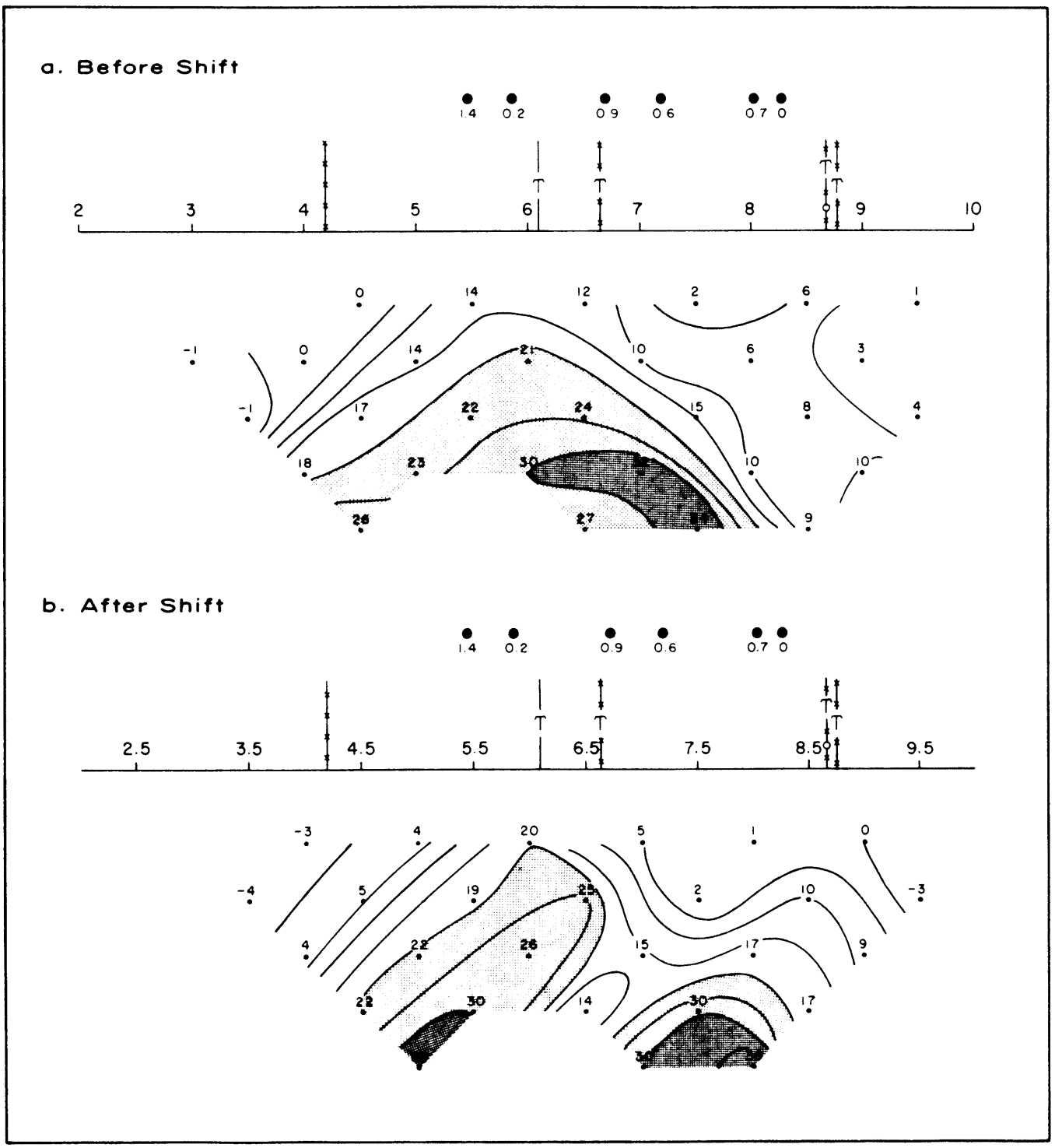

Figure 2.14. Apparent polarization field data, Garza Field, comparing the first data set to the second data set, in which the electrodes were shifted by 0.5 a-spacing (see text). Contour interval: 0, 5, 10, . . . milliradians. For explanation of symbols, see Figure 2.10.

PROBLEMS WITH SURFACE IMPEDANCE DETERMINATION

The well-casing modeling of Garza Field was accomplished by adjusting the complex surface impedance assigned to the casings in order to achieve a best fit with the polarization data. In a very real sense, this is forcing the model to look like the data, and it injects a note of arbitrariness into the modeling process.

The solution to this is to measure the impedance of each well casing within at least one a-spacing of the line. This is not at all a trivial task, since it is difficult to measure a complex surface impedance to any degree of accuracy, and modeling shows that the figure must be very accurate. Some research is underway at Zonge Engineering to measure the real component of the surface impedance of a well casing in order to compare it to field data; initial indications are that this process would be prohibitively expensive if numerous well casings had to be measured in a typical survey.

The surface impedance problem indicates that, in most instances, the best use of modeling data is to evaluate overall trends in the field data, not specific features or magnitudes of responses.

PROBLEMS WITH THE HOMOGENEOUS EARTH ASSUMPTION

Layering effects can radically alter the appearance of data affected by lateral features such as well casings. Unfortunately, since "PIPE" does not permit layering effects to be included in the modeling, the model data and the field data are often difficult to compare properly. Holladay (1983) is developing an improved algorithm which may alleviate this problem.

PROBLEMS WITH VARIATIONS IN WELL-CASING GEOMETRY

The present modeling routine accepts only a single casing diameter, whereas wells are normally set with several sizes of surface and production casing. Modeling indicates that casing size has an appreciable effect upon the magnitude of the calculated effect. A related problem is that "PIPE" assumes an infinitely long casing, which may not be a viable assumption.

Well casings are often interconnected mechanically and electrically by supply pipelines. Considering the dramatic effects which pipelines alone can have on field data, connections with well casings could produce an overwhelming effect, as noted over Desert Springs Field (Chapter 4). Unfortunately, the solution of this kind of a problem is unlikely with an integral equation technique like "PIPE" (Wait, 1983).

PROBLEMS WITH THE DC APPROACH

"PIPE" calculates a strictly DC galvanic effect. It involves no electromagnetic effects whatever. This is an inconvenience, particularly when REM effects are interpreted, but a minor one when compared to other restrictions of the model.

Use of "PIPE" in the Case Histories

The preceding discussion urges great caution when using "PIPE" or any other model which oversimplifies a situation being modeled. However, it is beyond question that well casings have an effect on some data sets, despite the extreme variability of response from well to well. Therefore, we have elected to use "PIPE" in this volume of case histories under the very restrictive condition that only the *qualitative* aspects of the calculated data be used for interpretation. Again, we summarize the restrictions of the model:

1. "PIPE" treats all casings alike, despite field evidence that casing effects are highly variable.
2. The surface impedance of the model is arbitrary, i.e., unless surface impedance measurements are made in the field, the parameters must be varied

arbitrarily to resemble the field data, especially in modeling apparent polarization data.
3. Geoelectric layering effects cannot be accommodated by the model.
4. Different well-casing sizes, interconnection of casings via surface pipelines, or finite-length casings cannot be modeled.
5. "PIPE" applies strictly to the DC case—no EM effects are calculated.

As a result of these problems, and the fact that "worst-case" parameters are often used to force an anomaly, "PIPE" often tends to "overmodel" field data by calculating a larger effect than is observed. Its chief utility, therefore, is to estimate the overall shape of the model data for comparison to the overall shape of the field data.

CALCULATION OF "RESIDUAL" DATA

In order to facilitate comparison of these data sets, a simple superposition technique has been used for apparent resistivity data in the case histories. The technique involves a point-for-point calculation of the ratio of the background resistivity (ρ_B) used in the model to the calculated apparent resistivity (ρ_C), and then multiplying it by the corresponding apparent resistivity (ρ) measured in the field, to yield the "residual" apparent resistivity ($\rho_{residual}$):

$$\rho_{residual} = \rho\,(\rho_b/\rho_c) \tag{2.9}$$

The residual data, then, represent what is left over when calculated well-casing effects are removed from the field data. This in no way implies total acceptance of the well-casing model; it merely shows a residual under the temporary assumption that the well-casing model is correct. The chief restriction of the residual calculation itself is that apparent resistivities measured in the field are close to the background resistivity used in the model; extreme differences will cause too large or small a correction to be applied to the data. In general, however, the residual calculation represents the difference between modeled and field data fairly, as long as field resistivities are within 50 to 100 ohm-meters of the assumed background resistivity used in the model.

MODELING PARAMETERS USED

Our approach in using "PIPE" is to try to show the *worst* effects which can reasonably be calculated with the model. If worst-case effects are removed from the data, and a residual anomaly remains, then one would be inclined to conclude that the anomaly cannot be caused entirely by well-casing effects, especially if the character of the field data differs from the character of the model data in a fundamental way. It should be borne in mind that this is really an extreme perspective taken only to argue a point of logic; in actuality, the well-casing effects observed in the field are frequently much less than those calculated by the model. This is demonstrated in several of the case histories.

In order to achieve a reasonable worst-case model, the following parameters were used:

1. Well-casing diameter is the diameter of the largest well casing used in the field at depths greater than 0.25 a-spacing. Inner diameters are, by industry convention, fixed by the outer diameter.
2. Well-casing resistivity is 2.0×10^{-7} ohm-meters, the value of the most conductive material normally used for casing and drill stem (U.S. Steel, 1983).
3. All cased wells within three a-spacings of the line were included in the model. All are assumed to have a maximum electrical response.

4. Real and imaginary coefficients for the complex surface impedance were usually set equal, and the value was adjusted in order to force the polarization model into a best fit of the field polarization data.
5. No attempt was made to model cementation effects, since modeling indicated that these were relatively minor, and since cementation practices vary with depth in many of the wells included in the case histories.
6. Wave number bounds were set between zero and −17, as suggested by Holladay and West.
7. Wells were located by Petroleum Information lease-ownership maps. All wells in progress at the time of the survey were included, under the assumption that the electrical effects due to drill stem should be similar to those of cased wells.

2.6 SURFACE CULTURE EFFECTS

Surface Pipelines

Well casings are by no means the only source of cultural contamination in surface electrical measurements over oil and gas fields. Perhaps the worst offenders are grounded metal pipelines, which are common in most producing fields. Pipelines may produce artificial low resistivities, high polarization values, both, or neither; responses are generally unpredictable. Usually, a pipeline effect is strongest at the surface, with strong diagonals in an inverted chevron shape, as shown in the model data of Figure 2.15. The appearance varies considerably, depending upon the relative location of the pipeline with respect to the electrodes, as shown by the comparison of Figures 2.15a and 2.15b. An example of pipeline contamination of apparent resistivity data is provided in the discussion of Desert Springs Field in Chapter 4; an example of pipeline contamination of apparent polarization data is provided in the discussion of Line 2 at Lisbon Field in Chapter 6. Multiple pipeline effects are shown in the discussion of line 1 at Little Buck Creek, presented in Chapter 5.

As pointed out by Wynn and Zonge (1975), cathodic protection on pipelines can produce an additional coupling effect, especially at higher frequencies. Consequently, it is often advisable to have the protection turned off for the duration of the survey, especially to avoid the noise effects due to the unstable rectified waveform.

The situation to be avoided most is locating the survey line close to a parallel, grounded pipeline. This arrangement may cause severe coupling contamination of the data, wiping out any useful interpretation. The reason for this is that two parallel line elements are in a maximum coupling configuration. It is best to run survey lines perpendicular to pipelines—the minimum coupling configuration.

The extreme variability of pipeline effects is not understood, but it is a commonly encountered phenomenon and may be related to the quality of contact a given pipeline makes with the ground. Data on a number of survey lines have shown strong effects due to one pipeline but not the other. Effects cannot be predicted without making detailed surface impedance measurements. However, it is important to note that pipeline effects, when they are present in a set of data, can be recognized for what they are and are not easily confused with true alteration anomalies.

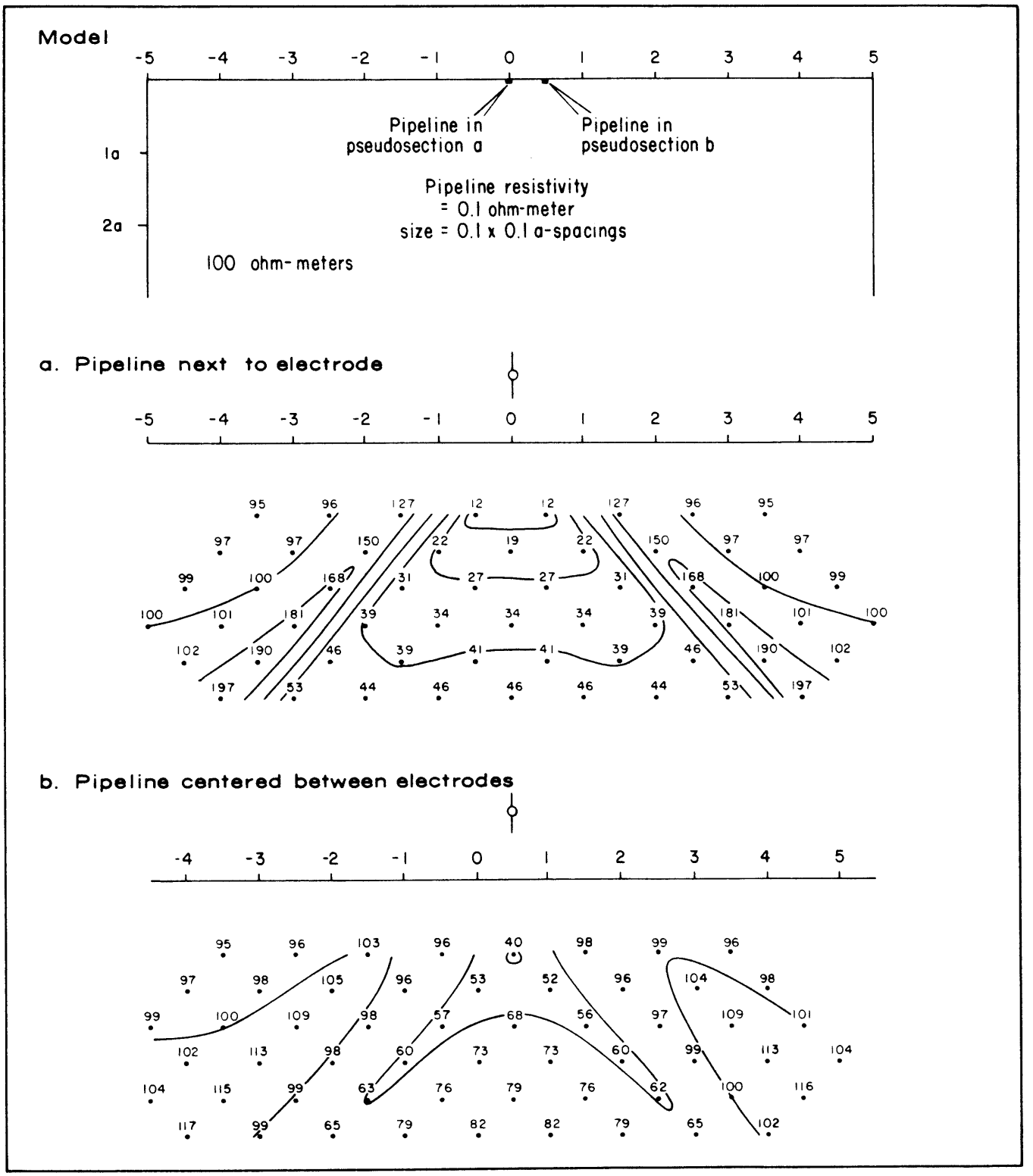

Figure 2.15. Two-dimensional resistivity model ("2DIP") of a pipeline, simulated by a very small solid conductor with rectangular cross-section, crossing the line at right angles. The pseudosections show the data resulting from a pipeline crossing the line at an electrode and crossing between two electrodes. Contour interval: 10.0, 15.9, 25.1, 39.8, 63.1, 100.0, . . . ohm-meters.

Powerlines

Powerlines, especially high-voltage, grounded ones, can produce fairly large effects on apparent resistivity and apparent polarization data. An example of powerline effects is noted above in the discussion of Garza Field (section 2.5). Powerline effects are less frequently seen in the data than are pipeline effects, and these effects are often (but not always) less than those due to pipelines. Powerline effects take on the expected diagonal or chevron appearance exhibited by other cultural features. The exception to this is a powerline running parallel to the survey line within one a-spacing. This kind of a situation is avoided in the field whenever possible due to the peculiar data contamination it often produces.

Fences

Fences can also produce strong diagonal effects in the data. The response or non-response of the fence is not predictable without making the necessary impedance measurements (Nelson, 1977); however, fence effects are usually easily recognized as such when they do appear. The worst effects are associated with well-grounded, metal-stake fences which extend over large distances and fall close to electrode stations. Fences which run parallel to the line within one a-spacing may severely compromise the integrity of the data. If possible, lines are oriented so that the fences cross at high angles and between electrodes.

Other Cultural Features

Other cultural features encountered in oilfield surveys involve buried cables, metal buildings, irrigation ditches, and so forth. These features may occasionally produce spurious responses in the data, but no examples of such are present in any of the case histories of this volume.

2.7 TOPOGRAPHIC EFFECTS

Introduction

Apparent resistivity calculations, and to a lesser extent REM calculations, are affected by topography in that the relative dipole orientations are changed, as are the current distribution patterns in the earth. Strong effects can result from slopes of over 10 degrees, as described by Fox, Hohmann, and Rijo (1978). The approach taken in this study to deal with topography is to process the data normally, as if it were obtained from a strictly collinear, flat-earth dipole-dipole array, and then to interpret the nature of topographic effects by computer modeling.

The "2DIP" Algorithm

The algorithm used for all two-dimensional IP modeling in this volume is "2DIP," a finite-element routine which calculates apparent resistivity and apparent polarization effects for the dipole-dipole array. The model can include topography as well as buried structures and layers. Up to nine finite bodies can be modeled. A fine triangular mesh (69 x 20) is normally used for modeling in order to minimize edge-boundary effects.

The "2DIP" algorithm has shown its reliability in in-house modeling at Zonge Engineering for about two years. A number of reliability and limitations tests have been performed. The only significant problem which has been discovered is an artificial, low-over-high layering imprint upon all data, including a homogeneous earth model. Resistivities vary about 10 percent from n=1 to n=6, and the reader should bear this in mind when considering the model results. Two modeling limitations should also be borne in mind. One problem is that any off-line effects, such as those due to mesas and cliffs, cannot be modeled. This also means off-line

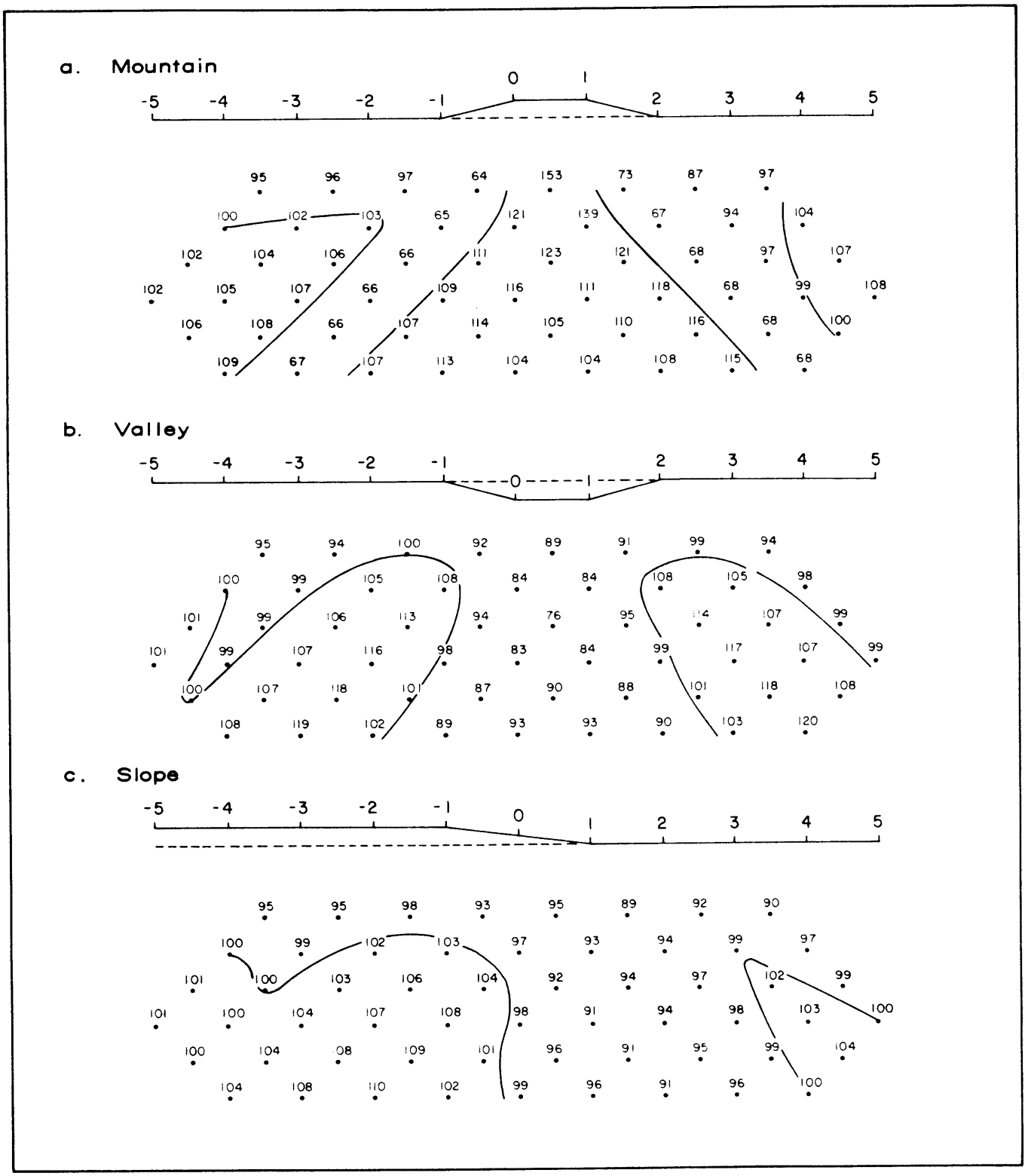

Figure 2.16. Two-dimensional resistivity model ("2DIP") of topographic effects due to a mountain, a valley, and a monoclinal slope change. The elevation change in each model is 0.25 a-spacing. Contour interval: 10.0, 15.9, 25.1, 39.8, 63.1, 100.0, . . . ohm-meters. Background resistivity is 100 ohm-meters.

buried structural changes and non-perpendicular structures, such as subparallel faults and plunging folds, cannot be modeled accurately. Another limitation of "2DIP" is that model parameters are completely arbitrary and non-unique. Since resistivities and phase angles of each body may be adjusted in order to force-fit the model data to a set of field data, "2DIP" models present only one possible geoelectrical solution, not a unique geoelectrical solution.

Examples of Topographic Effects

The effects of topography on apparent resistivities of a homogeneous earth are predictable in the two-dimensional case. A mountain (Figure 2.16a) will produce a high resistivity feature beneath it in the pseudosection, flanked by low resistivity diagonals extending to depth. A valley (Figure 2.16b) will produce essentially the opposite effect, i.e., a central, low resistivity zone flanked by high resistivity diagonals. Note that a "valley effect" of this type could conceivably enhance or even produce a false low resistivity anomaly at depth. This emphasizes the importance of careful topographic modeling on projects with appreciable topography. A third example of topographic effects involves a change in slope from a high area to a lower area (Figure 2.16c). In this case, one obtains an asymmetric pseudosection in which a low resistivity diagonal points in the direction of the change in slope.

Additional complicating factors arise when a layered or dipping stratigraphic section of alternating resistivities intersects a surface of varying topography. In this case, it is often necessary to model both the effects of topography and geology. An example is shown in the following discussion.

2.8 SUBSURFACE GEOLOGIC EFFECTS

Stratigraphic and structural changes in the subsurface often influence the data significantly, and this is often an aid to interpreting data in areas with poor geologic control. While it is true that electrical techniques typically detect only changes in conductivity and polarizability, these properties are often intimately tied to lithology. Good examples of geoelectric mapping are presented in the case histories.

The main goal in making electrical measurements, however, is not to map lithology, since this can be done in greater detail and with much better depth control using reflection seismic techniques. Rather, the real utility of electrical measurements in petroleum applications is the detection of anomalous behavior which is indicative of oil or gas at depth. In this context, the imprint of subsurface geology must be well understood in order to avoid confusing it with true hydrocarbon responses.

There are several commonly encountered situations which make interpretation difficult. The first, and perhaps the worst, is the problem of a discontinuous high resistivity surface cover, such as volcanics. Resistive blocks tend to channel current flow around them, creating an artificial low resistivity zone below them in the pseudosection. This kind of an effect is illustrated in Figure 2.17. Since one of the features being looked for in hydrocarbon surveys is low resistivities at depth, it is critical to evaluate whether such features are due to surface effects or to hydrocarbon-related "deep" anomalies. This kind of an evaluation is best done with the aid of computer modeling and geologic information.

Another situation which engenders some difficulties involves selective topographic exposures of layered stratigraphy. The effects which are observed from such a situation depend upon the resistivities of the layers and their outcrop positions with respect to the electrodes. Figure 2.18 shows a typical example of the problems

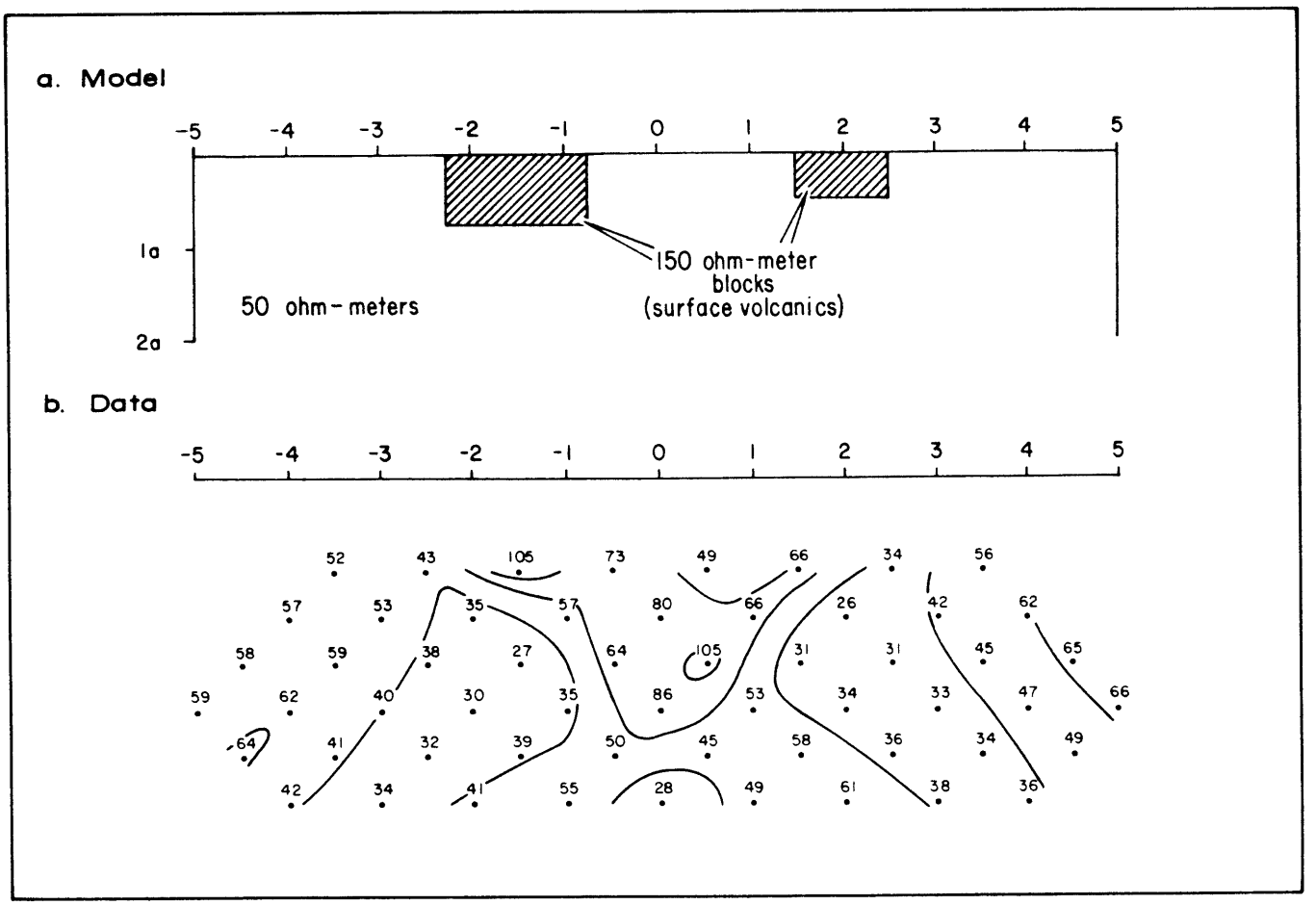

Figure 2.17. Two-dimensional resistivity model ("2DIP") of the effect of two discontinuous high resistivity blocks at the surface of a homogeneous earth. The geometric low resistivities produced by current channeling around those blocks could be misinterpreted as "deep anomalies" if care is not taken in evaluating the data. Contour interval: 10.0, 15.9, 25.1, 39.8, 63.1, 100.0, . . . ohm-meters.

which can arise. The model shows the effects when topography cross-cuts horizontally-layered stratigraphy. In this case, some complexity is evident in the data, and a strong low resistivity anomaly at depth is apparent. Without adequate geologic knowledge, interpretation experience, and modeling facilities, there can be serious difficulties in distinguishing this topographic-structural anomaly from a "deep anomaly" due to conductive alteration above a hydrocarbon trap. In order to deal effectively with this problem, extensive two-dimensional modeling is quite useful.

Obviously, complicated geologic stratigraphy and structure make interpretation more difficult when no geologic information on the field site is available. Without geologic knowledge, it is certainly possible to come up with a geoelectric interpretation, but that interpretation will be unconstrained by geology and might include assumptions which are unrealistic. Hence, it is important to combine the geophysical and geologic data in order to arrive at a reasonably useful electrical model of the subsurface.

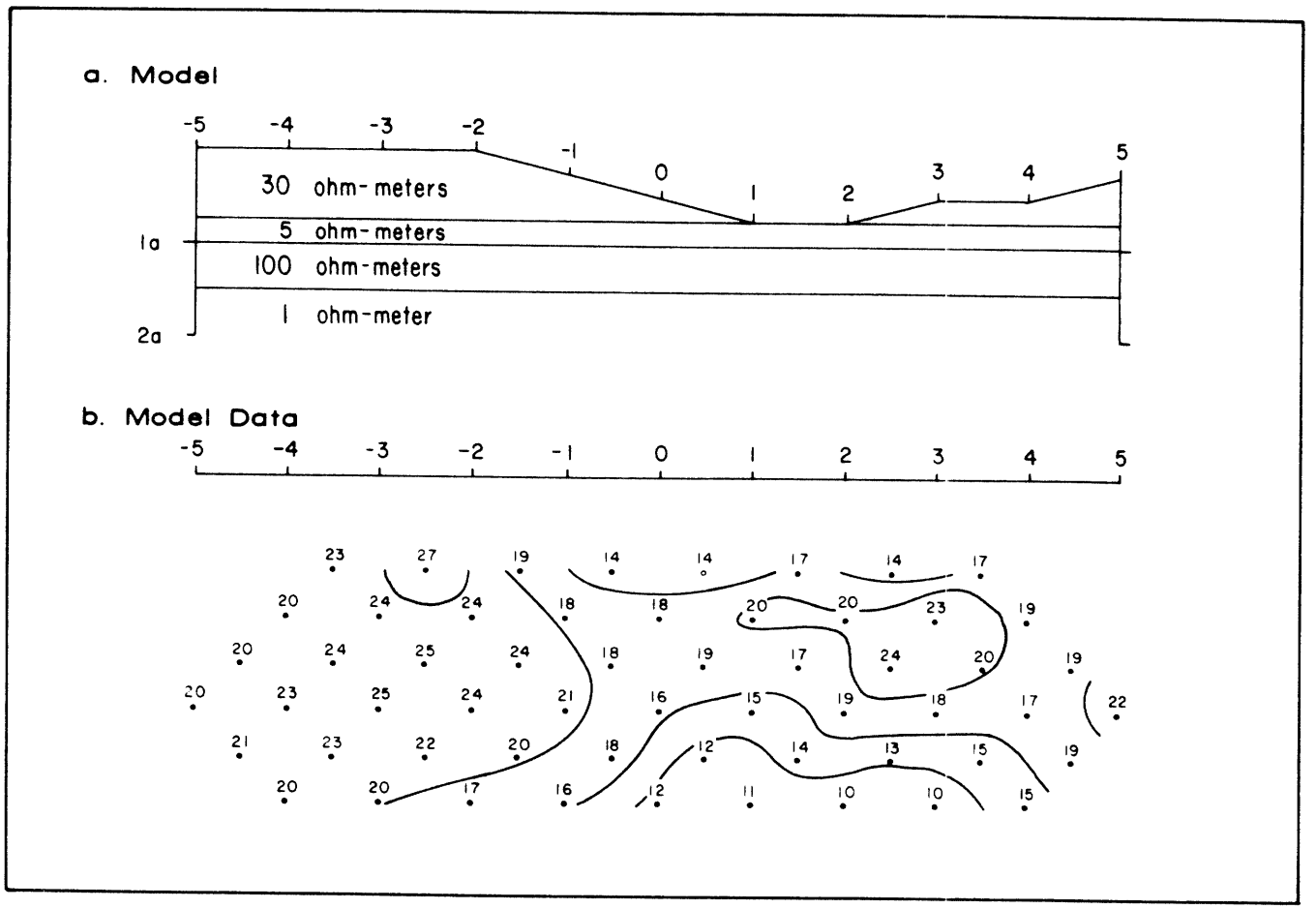

Figure 2.18. Two-dimensional resistivity model ("2DIP") of the effects due to layering which is cross-cut by varying topography. Note the artificial low resistivity zone at depth, which spuriously resembles a "deep anomaly." Contour interval: 10.0, 12.6, 15.9, 20.0, 25.1, 31.6, 39.8, 50.1, 63.1, 79.4, 100.0, . . . ohm-meters.

2.9 ANOMALIES DUE TO HYDROCARBON ALTERATION— WHAT TO LOOK FOR

We have seen some examples of spurious effects due to culture, topography, and geology in the preceding sections, but what should anomalies due to alteration by hydrocarbons look like? There is no simple answer. While endless speculations can be made regarding what alteration anomalies should look like based upon preconceived notions about the mechanisms which produce them, it is more useful to review some empirical observations which have been made over the past five years of Zonge Engineering surveys.

Conductive anomalies are often found over existing oil and gas fields. The responsive material is usually rather deep, but it can sometimes have a near-surface expression as well. An increased conductivity with depth has been indicated on some surveys. The conductive material is generally column-shaped; electrical structure within the column has not yet been resolved. The appearance of the conductor may change substantially, depending upon whether the ground shows high-over-low or low-over-high layering, what the background resistivities are, what kind of structure exists, and so forth. However, the main thing to look for is a lateral change at depth to lower resistivities which is well-bounded and cannot be explained by culture, topography, structure, or other effects. A good example of this type of anomaly is provided in the Whitney Canyon case history (Chapter 3).

Polarizable anomalies over hydrocarbons are much less common than conductive anomalies. Deep, strong, diagonally-controlled anomalies of the type seen at Garza Field (section 2.5) are generally regarded with some suspicion due to the possibility of cultural effects; shallow, well-bounded anomalies of the type seen at Ryckman Creek Field (Chapter 3) are more easily related to near-surface alteration. The strongest polarization anomalies in the Rocky Mountain and midwestern United States are often found in Texas and Oklahoma, so the polarization parameter may be more indicative of hydrocarbons in that province than elsewhere. However, it is important not to be tied too strongly to observations such as this, for they are made at a point in time when few hard facts are available on what hydrocarbon-related anomalies should really look like.

The case histories provide some interesting and illustrative examples of how oilfield anomalies can be interpreted in light of current understanding.

REFERENCES

Azad, J., 1973, Direct oil prospecting with electrical transient reflections: Canadian Jour. of Geophysics, v. 9, Dec., p. 1-11.

Barker, C., 1980, Primary migration: the importance of water-mineral-organic matter interactions in the source rock, *in* Problems of petroleum migration: AAPG studies in geology, no. 10, p. 19-31.

Bredehoeft, J.D., and Papadopulos, I.S., Rates of vertical groundwater movement estimated from the earth's thermal profile: Water Resources Research Jour., v. 1, p. 325-328.

Carlson, N.R., Hughes, L.J., and Zonge, K.L., 1982, Hydrocarbon exploration using induced polarization, apparent resistivity, and electromagnetic scattering (abs.): Geophysics, v. 47, p. 451. Full paper available in Technical papers, 51st Annual International Meeting and Exposition, SEG, Los Angeles, v. 3, p. 1339-1358.

Clavier, C., Heim, A., and Scala, C., 1976, Effects of pyrite on resistivity and other logging measurements, *in* SPWLA 17th Annual Logging Symposium, Jun. 9-12, p. 1-34.

Davis, J.B., 1969, Microbiology in petroleum exploration, *in* Unconventional methods in exploration for petroleum and natural gas: Dallas, Southern Methodist University, p. 139-157.

Dolan, W.M., 1967, Considerations concerning measurement standards and design of pulsed I.P. equipment: Proc. of the Symposium on Induced Electrical Polarization, University of California, Berkeley.

Donovan, T.J., 1974, Petroleum microseepage at Cement, Oklahoma—evidence and mechanism: AAPG Bull., v. 58, p. 429-446.

Donovan, T.J., Forgey, R.L., and Roberts, A.A., 1979, Aeromagnetic detection of diagenetic magnetite over oil fields: AAPG Bull., v. 63, p. 245-248.

Duchscherer, W., Jr., 1980, Geochemical methods of prospecting for hydrocarbons: Oil & Gas Jour., Dec. 1, p. 194-208.

———,1981, Nongasometric geochemical prospecting for hydrocarbons with case histories: Oil & Gas Jour., Oct. 19, p. 312-327.

Duckworth, K., 1981, Paradoxical resistivity anomalies due to sulphides in sedimentary rocks associated with hydrocarbons: Jour. Canadian Soc. of Exploration Geophysicists, v. 17, p. 72-74.

Ferguson, J.D., 1979, The subsurface alteration and mineralization of Permian red beds overlying several oil fields in southern Oklahoma: The Shaleshaker, v. 29, Apr., p. 172-178, and May, p. 200-208.

Fox, R.C., Hohmann, G.W., and Rijo, L., 1978, Topographic effects in resistivity surveys: Salt Lake City, Earth Science Laboratory, University of Utah Research Institute.

Harwood, R.J., 1973, Biodegradation of oil, *in* The geology of fluids and organic matter in sediments: National Conference on Earth Science, Banff, Alberta, p. 149-156.

Hedstrom, H., 1930, Geo-electrical exploration methods: Oil Weekly, v. 58, no. 6, Jul. 25, p. 34-36.

Holladay, J.S., 1983: personal communication.

Holladay, J.S., and West, G.F., 1982, Effect of well casings on surface electrical surveys (abs.): Geophysics, v. 47, p. 439. Full paper available in Technical papers, 51st Annual International Meeting and Exposition, SEG, Los Angeles, v. 2, p. 815-838.

Horvitz, L., 1969, Hydrocarbon geochemical prospecting after thirty years, *in* Unconventional methods in exploration for petroleum and natural gas: Dallas, Southern Methodist University, p. 205-218.

———, 1982, Hydrocarbon geochemical prospecting after forty years, *in* Unconventional methods in exploration for petroleum and natural gas: Dallas, Southern Methodist University, p. 83-95.

Madden, T.R., and Cantwell, T., 1967, Induced polarization, a review: *in* Mining geophysics, v. 2, p. 373-400.

Magara, K., 1981, Hydrodynamics—does it trap oil?: Jour. Petroleum Geology, v. 4, p. 177-186.

Meinhold, R., 1971, Hydrodynamic control of oil and gas accumulation as indicated by geothermal, geochemical, and hydrological distribution patterns: 8th World Petroleum Congress (Moscow), v. 2, p. 55-66.

Mogilevskii, G.A., 1940, The bacterial method of prospecting for oil and natural gas (in Russian): Razvedka Nedr, v. 12, p. 32-43. Trans., (RJ-1372) Associated Technical Services, East Orange, N.J., 1953.

Myres, S.D., 1977, The Permian Basin, era of advancement: El Paso, Texas, Permian Press, p. 266.

Neglia, S., 1979, Migration of fluids in sedimentary basins: AAPG Bull., v. 63, p. 573-597.

Nelson, P.H., 1977, Induced polarization effects from grounded structures: Geophysics, v. 42, p. 1241-1253.

Nisle, R.G., 1941, Consideration of the vertical migration of gases: Geophysics, v. 6, p. 449-454.

Oehler, D.Z., and Sternberg, B.K., 1982, Induced polarization for hydrocarbon exploration: geochemical/geological interpretation (extended abs.), *in* Technical program abstracts and biographies: 52nd Annual International Meeting and Exhibition, SEG, Dallas, p. 445-448.

Ostrander, A.O., and Zonge, K.L., 1979, Complex resistivity measurements of sulfide-bearing synthetic rocks (abs.): Geophysics, v. 44, p. 409. Full paper available in Induced polarization for exploration geophysicists (short course): Johannesburg, South Africa, University of Witwatersrand, p. 71.

Pirson, S.J., 1969, Geological, geophysical and chemical modifications of sediments in the environment of oil fields, *in* Unconventional methods in exploration for petroleum and natural gas: Dallas: Southern Methodist University, p. 159-186.

———, 1980, Pirson, oil is confined in the earth by redox potential barriers: Oil & Gas Jour., Jul. 7, p. 153-158.

Powell, J.A., 1981, Electrical transient surveys for hydrocarbon (abs.): Geophysics, v. 46, p. 432. Full paper available in Technical papers, 50th Annual International Meeting and Exhibition, SEG, Houston, v. 3, p. 1773-1794.

Richers, D.M., Reed, R.J., Horstman, K.C., Michels, G.D., Baker, R.N., Lundell, L., and Marrs, R.W., 1982, Landsat and soil-gas geochemical study of Patrick Draw Oil Field, Sweetwater County, Wyoming: AAPG Bull., v. 66, p. 903-922.

Roberts, A.A., 1982, Helium emanometry in exploring for hydrocarbons: part II, *in* Unconventional methods in exploration for petroleum and natural gas: Dallas, Southern Methodist University, p. 135-149.

Roberts, W.H., III, 1980a, Design and function of oil and gas traps, *in* Problems of petroleum migration: AAPG studies in geology no. 10, p. 217-240.

———, 1980b, Some uses of temperature data in petroleum exploration, *in* Unconventional methods in exploration for petroleum and natural gas: Dallas, Southern Methodist University, p. 8-49.

Snyder, D.D., Kolvoord, R.W., Frangos, W., Bajwa, Y., Fleming, D.B., and Tasci, M.T., 1981, Exploration for petroleum using complex resistivity measurements, *in* Advances in induced polarization and complex resistivity: Tucson, short course reprints, University of Arizona, p. 209-253.

Soli, G.G., 1957, Microorganisms and geochemical methods of oil prospecting: AAPG Bull., v. 41, p. 134-140.

Sumner, J.S., 1967, Principles of induced polarization for geophysical exploration: New York, Elsevier Scientific Publishing Co., 277 p.

Tóth, J., 1980, Cross-formational gravity-flow of groundwater: a mechanism of the transport and accumulation of petroleum (the generalized hydraulic theory of petroleum migration), *in* Problems of petroleum migration: AAPG studies in geology, no. 10, p. 121-178.

U.S. Steel, 1983: personal communication with materials experts.

Wait, J.,1983: personal communication.

Wynn, J.C., and Zonge, K.L., 1975, EM coupling, its intrinsic value, its removal, and the cultural coupling problem: Geophysics, v. 40, p. 831-850.

Zonge, K.L., and Hughes, L.J., 1981, The complex resistivity method, *in* Advances in induced polarization and complex resistivity: Tucson, short course reprints, University of Arizona, p. 163-208.